Heat Transfer Analysis In Steel Structures

by

Vikas Adarsh Narang

A Thesis

Submitted to the Faculty

of the

WORCESTER POLYTECHNIC INSTITUTE

in partial fulfillment of the requirements for the

Degree of Master of Science

in

Civil Engineering

May 2005

APPROVED:

_____

Professor Leonard D. Albano, Major Advisor
Civil and Environmental Engineering

_____

Professor Robert W. Fitzgerald, Co-Advisor
Civil and Environmental Engineering

_____

Professor Fredrick L. Hart, Head of Department
Civil and Environmental Engineering

ACKNOWLEDGEMENT

ABSTRACT

The potential hazard of fire is one of the major concerning issues after the recent events of 9/11 and others. A lot of studies and research work is being carried out presently, to ensure the safety of buildings. But, there is no accurate method to estimate the fire endurance/resistance for a building due to the variability of fire characteristics, material properties of construction material, and other characteristics of a building. One can only provide guidelines and can adopt from the lessons learnt in the past to ensure better quality to make the buildings more fire proof, so that they can withstand high temperatures and stresses for a longer time, before collapse mechanism occurs. From a long time, live laboratory tests have been conducted to study the performance of assemblies by subjecting them to appropriate time-temperature histories that are derived from standardized fire curves. The performance-based approach is very time consuming and also involves high costs. In recent times, due to the advances in technology, computer models have been developed, that aid towards the simulations of assemblies and other components of a building that are subjected to a fire event. This approach helps in attaining reasonable results, thereby providing an alternative to the prescriptive and performance-based approaches.

This project deals with the study of heat transfer mechanism that takes place in steel structures in case of a fire event. For proper and accurate simulation process, the use of software is a must along with the support of technical resources. Due to high thermal conductivity of steel the heat gets transferred rather fast in the steel section which creates non-uniform temperature distributions because of variable thermal properties, like thermal conductivity and specific heat. 3-D finite element software TAS (Thermal Analysis Software) was used to study the non-uniform temperature distributions in case of a W 12x27 beam protected with vermiculite coating. The results were compared with the studies done by Professor Bletzacker, which involved the furnace testing of a W 12x27 beam by subjecting it to ASTM E-119 curve time-temperature history. In addition to this, the sensitivity of results was evaluated based on the variation of thermal properties for concrete, vermiculite, and gypsum board. Different beam models for

W12*x*27 section protected with vermiculite and gypsum board coatings were simulated to justify their performance based on temperature rise within the assembly. Also, simulations were performed for analyzing the behavior of the beam when subjected to different fire curves like ASTM E-119 and ENV. Analytical analysis was also carried out using the method of Lumped mass parameter method to provide a comparison of results from different models. Finally, conclusions and recommendations were made to ensure further development and understanding in the field of Structural and Fire Protection Engineering.

TABLE OF CONTENTS

List of Figures

List of Tables

Notations

A = surface are for heat transfer

A_p = area of steel protection per unit length exposed to fire

c_p = specific heat of gases

C = specific heat of air

C_{pc} = specific heat of concrete

C_{ps} = specific heat of steel

d_p = insulation thickness

dT = temperature difference

e = emissivity of steel

E_{b1} is the thermal radiation per unit surface of A_1

E_0 = initial Young's modulus at 20°C

E_T = Young's modulus at time T

F = opening factor

F_{y0} = initial Yield strength at 20°C

F_{yT} = Yield strength at time T

g = acceleration due to gravity

Gr = Grashof number

h_a are the overall heat exchange coefficients

h_c = convective heat transfer coefficient

k_s = thermal conductivity of steel

k_c = thermal conductivity of concrete

k = thermal conductivity of material

L = length of solid surface

Nu = Nusselt number

Pr = Prandtl number

$q_{t,d}$ = design fire load per unit area of compartment boundary

$\dot{Q}$ = rate of heat transfer across material thickness of dx

q = heat transferred per unit time (W)

Rd = Reynold's number

Ra = Raleigh number

t = time (*minutes*)

t^* = parametric time for determining compartment temperature-time response

t_d^* = parametric fire duration

T_s = temperature of steel

T_{fi} = fire temperature

T_a = air temperature

T = absolute temperature in K.

U_o = flow velocity

α = absorptivity

β = coefficient of thermal expansion for the fluid

τ = transmissivity

Γ = parameter to calculate parametric compartment temperature-time response

ε_{th} = free thermal strain

θ_a = structural steel temperature

λ_p = thermal conductivity of protection material

μ = absolute viscosity of fluid

$\sqrt{\rho c \lambda}$ = thermal inertia of the compartment boundary

ρ = density, reflectivity

ρ_p = density of insulation

ρ_a = density of structural steel

σ = Stefan-Boltzmann constant = $5.67x10^{-8}$ W$/$ m^{2}K^4

Φ = configuration factor for radiation, insulation heat capacity factor

v = relative viscosity of the fluid

$\Delta\theta_t$ = incremental increase in steel temperature

1 INTRODUCTION

1.1 Background

Fire hazard is one of the biggest challenges that any building could face during its service life. If not properly designed and managed, a fire could lead to a large amount of destruction in terms of property, loss of life, money. Historically a prescriptive approach to structural fire safety in the form of codes has been utilized which helps to solve the problem to a certain extent by regulating design and construction quality. The validity of prescriptive approach and its level of safety is now a concern **[8]** due to the development of performance-based approaches. A performance-based approach is a representation of the actual stages and developments that may occur in a structure during a fire event.

During the early stages, building codes were the only source to provide specifications for a building in case of a fire event. Building codes provided measures on how to curb a fire event after a fire had occurred in a building. The codes served as guidelines for the number of sprinklers required, the location and design of exits and other issues rather than emphasizing more on protection of a building even before a fire event occurred. The awareness was really not there and it was only after incidents like September 11, 2001, and others that the real importance of fire protection was recognized. The awareness led to more concrete research and testing which observed the evolution of performance-based approach in the form of live laboratory testing. Specifications have been provided by ASTM, NIST, and UL directory from the lab tests that are conducted by these associations. The results pertaining to the thickness requirements and hourly ratings of assemblies have been incorporated into building codes. Architects and structural engineers have been following these specifications without actually analyzing and studying the behavior of the building in a fire event. But, there have been fingers raised to the fact that how reliable these laboratory tests are, and whether it is possible to reproduce these results. In the late 1990's the and early 2000's the technique of finite element software caught the eye of researchers, and since then various tools have been developed to provide simulations of fire environments and structural performance thereby reducing the cost of expensive performance-based tests.

With so much research going on for steel design and its thermal properties **[14]** such as thermal conductivity and specific heat of how it would behave with respect to the change in temperature, it has become very important to use tools such as finite element software **[3]** which aid in facilitating the design procedure for the building. Simultaneously, to make steel more effective and protect it from fire hazards the insulating materials have gained significance importance in the market which leads to more and more research on their properties and behavior when exposed to fire conditions **[14]**. The variation in thermal characteristics of insulating materials such as vermiculite spray-on, and gypsum board play a major role in the heat transfer process that occurs through the insulation and then within the steel. This leads to research and development of new and improved fire protection materials. The use of different finite element tool such as SAFIR **[3], [21]** presents a reasonable picture of how the building component or structure would behave with the increase in temperature. The recognition of important characteristics such as elongation, thermal stresses, fire endurance points, boundary conditions and deflections **[1]** would help the engineer to better understand the key points of design and thus to make the building more sound in terms of fire exposure.

1.2   Aim

The purpose of this thesis is to study the heat transfer analysis in case of steel structures with the aid of finite element software. The main purpose is to study the processes of conduction, convection and radiation occurring in a member and then to analyze the sensitivity of the thermal analysis to the properties of steel and insulating materials. It is also intended to correlate the analytical results with Professor Bletzacker's experimental studies **[1]** and to extend his work with the help of modern tools like TAS **[25]**.

1.3   Objectives

The main objective of this study is to understand the concept of heat transfer through the section of a steel beam and gain experience with finite element software and analytical techniques. A second objective is to investigate the sensitivity of heat transfer analyses to thermal properties, such as thermal conductivity and specific heat.

1.4 Scope of work

The scope of activities included the following:

- ➤ Background research and understanding of the field of Fire Protection Engineering

- ➤ Analysis of heat transfer in steel structures by use of 3-D finite element software TAS (Thermal Analysis Software)

- ➤ Exploration of the effect of boundary conditions on the thermal behavior of a member

- ➤ Sensitivity analysis of the parameters that play an important role in heat transfer mechanism towards the assemblies in the form of convection and radiation and within the assemblies in the form of conductivity

- ➤ Investigation of the different types of coatings used for fire protection and their impact on the temperature profile of the steel during exposure to various time – temperature curves

- ➤ Study of the effects of different fire curves and to compare these results with those obtained from a simple, analytical methodology

1.5 Related activities

The project was carried out in a step-by-step manner by modeling different components of a structural assembly and studying the associated thermal properties and effects. Figure 1.1 presents the activities that were identified for achieving the goals for this project.
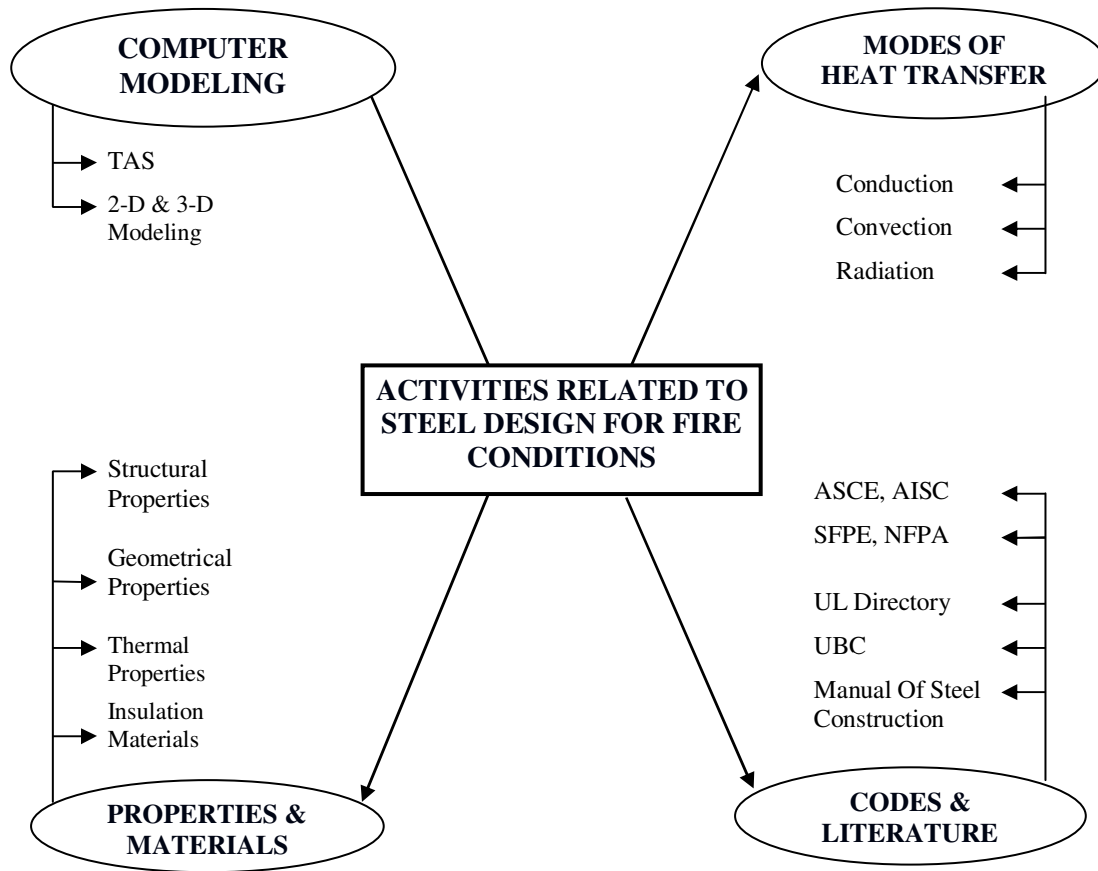
Figure 1.1 Related activities

For the TAS model development and simulations, different areas were explored which resulted in the study of various parameters. Some of the activities related to this project are explained below:

➢ Thermal conductivity, specific heat, and other thermal properties vary with temperature and thus were modeled as temperature-dependent parameters in the numerical analyses.

➢ Equations have been suggested for the variation of thermal conductivity and specific heat with respect to time. These equations are presented in Chapter IV.

➢ Information and data for the model were gathered from the experimental studies done by Professor Bletzacker [1].

➢ The insulation materials that were studied were gypsum board and spray-on vermiculite with different thicknesses and variation in their respective thermal properties.

➢ Influencing parameters like emissivity, conductivity were studied. The data for these varying parameters was taken from the formulation provided by sources such as Eurocode **[22]**.

➢ A comparison would be made with the data obtained from Bletzacker's experiments **[1]** and that obtained by TAS so as to study the effectiveness of computer modeling as an alternative to the high cost furnace test.

2   LITERATURE REVIEW

2.1   General

This section provides an overview of previous studies that have been conducted by researchers in the fields of Structural Engineering and Fire Protection. Different sources were reviewed in order to understand the techniques and key studies that have been conducted.

2.2   Research Studies

2.2.1   *Wong M.B. and Ghojel J.I.*

Wong and Ghojel **[23]** conducted a sensitivity analysis in order to determine the appropriateness of the guidelines provided by Eurocode 3. The parameters of thermal conductivity, specific heat, and emissivity were evaluated to determine the change in temperature of steel when subjected to a fire event. An equation for thermal conductivity variation for concrete was also proposed. For insulations having high thermal characteristic values, it has been suggested that the results due to the Eurocode 3 formulation and the exact solution may differ significantly.

2.2.2   *Sakumoto Y.*

Sakumoto **[14]** conducted a fire test on an office building to identify the critical parameters and the necessity of research on new fire protection materials. A four-story office building with floor dimensions, 22.0 m x 12.2 m x 3.5 m, coated with 12.5 mm thick plaster board was considered for the tests. Firstly, analysis was done on a one layer model was analyzed to define the effect of openings and fire load on the overall rise of temperature in a structural member. The results suggested that larger opening area resulted in a higher temperature rise but shorter fire duration, due to the inflow of fresh air. Secondly, temperature data was gathered from a fire test that was conducted on a steel column with intumescent coating. This data was used to study the high temperature performance for different grades of steel by varying their chemical composition. The results of these studies indicated the effectiveness of different grades of steel as a strategy to reduce the loss of strength and stiffness at elevated temperatures.

2.2.3 *Chitty R. and Foster J.*

Chitty R. and Foster J. **[3]** used the technique of computer modeling to evaluate the thermal response of structures that had undergone a real fire event. The computer tools JASMINE, CFAST, and CRISP were used to study the thermal response of a school building and a residential tower block. Temperature assumptions for different locations in the buildings were made based on observations and data collected. A comparison of results obtained from the different software was also presented. The paper summarizes the significance of finite element modeling by proceeding from simpler to complex methods in order to study thermal responses of a building. The authors conclude and draw attention to the variability and difficulty in modeling different parameters that are associated with fire design.

2.2.4 *Ioannides S.A. et al.*

The paper **[13]** addresses a method to determine the thickness of spray – applied fire resistive material based on the prescriptive code approach. It addresses the standard test of ASTM E-119 and proposes equations based on steel temperatures for calculating required thickness of insulation. These equations are supplemented with two examples that also identify the strategy for reducing high costs by avoiding unnecessary thickness of insulation.

2.2.5 *Poh K.W.*

Poh K.W. **[11]** presented a mathematical relationship to represent the stress-strain behavior of steel at elevated temperature. Experimental data was used in conjunction with the technique of curve fitting to replicate the curve. Different stress-strain relationships and their drawbacks have also been discussed. The proposed equations are highly versatile and can be easily incorporated into computer models for analyzing behavior of steel at higher temperatures.

2.2.6 *Lie T.T.*

Lie T.T. **[9]** suggested an analytical formulation for calculating steel temperature in a fire event. Equations were proposed for determining fire load and temperature of steel section for different conditions. Two examples were also been presented to illustrate the use of

the equations. Further, these equations were justified by comparing the analytical results with data from other experimental studies.

2.2.7 *Summary of studies*

From the previous studies, some points of interest can be drawn to create an awareness of the trends that exist in the fields of Structural and Fire Engineering. These points are summarized as below:

1. Finite element analysis has gained significant importance as a possible alternative to fire testing in order to save high costs. Efforts are being made to develop a software that can handle both thermal and structural responses.

2. Strategies and formulations have been developed to boost the ease and significance of analytical techniques. Studies and modifications are still being done for existing formulations and ASTM E-119.

3. The studies suggest that the current practice of furnace testing may be significantly different from an actual room fire due to factors such as opening factor and fire load which have not been studied with greatly.

According to these studies, the best understanding was provided by the study of sensitivity issues and parameters that are necessary to be modeled properly for accurate and reliable results. This was indicated by the studies conducted by **Wong *et al.* [23]** who conducted an in depth study to provide a foundation for future researchers.

2.3 Bletzacker's Experiments

In September 1966 a report titled "Effect of Structural Restraint on the Fire Resistance of Protected Steel Beam Floor and Roof Assemblies" **[1]** was submitted by Professor Richard Bletzacker. The research was sponsored by "American Iron and Steel Institute". This report presented the findings from Professor Bletzacker's experiments based on physical tests that were carried out on twelve separate beams with different restraining conditions and different compositions such as composite and non-composite slabs.

The type of beam used for Bletzacker's experiments was a W12*x*27 which was also used in this project so as to create a benchmark for the obtained results. Time-temperature data, which was gathered from thermocouples, was presented in his report, and this data was used in this project for comparison between his findings and the capabilities of the TAS models.

The physical testing process was conducted at Ohio State University. The entire setup for the mechanical systems was possible due to the valuable help of agencies and different people. Once the setup was established, member restraints and material composition were varied to provide a detailed analysis and comparison of the twelve members that were subjected to fire. In all cases Professor Bletzacker used the ASTM E-119 time-temperature curve **[24]** to control the temperature of the furnace during the course of the experiment. The temperature profile for the steel beam was extracted at different locations within the cross-section by the use of thermocouples. The data obtained from these readings thus helped in developing plots to determine the pattern for the increase in steel temperature over the period of time. The data was used to estimate fire endurance time which was the time to when the beam could not carry the loads any longer and ultimately resulted in a failure or collapse. Similarly, plots for deflection and stress were also developed from this data. These studies were significant from the view point of determining endurance times by modeling the beam as expected in the real world. The beam was subjected to loads and moments with the help of hydraulic jacks and other mechanical devices. However, it was not possible to represent an actual loading condition by the use of finite element software. Due to this reason, it was not possible to evaluate the stress, strain, and deformation results by the use of TAS **[25].**

2.4 Finite Element Software

2.4.1 *General*

Building codes by far have been the most accepted solution to structural and fire design. The performance demonstrated by physical tests is incorporated within the building codes for designing purposes. Over the course of time, finite element models have gained significant importance, and research has been ongoing to establish an alternative to

expensive and highly time consuming fire tests. Computer models have been developed to provide timely and economical simulations for results of a fire test. Researchers prefer finite element modeling to fire testing because the simulations can be used to target sensitive parameters that affect the overall fire event.

2.4.2 *FEAST*

2.4.2.1 *General*

FEAST stands for "Finite Element Analysis of Structures at Temperatures". This software was developed at the University of Manchester by Dr. T.C.H. Lui **[22]**. The program in itself is very versatile and has a detailed library for shell, solid, bolt, gap, and contact elements. Therefore, it can be utilized to analyze the local behavior of steel beams and columns.

2.4.2.2 *Applications*

The program is mainly used to study the behavior of steel framed connections and the effect of connections on the performance of steel beams exposed to fire conditions. Results from FEAST have shown a good correlation with laboratory tests.

2.4.2.3 *Limitations*

Presently, FEAST is not capable of simulating buckling behavior in a steel member. Also, it is not capable of analyzing the non-linear behavior of large scale steel frames with many members. It cannot be used to simulate composite structural behavior.

2.4.3 *SAFIR*

2.4.3.1 *General*

SAFIR **[26]** was developed at the University of Leige, Belgium by *Franssen et al. 2000* **[22]**. SAFIR has the capabilities of simulating structural as well as thermal problems. Beam, truss, shell elements and 3-D solid elements are used for structural modeling and analysis. The arc length method (Crisfield 1991) is included in the program to analyze post-buckling behavior but only for simple structures at present. Unlike FEAST, SAFIR does not have the capability to simulate connection behavior.

2.4.3.2 *Limitations*

Thermal analysis features are not very well-developed. The user has to conduct a thermal analysis for each part of the structure, and then prepare a library of temperature files to be used as an input for a subsequent structural analysis to evaluate forces, stresses, and deformations.

2.4.4 *TAS (Thermal Analysis Software)*

2.4.4.1 *General*

TAS **[25]** is a general purpose tool used to computer-simulate thermal problems. The version of TAS which was used for this thesis project was **Version 7.0.8,** and it was developed at Harvard Thermal Inc. located in Boston, Massachusetts. The version was compiled on June 30, 2003. TAS is designed on the basis of Windows platform that provides the user with a single, integrated, graphical and interactive environment for model generation, execution and post-processing of the results.. The provision of dialog boxes to facilitate data input and prompts for avoiding common input errors makes TAS a user friendly software. The generation of brick elements and full use of boundary conditions helps in developing the model more precisely in order to achieve reasonable results. Three-dimensional geometry can be created using two-dimensional plate and three-dimensional brick and tetrahedron elements. The addition of heat sources in the form of radiation and convection sources facilitates the process of modeling heat transfer. Arrays for different properties and parameters, such as thermal conductivity, specific heat, and temperature can be provided in the form of temperature, temperature difference, time and time cyclic dependent. Heat loads can be supplied at specified points, locations or regions in the form of nodal or surface loads.

TAS uses a finite element technique to model and solve the governing equations. This offers the versatility to easily create complex models involving many of the nonlinear cases often encountered. These include radiation, temperature-dependent thermal conductivity, and heat transfer coefficients that can be a function of temperature difference. The accuracy of the software has been proven over the past years. The results of numerous models have been compared to classical solutions and the results of other

programs such as MSC/NASTRAN, ANSYS and SINDA. The program was written entirely in the C++ language. This ensures speed in the graphics and the solution. The program dynamically and efficiently allocates PC memory sufficient for the particular model being investigated.

2.4.4.2 *Limitations*

One of the drawbacks of TAS is that it is not appropriate for combined thermal-structural analysis. It does not have a feature to add general point loads or uniformly distributed loads to the analysis of thermal stresses; it is limited to gravity loads only. Due to this reason it was not possible to obtain stress, strain, and deformation results, and thereby the structural failure due to the effect of temperature could not be evaluated. Steps are being taken at Harvard Thermal to incorporate features that would make TAS efficient enough to solve structural-related problems and give more detailed results in terms of stress, strain, and deformations.

3   FIRE TESTS

3.1   General

Most countries around the world rely on fire resistance tests to determine the performance of building materials and structural elements. The time-temperature curve used for a test is called a fire curve. There are different types of fire curves that have been established by researchers, viz. ASTM E-119 **[24]**, and Eurocode **[8]**. In USA, the temperature profile and duration of a standard fire for designing and testing purposes is based on the provisions of ASTM E-119 **[8], [24]**.

3.2   ASTM E-119

ASTM E-119 **[8], [24]** is the widely recognized standard for fire testing in the United States. The first edition was published in 1918 **[8]**, with the most recent published in 2000. Technical committees help in setting up a standard, and this standard is revised as technology and understanding changes. There has been significant debate on the validity of ASTM E-119 data and methodology **[8]** due to the recent events of 9/11. One has to understand that ASTM E-119 is a guideline for fire safe design of buildings and not a predictor of behavior in an actual fire. Real fires are a function of many variables, such as fuel load, thermal radiation, heat flux, ventilation factor, and area of openings **[8], [9], [23]** which are related to the type of construction, building occupancy, and design. The main purpose of using the ASTM E-119 protocol is to establish and document the fire rating of different elements of a building. The test does not cover flame spread, fuel contribution, or smoke density. ASTM E-119 describes different strategies for conducting fire tests on the following structural assemblies and elements:

1. Bearing walls and partitions
2. Non-bearing walls and partitions
3. Floors and roofs
4. Loaded restrained beams
5. Columns

3.3 Lab Tests

3.3.1 *General*

Lab testing is a very common method for determining the performance of a structural member from the view point of fire resistance. The main reason for conducting lab tests is essentially to test a structural element in a furnace from the viewpoint of critical temperature and fire endurance time or collapse mechanism **[8], [14]**. The element is then heated according to a standard time-temperature profile such as the ASTM E-119 curve **[24]**. The heating process is continued until failure of the element occurs so that specific data can be taken regarding the deflections, stresses, strains, etc. This data however is not available to public, and only the critical values are published in the codes. Figure 3.1 presents a traditional setup of a lab conducted fire test.
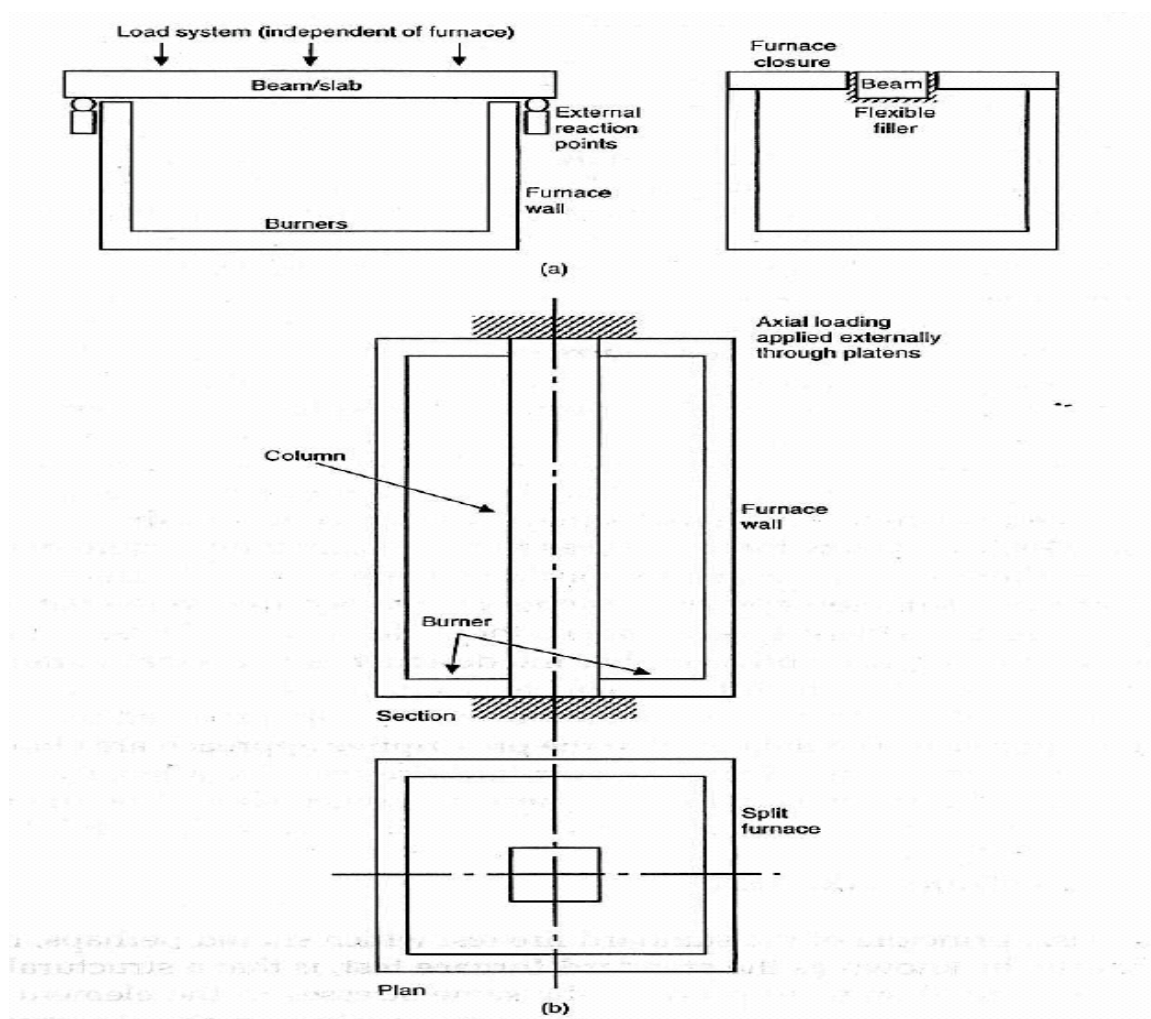
Figure 3.1 Assembly setup for a furnace test:(a)beam;(b)column [12], Chapter 3

Currently, there are studies being done and revisions are being made for the standard fire test procedure **[8]**. It is suggested by British Steel and the Building research development, 1998 **[8],** on the basis of full scale fire test results at Cardington, UK that the actual temperature of an element when tested separately in a furnace is quite different from the temperature of the same element when exposed to a fire within a building. This is observed due to the various connections and differences in boundary conditions that occur when the beam or an element acts as a part of a frame. However, research is ongoing and it will take some time to arrive at a clear conclusion.

3.3.2   *Time-Temperature Curves*

ASTM E-119 is the most common time-temperature curve that is used for the purpose of testing and simulations. Figure 3.2 presents the time-temperature profile for ASTM E-119.
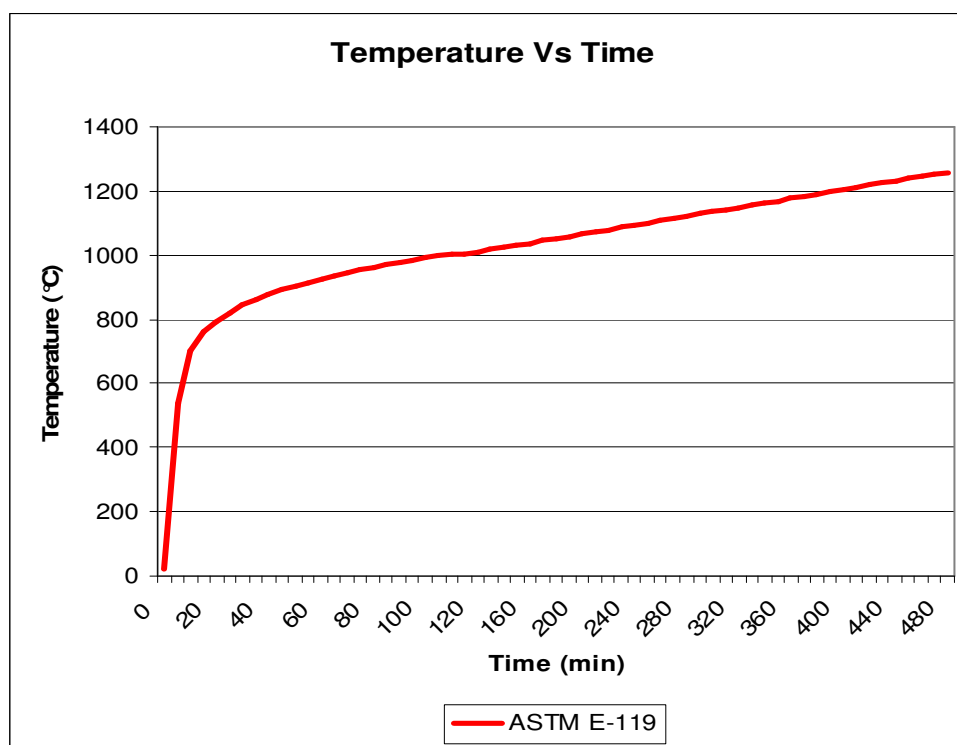
Figure 3.2 ASTM E-119 Time-temperature curve

However, different curves can be formulated for fire tests, based on the standard equations. The current version of **ISO 834**, **[12]** suggests that the time-temperature curve for the furnace tests is controlled by the following equation.

$$\theta_g = 20 + 345 \log(8t + 1)$$ - [3-1]

where, θ_g = furnace temperature $(°C)$

t = temperature (*minutes*)

There are various other mathematical equations that have been suggested. Some of them are given below.

Equation proposed by Williams – Leir (1973)

$$\theta_g = \theta_o + a_1\left(1 - e^{-a_4 t}\right) + a_2\left(1 - e^{-a_5 t}\right) + a_3\left(1 - e^{-a_6 t}\right)$$ - [3-2]

where, $a_1 = 532$, $a_2 = -186$, $a_3 = 820$, $a_4 = 0.01$, $a_5 = 0.05$ and $a_6 = 0.20$ and θ_0 is the ambient temperature.

Equation proposed by Fackler (1959)

$$\theta_g = \theta_o + 774\left(1 - e^{-0.49\sqrt{t}}\right) + 22.2\sqrt{t}$$ - [3-3]

In these equations above, the base temperature or ambient temperature θ_o is not considered to be 20°C which usually is the current practice.
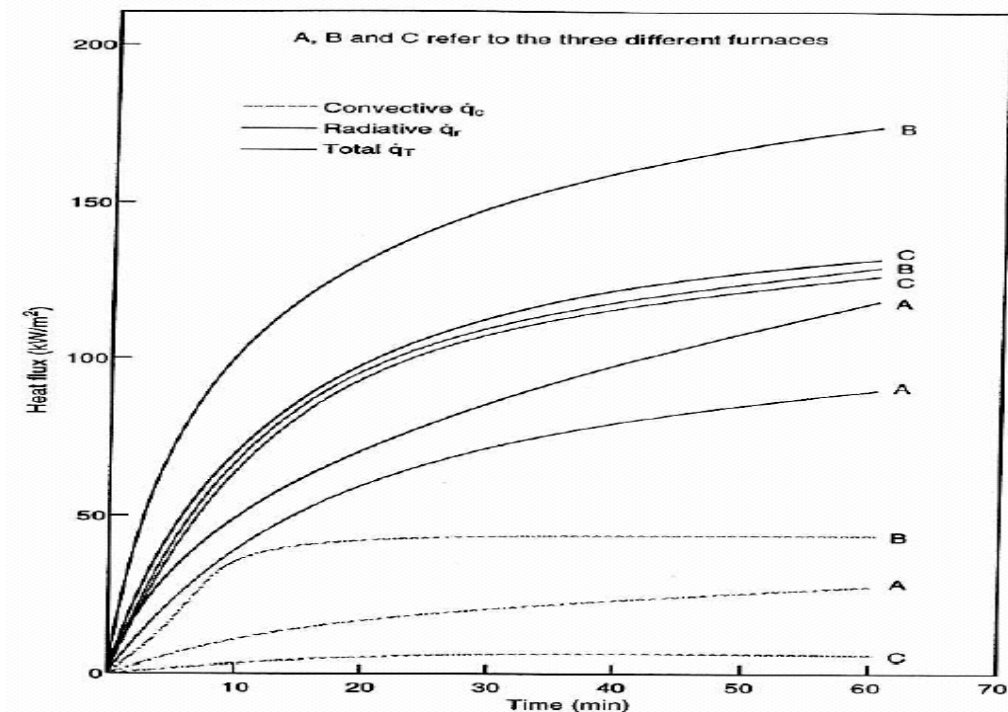
Figure 3.3 Heat flux Vs Time for different furnaces [Castle, 1974], [12]
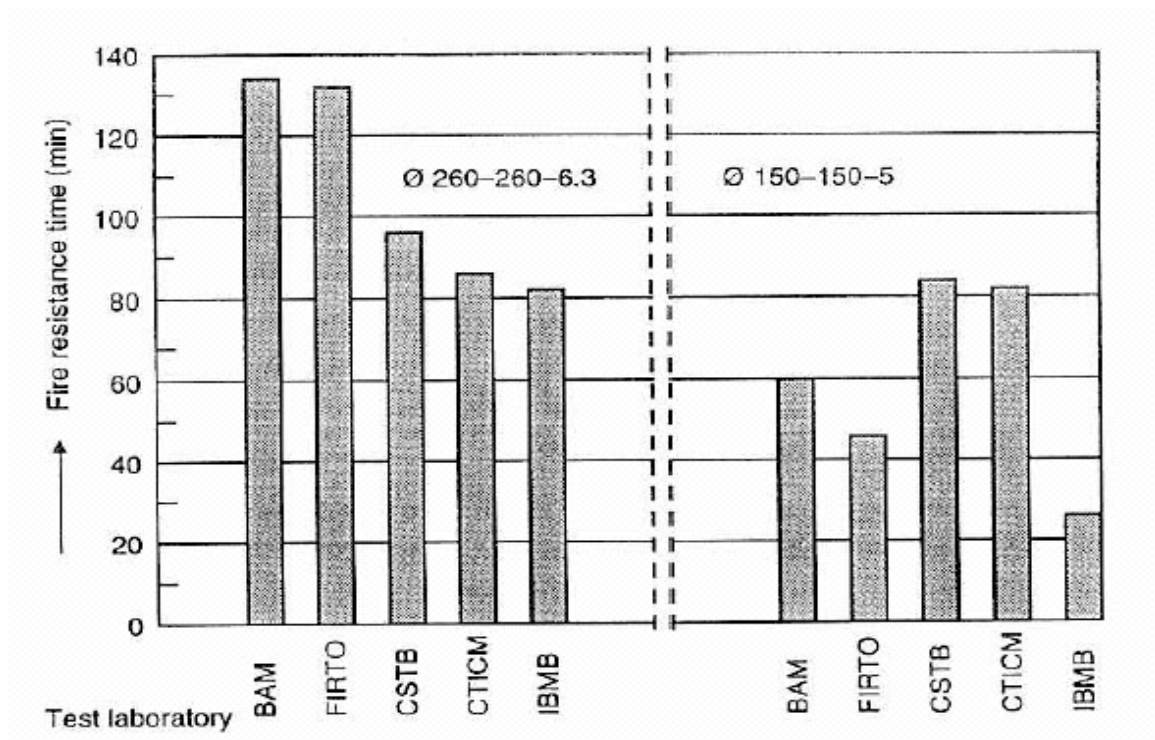
Figure 3.4 Effect of furnace characteristics on fire test results
[Witteveen and Twilt, 1981/2], [12]

3.3.3 *Drawbacks of Fire Tests*

Fire tests may present variable results depending on the furnace conditions and other parameters. Some of the drawbacks of fire tests are listed below,

> ➢ Cost of specimen preparation and actual test procedure is very expensive
>
> ➢ The test results are applicable only to a particular set of parameters that are already set and may not be true for an actual building construction
>
> ➢ It is difficult to test large assemblies due to the space limitations of a furnace
>
> ➢ It may not be possible in every case to supply the necessary loadings, restraints and moments to which a member would be subjected in actual construction
>
> ➢ Redistribution effects cannot be studied in detail because of the limitations of testing one member at a time
>
> ➢ The results obtained from a fire test are highly confidential from a manufacturer's point of view and cannot be applied for the purpose of research or further studies

➢ The thermal characteristics of a furnace play an important role in fire performance of elements and these parameters may vary from a furnace to furnace. Figure 3.3 presents the variability in heat flux for three different furnaces A, B, and C

➢ Reproducibility of results is not possible because of the variable thermal characteristics of a furnace. Harmanthy, 1969, suggested that the temperature rise in a furnace is a function of the thermal characteristics of furnace. Figure 3.4 illustrates the variability of results from a series of tests conducted by Witteveen and Twilt, 1981/2, **[12]** on similar beams within different furnaces

3.4 Behavior of actual fire

3.4.1 *General*

Compartment condition in an actual fire is an important study in the field of fire protection. Numerous curves have been suggested to explain the relation between temperature and time once a fire event takes place. It is important to note that factors such as thermal inertia, heat release rate, the presence of combustible materials, and the ventilation factor **[8]** play a critical role in the development of these fire curves. The behavior of compartment fire is described by three main phases, namely,

1. Growth
2. Fully developed fire
3. Decay period

Figure 3.5 represents the different phases that develop in the case of a compartment fire.
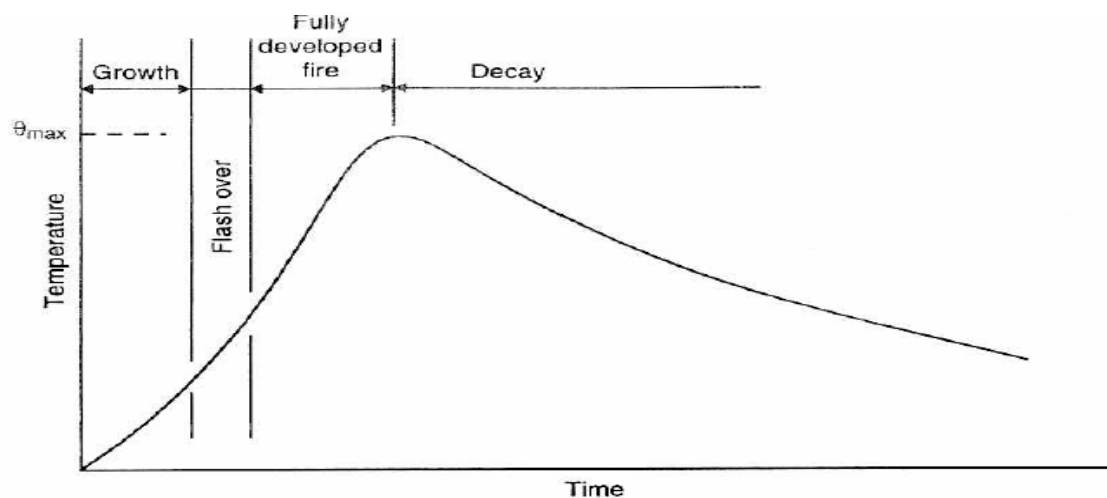
Figure 3.5 Different phases in a fully developed fire [12], Chapter 4

3.4.2 *Growth*

Growth is the initial phase of fire development. During this stage, combustion is restricted to certain areas of the compartment that may however result in significant localized rises in temperature. It may happen that many fires may not surpass this initial stage of fire development, due to insufficient fuel loads, limited availability of air supply, or human intervention.

3.4.3 *Fully developed fire*

The rate of increase in temperature is directly proportional to the heat release rate. Therefore, during this stage there is a large increase in the temperature of the compartment with temperatures reaching to about 1000°C. The duration of this phase depends on the volatile matter that is present in a compartment. As the rate of generation of volatile material decreases, or when there is insufficient heat available to generate such volatiles, the phase begins to cease gradually.

3.4.4 *Decay phase*

The word "decay" means decrease. As the name clearly suggests, there is a decrease in the fire intensity during this phase due to the decrease in the available fuel and the rate of fuel combustion. This phase occurs when the quantity of volatile matter continues to decrease and is consumed, after the initial stages of fire.

3.5 Parametric Curves

Time-temperature curves other than ASTM E-119 **[24]** are formulated on the basis of standardized equations and these curves are known as parametric curves. The approach is based on compartment fire response whereby certain parameters need to be established before the temperature response is calculated. There are, however, certain assumptions that need to be made for analyzing the response **[12]**.

1. Combustion is complete and occurs totally within the boundaries of the compartment.
2. No temperature gradient exists in the compartment.

3. Heat transfer characteristic known as thermal inertia, **"b"**, is a critical parameter for the determination of fire response. This parameter depends on several quantities including material density, thermal conductivity and specific heat.

4. Heat flow through compartment walls is assumed to be unidirectional.

It was suggested by Wickstrom (1981/2, 1985 a), **[12]** that the compartment fire is dependent on the ratio of opening factor to the thermal inertia. A ventilation factor of 0.04 m and a thermal inertia of 1160 $Ws/m^2\,°C$ were assumed as reference values for a typical room for an office building to establish the standard furnace curve.

In general, the temperature-time relations are expressed by the following equations,

For the heating phase,

$$\theta_g = 1325\left[1 - 0.324e^{-0.2t^*} - 0.204e^{-1.7t^*} - 0.472e^{-19t^*}\right]$$ - **[3-4]**

t^* = parametric time for determining compartment temperature-time response.

t^* is given by, tΓ

Here,   t = time

Γ = parameter to calculate parametric compartment temperature-time response.

Γ is defined as,

$$\Gamma = \frac{\left(\dfrac{F}{\sqrt{\rho c\lambda}}\right)^2}{\left(\dfrac{0.04}{1160}\right)^2}$$ - **[3-5]**

where, F = opening factor

$\sqrt{\rho c\lambda}$ = thermal inertia of the compartment boundary.

For the cooling phase:

for $t_d^* < 0.5$ hours

$$\theta_g = \theta_{max} - 625\left(t^* - t_d^*\right)$$ - **[3-6]**

for $0.5 \leq t_d^* \leq 2$ hours

$$\theta_g = \theta_{max} - 250\left(3 - t_d^*\right)\left(t^* - t_d^*\right)$$ **- [3-7]**

for $t_d^* > 2$ hours

$$\theta_g = \theta_{max} - 250\left(t^* - t_d^*\right)$$ **- [3-8]**

θ_{max} is the maximum temperature that is reached during the heating phase, and t_d^* is

given by, $$t_d^* = \frac{0.13x10^{-3}q_{t,d}}{F\Gamma}$$ **- [3-9]**

$q_{t,d}$ = design fire load per unit area of compartment boundary.

Figure 3.6 illustrates the sensitivity of the time - temperature response for ENV 1991-2-2, from the theories of Wickstrom, and Lie.
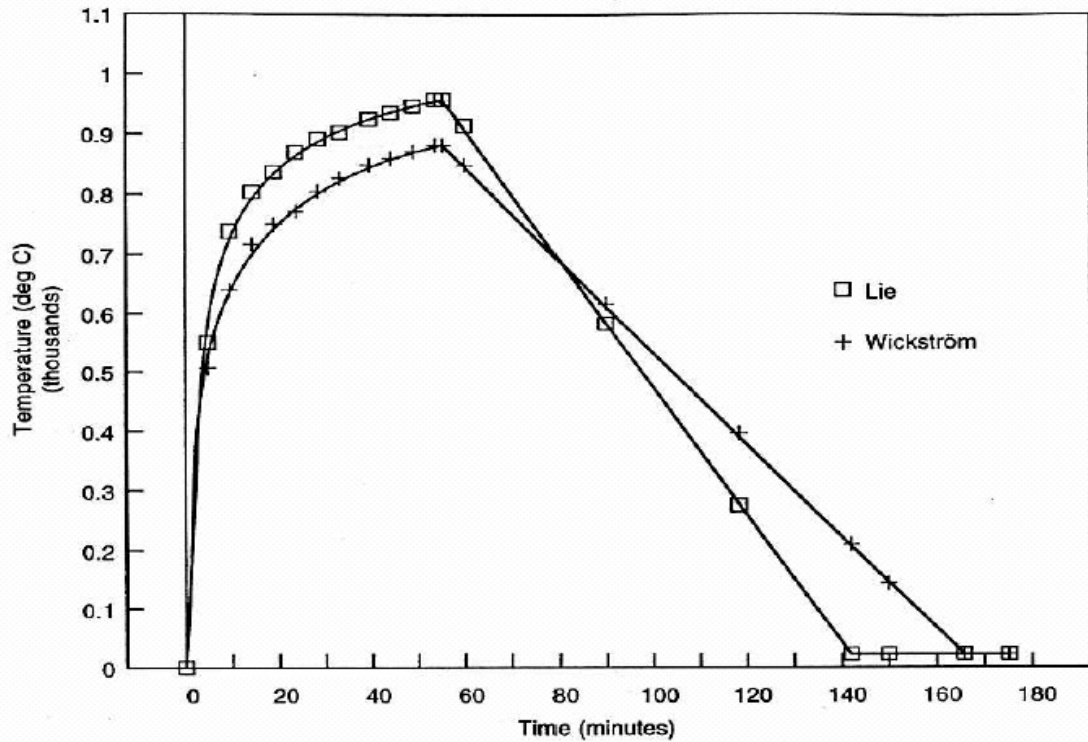
Figure 3.6 Comparison of time-temperature response using the theory of Wickstrom,and Lie [12]

From this chapter it was observed that there exists a significant amount of variability in the results that are obtained from furnace tests. Also, the behavior of fire curves from different formulations becomes an important area of study.

4 MATERIAL PROPERTIES AT ELEVATED TEMPERATURES

4.1 Introduction

This section provides an overview of the thermal properties of interest for typical construction materials such as steel, concrete, vermiculite and gypsum board. These properties were studied to facilitate the process of understanding and developing the models.

4.2 Definitions

4.2.1 *Density (ρ)*

Density is a physical property of matter. In a qualitative manner density is defined as the heaviness of objects with a constant volume. It is denoted as ρ. Common unit of density is kg/m^3.

4.2.2 *Thermal Conductivity (k)*

Thermal conductivity is defined as the amount of heat flux that would pass through a certain material depending on the temperature gradient over that material. Thermal conductivity plays an important role in many heat and mass transport phenomena as it is a function of Prandtl number.It is denoted as *k*. Commonly used units are W/mK and $cal/sec\text{-}cm\text{-}°C$.

4.2.3 *Specific Heat (C_p)*

Specific heat is an intensive property which means that it is independent of the mass of a substance Specific heat is defined as the amount of heat required to raise the temperature of one gram of a substance by one degree celcius. It is denoted as C_p. Common units for specific heat are J/kgK and J/kg°C.

4.2.4 *Coefficient of Thermal Expansion (ε_{th})*

The coefficient of thermal expansion is defined as the increase or elongation in

length occurring in a member per unit increase in temperature. It is denoted as ε_{th}.
Commonly used units are in/in/°C, cm/cm/°C.

4.2.5 *Thermal Diffusivity*

Thermal diffusivity is defined as the ratio of thermal conductivity to heat capacity.
Its values are obtained on the basis of density, thermal conductivity and specific
heat data for a particular material. It is denoted as $"\alpha"$. Common units are m^2/sec,
cm^2/sec, mm^2/sec.

$$\alpha = \frac{k}{\rho C_p} \qquad\qquad \textbf{- [4-1]}$$

where, k = thermal conductivity in W/mK

ρC_p = volumetric heat capacity measured in $J/m^3 K$

Substances with high thermal diffusivity rapidly adjust their temperature to that of
their surroundings, because they conduct heat quickly in comparison to their
thermal 'bulk'.

4.2.6 *Emissivitty*

Emissivity of a material is defined as the ratio of energy radiated to energy radiated
by a black body at the same temperature. It is a dimensionless quantity. It is
denoted as $"e"$.

4.3 Thermal Properties of Steel

4.3.1 *Introduction*

Steel is a metal alloy whose major component is iron, with carbon being the primary
alloying material. Different quality/grades of steel can be manufactured by varying the
amount of carbon and its distribution in the alloy **[14].** Fire resistant steel is manufactured
by adding molybdenum **(Mo)** and other alloying materials **[14]**. The behavior of steel
when exposed to high temperatures is of critical importance for the safety and stability of
the building. The temperature rise for a steel member is a function of the materials,
thermal conductivity and specific heat **[23]**. Thermal conductivity tends to decrease with
the increase in temperature while specific heat tends to increase with the increase in

temperature. The properties are discussed in the following sections with the help of graphs from different sources.

4.3.2 *Density*

The standard value for the density of structural steel proposed by Eurocode 3, Part 1.2 **[22]** is 7850 kg/m^3**.** For most calculations and research work density is assumed to be constant with the increase in temperature. Hence, a constant value was adopted for the modeling of the beam.

4.3.3 *Coefficient of Thermal Expansion*

The coefficient of thermal expansion for steel is denoted as ε_{th}. Thermal expansion is temperature dependent and can be evaluated based on the equations proposed in Eurocode 3, Part 1.2 **[22].** Figure 4.1 presents the plot for thermal expansion Vs temperature from Bletzacker's data.

$$\varepsilon_{th} = (-2.416x10^{-4}) + (1.2x10^{-5}T) + (0.4x10^{-8} xT^2) \quad \text{for } T \leq 750°\text{C} \qquad \textbf{- [4-2]}$$

$$\varepsilon_{th} = 0.011 \qquad\qquad\qquad\qquad \text{for } 750°\text{C} < T \leq 860°\text{C} \qquad \textbf{- [4-3]}$$

$$\varepsilon_{th} = -0.062 + (2x10^{-5}T) \qquad\qquad \text{for } T > 860°\text{C} \qquad\qquad \textbf{- [4-4]}$$
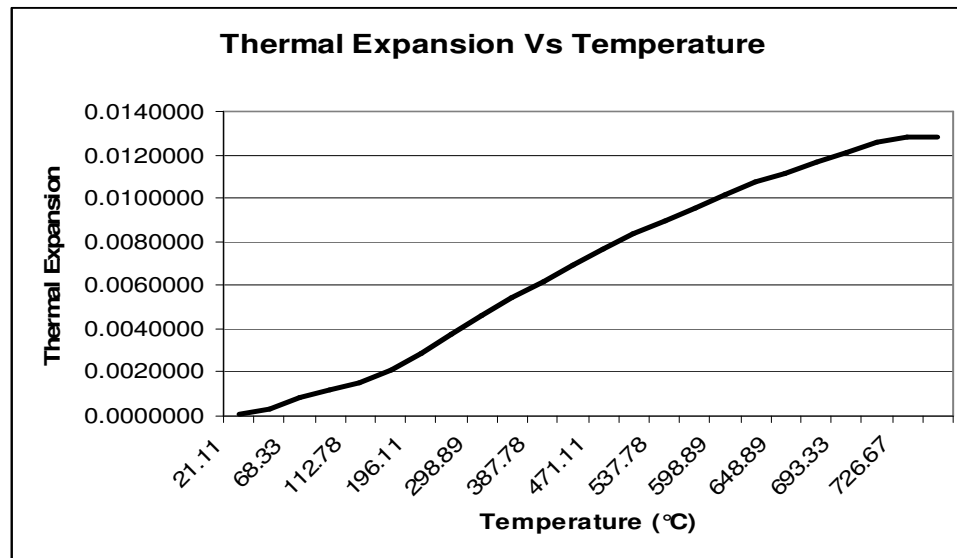
Figure 4.1 Thermal Expansion Vs Time based on Bletzacker's Experimental Data, [1]

4.3.4 *Thermal Conductivity*

Units for thermal conductivity are W/mK and W/cm°C. The standard value for thermal conductivity of steel as suggested by Eurocode 3, Part 1.2 **[22]** is 54 W/mK at 20°C. However, thermal conductivity (k_s) of steel varies with the change in temperature based on the relations established by Eurocode 3, Part 1.2 **[22].**

$$k_s = 54 - \left(\frac{T_s}{300} \right) \qquad \text{for } 20°C < T_s \leq 800°C \qquad \text{- [4-5]}$$

$$k_s = 27.3 \qquad \text{for } T_s > 800°C \qquad \text{- [4-6]}$$

Figure 4.2 represents thermal conductivity values based on Equations 4-5 and 4-6.
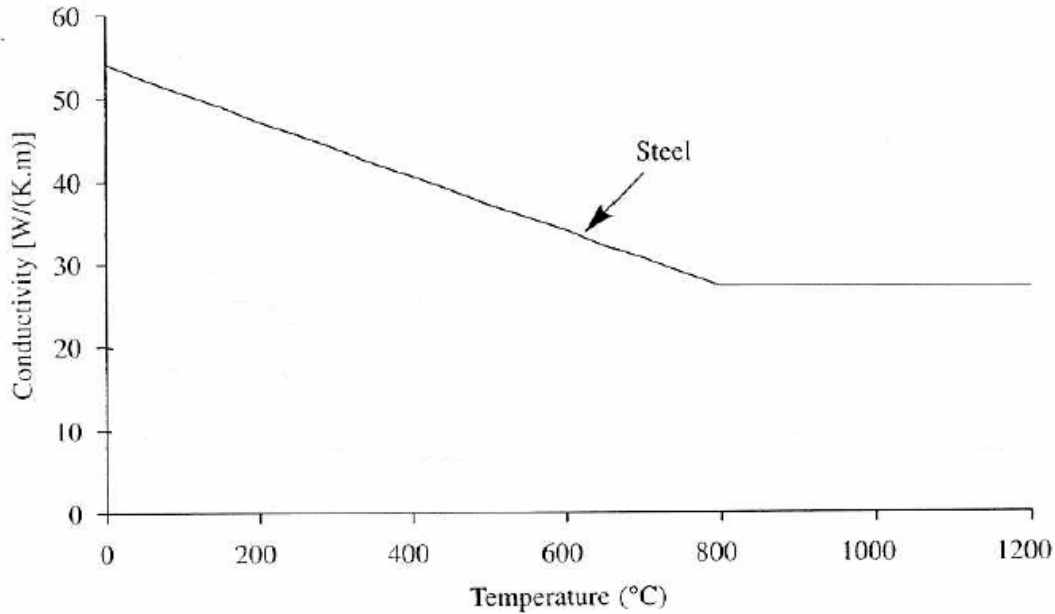
Figure 4.2 Thermal Conductivity Vs Temperature for Steel (CEN 2001), [22]

4.3.5 *Specific Heat*

Specific heat for steel is denoted as C_{ps}. Units for specific heat are J/lbs°C and J/kg K. The equations suggested by Eurocode 3, Part 1.2 **[22]** for change of specific heat of steel with temperature are presented below. The results of these equations are graphically represented in Figure 4.3.

$$C_{ps} = 425 + 0.733T_s + 0.000169T_s^2 + 2.22x10^{-6}T_s^3 \qquad \text{- [4-7]}$$

$$\text{for } 20°C \leq T_s \leq 600°C$$

$$C_{ps} = 666\left(\frac{13002}{T_s - 738}\right) \qquad \text{-[4-8]}$$

$$\text{for } 600°C < T_s \leq 735°C$$

$$C_{ps} = 545 - \left(\frac{17820}{T_s - 731}\right) \qquad \text{- [4-8]}$$

$$\text{for } 735°C < T_s \leq 900°C$$

$$C_p = 650 \qquad \text{for } T_s > 900°C \qquad \text{-[4-9]}$$
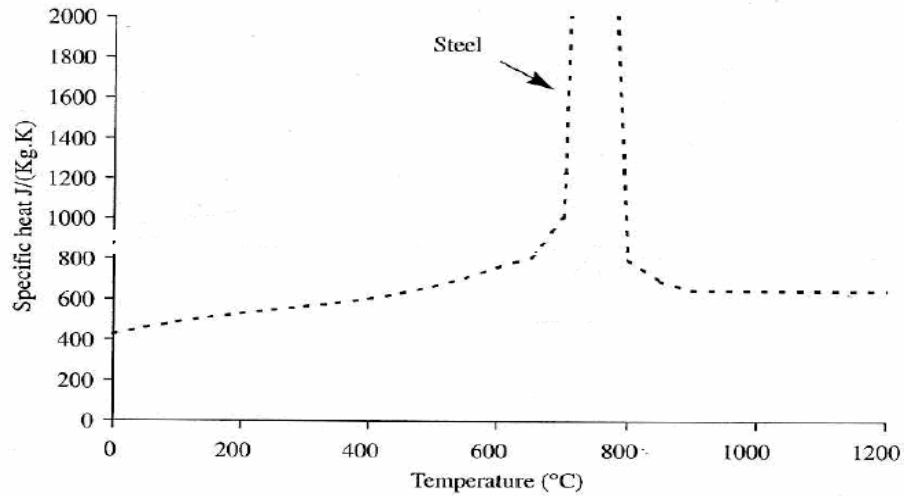
Figure 4.3 Specific Heat Vs Temperature for steel (CEN 2001), [12]

4.3.6 *Thermal diffusivity*

According to **Malhotra, [12]**, thermal diffusivity of steel shows a linear relationship up to a temperature of 750°C.

$$\alpha_a = 0.87 - (0.84x10^{-3}\theta_a) \qquad \text{- [4-10]}$$

4.3.7 *Emissivity*

Wong M.B. *et al* **[23]** confirmed through use of a heat transfer model that the resultant emissivity depends on temperature and is not a constant. However, due to the lack of research work most researchers assume constant values. **Eurocode 3** recommends a

constant value of **0.625** for steel. **Chitty *et al.*, 1992, [12], Chapter 5,** proved the significance of varying resultant emissivity to predict temperatures within a steel column. Figure 4.4 presents the results obtained from their tests. These tests prove that the results from a furnace test depend significantly on the thermal characteristics of a furnace and the geometry of the test element. These studies were significant from the view point of adopting constant values for emissivity to generate analytical solutions. However, due to the limitations of finite element analyses, constant values are adopted for the purpose of simulations.
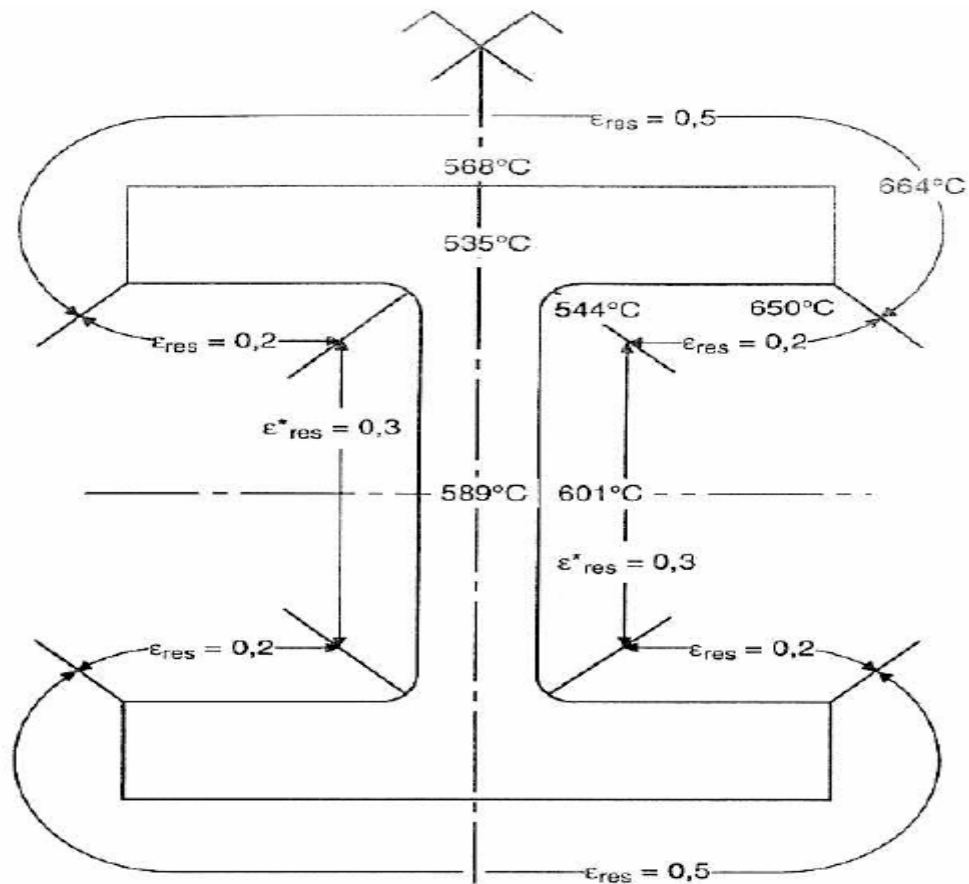
Figure 4.4 Temperature prediction within a steel column due to the variation of resultant emissivity [12], Chapter 5, p 77

4.4 Thermal Properties of Concrete

4.4.1 *General*

In construction, concrete is a composite building material made from a combination of aggregate, cement binder and water. The most common form of concrete is Portland cement concrete, which consists of mineral aggregate (generally gravel and sand), portland cement, and water. After mixing, the cement hydrates and hardens into a stone-like material. Since concrete is a hygroscopic material, the heat transfer process is affected by the migration of water. Due to the properties of concrete it can absorb a large amount of heat. In most methods, constant thermal values are assumed for design purposes **[23]**.

4.4.2 *Density*

The loss or change in density of concrete is not significant with the change in temperature. Therefore, constant density is assumed for design or modeling purposes. As suggested by **Eurocode [22]**, 2200 kg/m^3 was assumed for all the models.

4.4.3 *Thermal Conductivity*

The equation suggested by **ENV 1994-1-2** for change of thermal conductivity of concrete is presented below. The results from this equation are graphically represented in Figure 4.5. **Wong M.B.** *et al.* **[23]** conducted a sensitivity analysis and suggested that a constant value of **1.2 W/mK** may be assumed for modeling purposes. The equation below is a general equation which maybe applied to different grades of concrete.

$$k_c = 2.0 - 0.24\left(\frac{\theta_c}{120}\right) + 0.012\left(\frac{\theta_c}{120}\right)^2 \qquad \textbf{- [4-11]}$$

where, θ_c = temperature of concrete (°C)

k_c = thermal conductivity of concrete (W/mK)
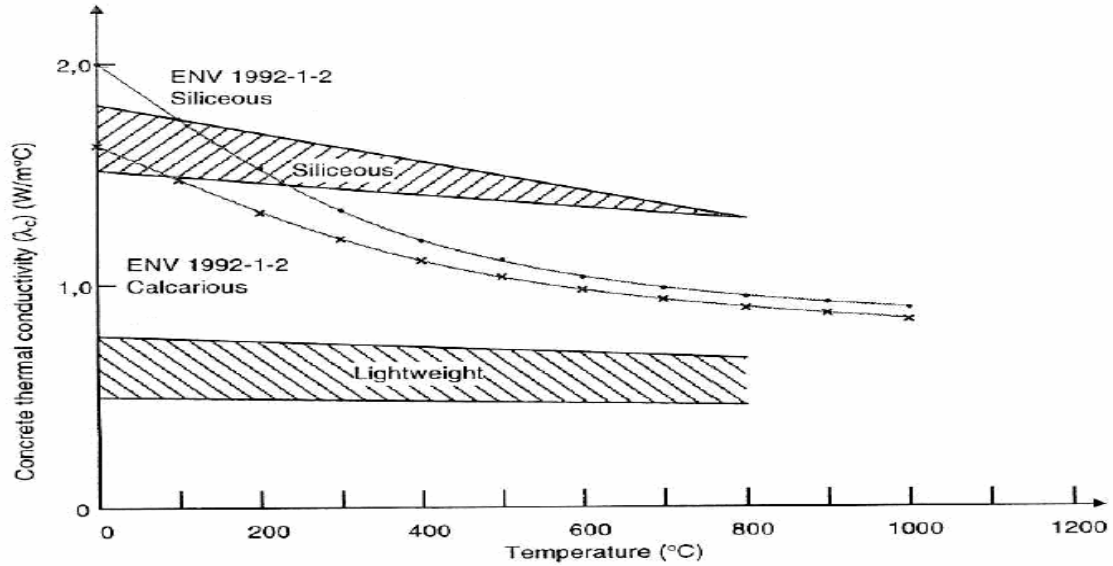
Figure 4.5 Thermal Conductivity Vs Temperature for soncrete (Schneider, 1986a), [12], Chapter 6, p 90

4.4.4 *Specific Heat*

Specific heat directly varies with temperature. The equation suggested by ENV 1994-1-2 **[12]** for changes in the thermal conductivity of concrete is presented below. The results of this equation and the values obtained from tests are graphically represented in Figure 4.6 As we can observe from the graph, the type of aggregate plays a critical role in the values.

$$C_{pc} = 900 + 80\left(\frac{\theta_c}{120}\right) - 4\left(\frac{\theta_c}{120}\right)^2$$ **- [4-12]**

where, θ_c = temperature of concrete (°C)

C_{pc} = specific heat of concrete (J/kgK)

A constant value of **840 J/kg°C** has been suggested by ENV 1994-1-2 for lightweight concrete. For this project, normal weight concrete was used for analyses.
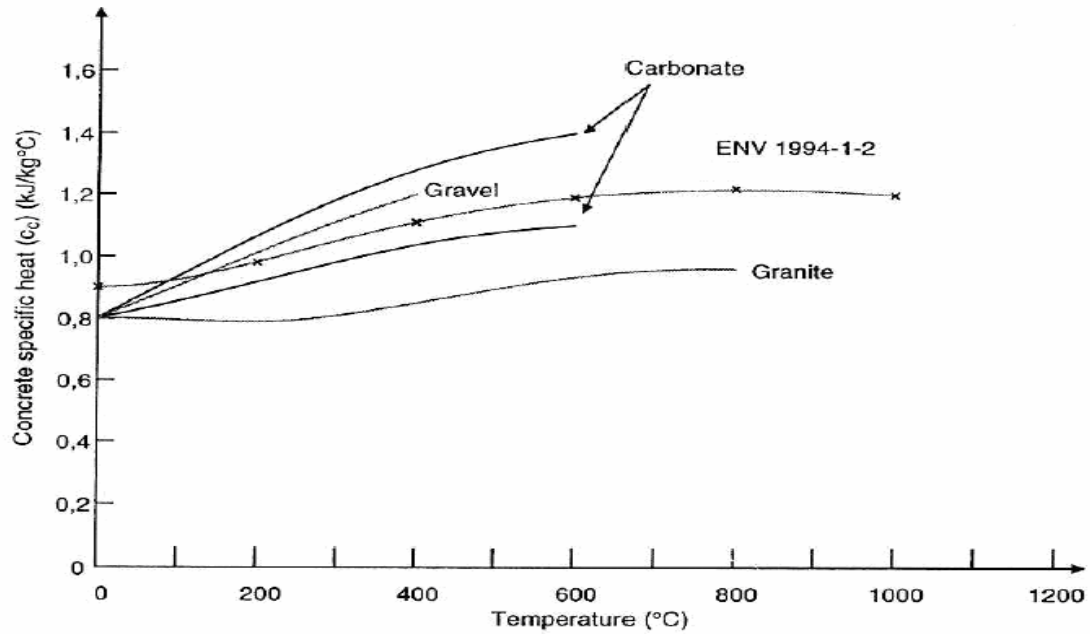
Figure 4.6 Specific Heat Vs Temperature for concrete (Schneider, 1986a), [12], Chapter 6, p 89

4.4.5 *Thermal Diffusivity*

The thermal diffusivity of concrete decreases with an increase in temperature. Figure 4.7 shows the nature of thermal diffusivity for normal and lightweight concretes.
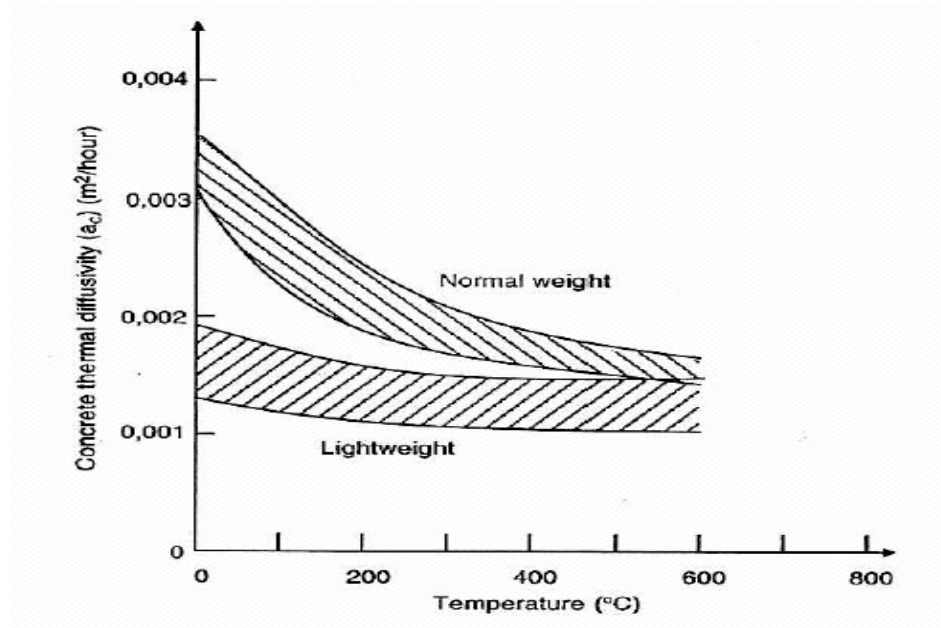
Figure 4.7 Thermal diffusivity Vs Temperature for concrete(Schneider, 1986a), [12], Chapter 6, p 91

4.5   Insulations and their Thermal Properties

4.5.1   *Definition of Insulation*

Insulation is a material or combinations of materials that retard the flow of heat energy. Some of the functions of insulations are:

1. Conserve energy by reducing heat loss or gain.

2. Control surface temperatures for personnel protection and comfort.

3. Facilitate temperature control of a process.

4. Prevent vapor flow and water condensation on cold surfaces.

5. Prevent or reduce damage to equipment from exposure to fire or corrosive atmospheres.

4.5.2   *Types of Insulations*

4.5.2.1   *Fibrous Insulation*

Fibrous insulation is composed of small diameter fibers that finely divide the air space. The fibers may be perpendicular or parallel to the surface being insulated, and they may or may not be bonded together. The most widely used insulators of this type are glass fiber and mineral wool.

4.5.2.2   *Cellular Insulation*

Cellular insulation is composed of small individual cells separated from one another. The cellular material may be glass or foamed plastic such as polystyrene (closed cell), polyurethane, and polyisocyanurate.

4.5.2.3   *Granular Insulation*

Granular insulation is composed of small nodules that contain voids or hollow spaces. It is not considered a true cellular material since gas can be transferred between the individual spaces. This type may be produced as a loose or pourable material, or combined with a binder and fibers to make a rigid insulation. Examples include calcium silicate, expanded vermiculite, perlite, cellulose, diatomaceous earth, and expanded polystyrene.

4.5.3 *Thermal Properties of Vermiculite*

4.5.3.1 *General*

The name Vermiculite is derived from the Latin word "Vermiculare" which means to breed worms. Vermiculite resembles mica in appearance. It is clean to handle, mold resistant, odorless and sterile due to the high temperatures to which it is subjected in production. Vermiculite exfoliates due to the presence of water which gets converted to steam. Vermiculite can be used for fire protection in the form of boards or as spray-applied plaster. The information presented below was obtained from a website for vermiculite **[27]**

Chemical Formula: $(Mg,Fe++,Al)_3(Al,Si)_4O_{10}(OH)_2 \cdot 4(H_2O)$

Composition:

Figure 4.8 represents the percentage composition of different elements that are present in vermiculite. Molecular Weight = 504.19 gm
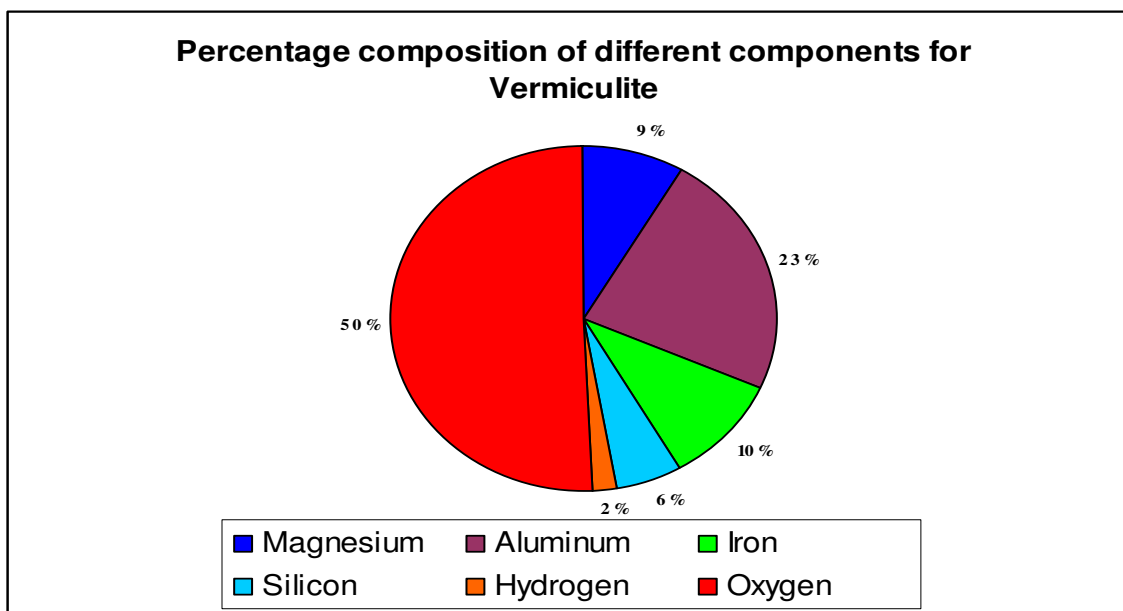
Figure 4.8 Percentage composition of different materials in case of vermiculite

Empirical Formula: $Mg_{1.8}Fe^{2+}_{0.9}Al_{4.3}SiO_{10}(OH)_2 \cdot 4(H_2O)$

4.5.3.2 *Advantages of Vermiculite*

- Vermiculite has reduced thermal conductivity.
- It is light in weight.
- It possesses improved workability.
- It is an excellent fire resistance material.
- It has improved adhesion properties.
- It has increased resistance to cracking and shrinkage.
- It is easy to install or apply.

4.5.3.3 *Thermal Conductivity*

The thermal conductivity of vermiculite increases with temperature, but after reaching a temperature in the range of about 1050°C to 1200°C the value decreases again.

"Hoben International", a leading professional engineering firm in England **[7]** has suggested that the thermal conductivity of vermiculite varies between **0.062 W/mK** to **0.065 W/mK** based on their laboratory tests. These tests also indicated that the melting point of vermiculite is around **1330°C**.

"SHUNDLER Company" [16], a US firm based in New Jersey, has also published test data for thermal resistance at specific temperature points. Since thermal conductivity is inversely proportional to thermal resistance, these values of thermal resistance can be used to obtain thermal conductivity values and incorporate them in the model.

Table 4-1 represents the values obtained from the lab tests conducted by Schundler Company for one cubic meter of vermiculite.

Table 4-1 Thermal Resistance data from tests done by Shundler Company, [16]

Temperature (° C)	Thermal Resistance (Km^2/W)
20	0.4
100	0.32
150	0.28
200	0.25
250	0.22
300	0.19
350	0.17
400	0.15
450	0.13

4.5.3.4 *Specific heat*

The specific heat of vermiculite has not been studied very deeply; it is an area of ongoing research with many unanswered questions. However, **"Hoben International"**, of England **[7]**, suggests a constant value of **1800 J/kg K**. Alternatively, Eurocode suggests a value of **1200 J/kg K, [12], Ch 6**. There is a large variation between these two values. A specific heat profile in accordance with temperature was suggested by **Toman Jan *et. al* [20]** based on their laboratory experiments. Due to non-availability of established equations, data points were read from the graph and were then adjusted according to the technique of curve fitting. Figure 4.9 presents a comparison between the two data sets.
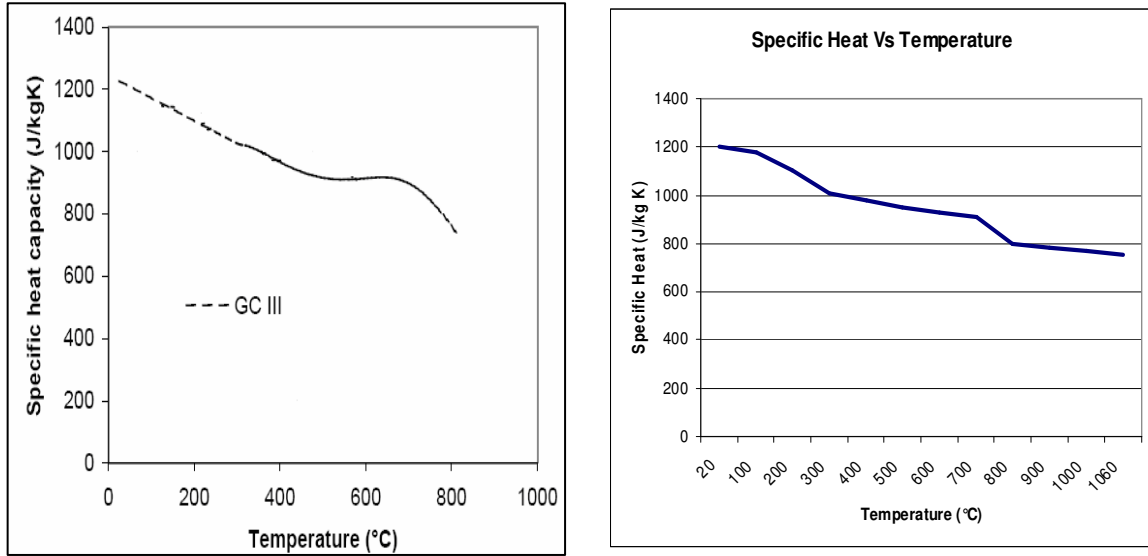
Figure 4.9 Comparison of graph of Specific heat Vs Temperature obtained from test data,[16] and from the technique of curve fitting(Interpolation)

4.5.4 Thermal Properties of Gypsum

4.5.4.1 General

Gypsum is a mineral found in sedimentary rock formations in a crystalline form known as calcium sulfate dehydrate. Gypsum rock is mined or quarried and then crushed into fine powder. The powder is heated and treated through a chemical process called calcining which is a process for removing chemically combined components. Gypsum boards are rigid sheets of building material made from gypsum and other materials. It is also known as drywall construction. The common type of gypsum board that is used for construction purposes is designated as Type X based on its composition and fire ratings. Also, gypsum may be used in a single layer or multiple layers, depending on the type of building and its significance. The determination of the number of layers required, depend upon the type of building and code compliance regulations.

Chemical formula: $CaSO_4-2(H_2O)$

Composition:

Figure 4.10 represents the percentage composition of different components that comprise gypsum.
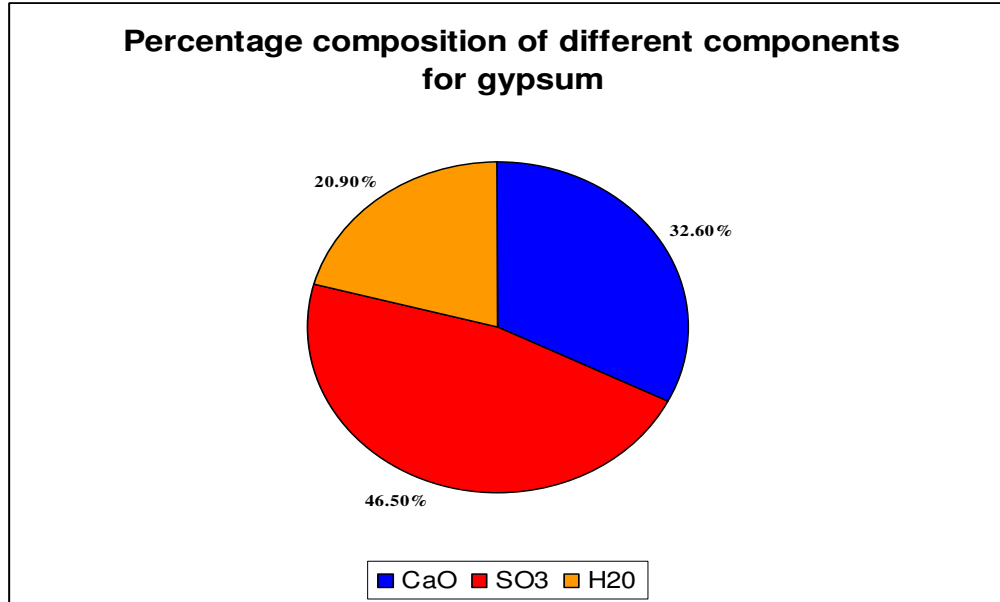
Figure 4.10 Percentage composition of different materials in case of gypsum

4.5.4.2 *Advantages of gypsum board*

- Gypsum is easily available
- Gypsum boards provide a durable surface for interior ceilings and walls
- They can be easily produced in the factory so there are no issues regarding moisture content
- Gypsum has a high melting point
- Gypsum panels are easy to install

4.5.4.3 *Thermal Conductivity*

Much research has been conducted at the **National Institute of Standards and Technology** also known as NIST. Cooper L.Y. **[4]** conducted lab tests on gypsum board to provide some understanding of how temperature influences properties of gypsum. As shown in Figure 4.11 thermal conductivity rises after a temperature limit of 400°C and also there is a steep increase beyond 800°C. The change in thermal conductivity values

over a temperature limit of 400°C depends upon the presence of shrinkage cracks in the gypsum board and also the intensity of the fire **[4]**.
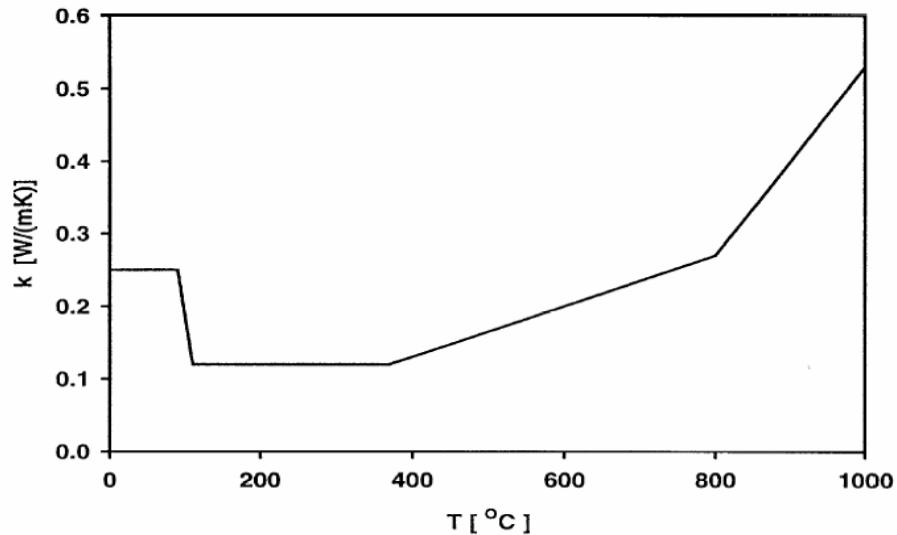
Figure 4.11 Thermal Conductivity Vs Temperature for gypsum, [4]

4.5.4.4 *Specific heat*

The specific heat of gypsum varies significantly with temperature increase **[4]**. Figure 4.12 represents the behavior of specific heat for gypsum board when subjected to high temperatures. The relationship is not linear and there is a large spike in the values during the initial heating period for temperatures in the range of 120°C to 200°C. Unfortunately, the reason for the spike was not known.
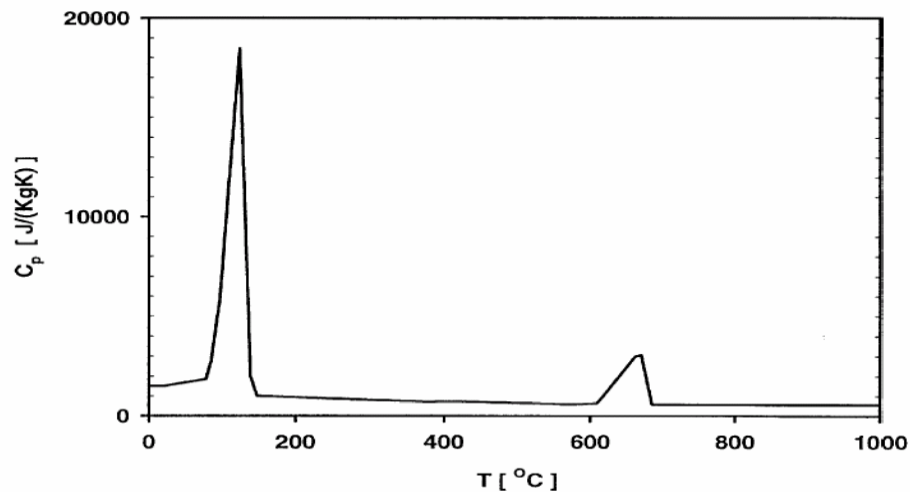
Figure 4.12 Specific Heat Vs Time for gypsum [4]

5   HEAT TRANSFER MECHANISMS

5.1   General

The science of heat transfer is an important aspect in the study of structural performance during a fire event. Heat transfer mechanisms involve numerous mathematical equations that describe the temperature distribution through a structure/material.

The mechanisms of heat transfer are:

1. Conduction
2. Convection
3. Radiation

5.2   Conduction

Conduction occurs within solids on a molecular scale without any motion of solid matter relative to one another. Figure 5.1 represents the conduction process occurring through an element of thickness Δx having constant thermal conductivity, k.
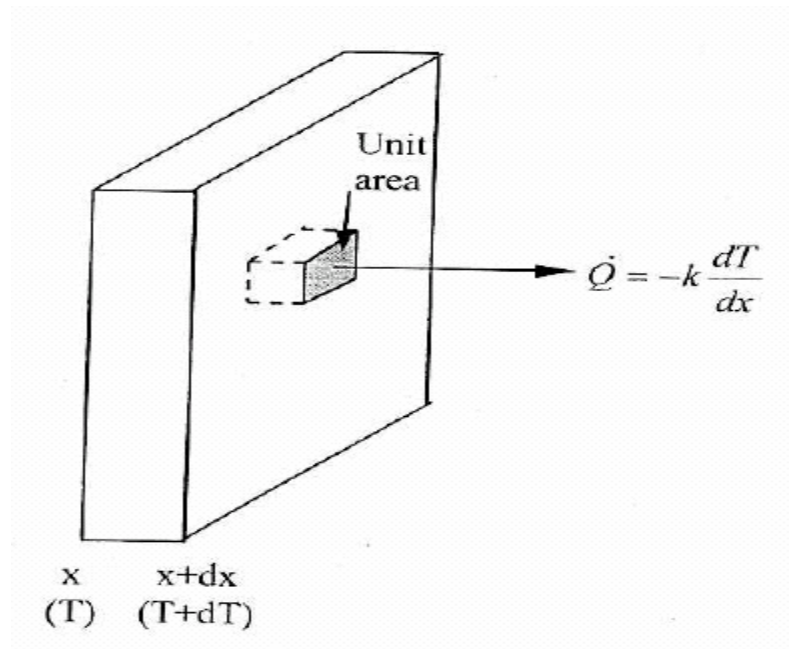
Figure 5.1 Temperature distribution with constant thermal conductivity [22], Chapter 6, p 171

The basic equation for conductive heat transfer is given by Fourier's law. The negative sign in the equation indicates that the heat flows from the higher temperature side to the lower temperature side.

$$\dot{Q} = -k\left(\frac{dT}{dx}\right)$$

- [5-1]

where, dT = temperature difference across a thickness of dx

$\dot{Q}$ = rate of heat transfer across material thickness of dx

k = thermal conductivity of material

So, for a material of thickness Δx with different temperatures T_1 and T_2 at its two faces, as shown in Figure 5.2,

$$\dot{Q} = -k\frac{(T_2 - T_1)}{\Delta x}$$

- [5-2]

5.2.1   *Boundary Conditions for one-dimensional heat conduction*

The exposed surfaces are in contact with fluids at elevated temperatures. These fluid temperatures are used as boundary conditions for determining the temperature distribution in construction element.
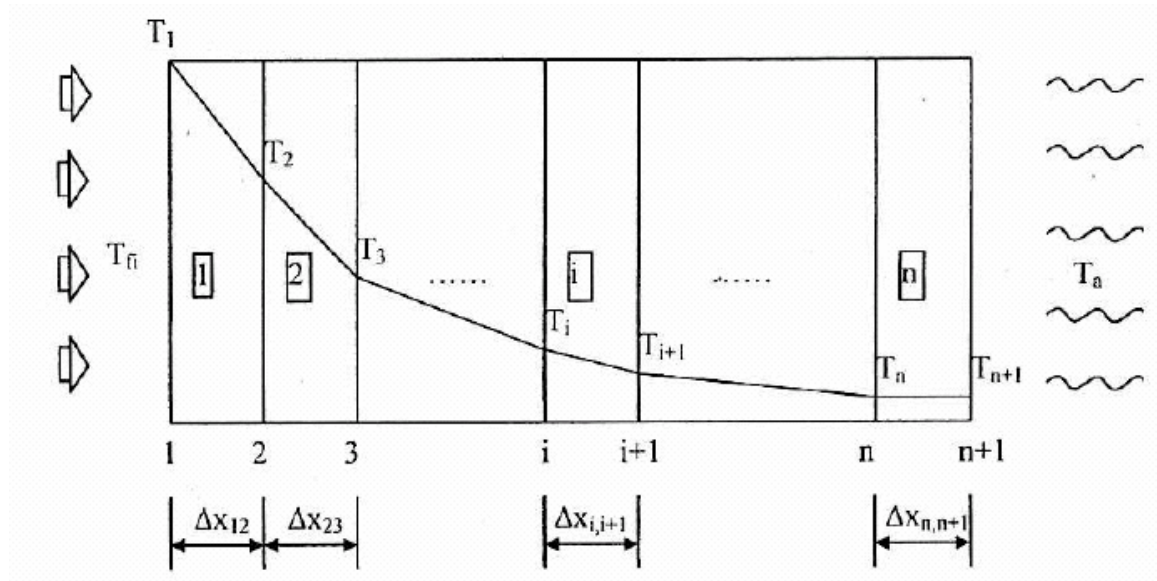
Figure 5.2 Boundary conditions for one-dimensional heat conduction [22], Chapter 6, p 174

Referring to Figure 5.2, the rate of heat transfer at the interface between the temperature T_{fi} and the material surface T_i is given by,

$$\dot{Q} = h_{fi}\left(T_{fi} - T_1\right)$$ **- [5-3]**

On the ambient air side,

$$\dot{Q} = h_a\left(T_{n+1} - T_a\right)$$ **- [5-4]**

T_{fi} = fire temperature, T_a = air temperature.

h_{fi}, and h_a are the overall surface heat exchange coefficients on the fire and air side respectively which depend on convective and radiative heat transfer.

5.3 Convection

Convection is defined as the transfer of heat by motion of or within a fluid. It may arise from temperature differences either within the fluid or between the fluid and its boundary, or from the application of an external motive force. Convection heat transfer is one of the very complex problem types in engineering science. Convection is difficult to study because it is highly unpredictable in nature, and one can only make the best effort to assume certain parameters to achieve the goal of safety from the view point of flame spread **[22].**

There are two types of flows:

1) Laminar

2) Turbulent

The type of flow would be an important area of study when the heat transfer process occurs through a fluid medium. In this case the heat transfer process occurs through the medium of air.

The study of convective heat transfer involves dimensionless numbers such as Nusselt,

$$N_u = \frac{h_c L}{k}$$ **- [5-5]**

Here, L = length of solid surface

h_c = convective heat transfer coefficient

k = thermal conductivity of fluid

There are primarily two types of convection processes,

1. Forced Convection
2. Natural Convection

The following two sections explain in detail the different convection processes.

5.3.1 Heat Transfer Coefficients for Forced Convection

Formulations as described below in Table 5-1 can be implemented to find the heat transfer coefficients for different types of flow conditions.

Reynolds number is given by,

$$R_e = \frac{\rho L U_o}{\mu}$$ - [5-6]

where, ρ = fluid density

U_o = flow velocity

μ = absolute viscosity of fluid

Prandtl Number is given by,

$$P_r = \frac{\mu C}{k}$$ - [5-7]

here, k = thermal conductivity, C = specific heat of air.

Table 5-1 Convective heat transfer coefficients for forced convection [22], Chapter 6, p 176

Flow type	Condition	Characteristic length	$Nu(=hL/k)$
Laminar flow, parallel to a flat plate of length L	$20 < Re < 3 \times 10^5$	L	$0.66 Re^{1/2} Pr^{1/3}$
Turbulent flow, parallel to a flat plate of length L	$Re > 3 \times 10^5$	L	$0.037 Re^{4/5} Pr^{1/3}$
Flow round a sphere of diameter L	General equation	L	$2 + 0.6 Re^{1/2} Pr^{1/3}$

5.3.2 *Heat Transfer Coefficients for Natural Convection*

Natural convection is caused by buoyancy forces due to density differences arising from temperature variations in the fluid. At heating the density change in the boundary layer will cause the fluid to rise and be replaced by a cooler fluid that also will heat and rise. This phenomenon is called natural or free convection. Boiling or condensing processes are also referred to as convective heat transfer processes. The heat transfer per unit surface through convection was first described by Newton, and the relation is known as the Newton's Law of Cooling.

The equation for convection can be expressed as:

$$q = \mathrm{k}AdT \qquad\qquad\qquad \textbf{- [5-8]}$$

where, q = heat transferred per unit time (W)

A = surface are for heat transfer (m²)

k = <u>convective heat transfer coefficient</u> for the process (W/m²-K or W/m²-°C)

dT = temperature difference between the exposed surface and the bulk fluid (K or °C)

Table 5-2 presents the variation in property values for air with increasing temperature. Air acts as a thermal barrier and thus provides protection to the main component or material. By modeling the thermal properties of air the process of precise model building in case of finite element techniques can be facilitated.

Table 5-2 Property values of air at atmospheric pressure, Thomas (1980) [22], Chapter 6, p 176

T(k)	ρ(kg/m^3)	C[kJ/(kg.°C)]	$\mu \times 10^5$ [kg/(m.s)]	$\nu \times 10^6$ (m^2/s)	K [W/(m·°C)]	Pr
200	1.7684	1.0061	1.3289	7.490	0.01809	0.739
250	1.4128	1.0053	1.488	9.49	0.02227	0.722
300	1.1774	1.0057	1.846	15.68	0.02624	0.708
350	0.9980	1.0090	2.075	20.76	0.03003	0.697
400	0.8826	1.0140	2.286	25.90	0.03365	0.689
450	0.7833	1.0207	2.484	28.86	0.03707	0.683
500	0.7048	1.0295	2.671	37.90	0.04038	0.680
550	0.6423	1.0392	2.848	44.34	0.04360	0.680
600	0.5879	1.0551	3.018	51.34	0.04659	0.680
650	0.5430	1.0635	3.177	58.51	0.04953	0.682
700	0.5030	1.0752	3.332	66.25	0.05230	0.684
750	0.4709	1.0856	3.481	73.91	0.05509	0.686
800	0.4405	1.0978	3.625	82.29	0.05779	0.689
850	0.4149	1.1095	3.765	90.75	0.06028	0.692
900	0.3925	1.1212	3.899	99.3	0.06279	0.696
950	0.3716	1.1321	4.023	108.2	0.06525	0.699
1000	0.3524	1.1417	4.152	117.8	0.06752	0.702
1100	0.3204	1.1600	4.44	138.6	0.0732	0.704
1200	0.2947	1.179	4.69	159.1	0.0782	0.707
1300	0.2707	1.197	4.93	182.1	0.0837	0.705
1400	0.2515	1.214	5.17	205.5	0.0891	0.705
1500	0.2355	1.230	5.40	229.1	0.0946	0.705

The general equation for Nusselt number for the case of natural convection is given by,

$$N_u = BRa^m \qquad \text{- [5-9]}$$

The values of unknowns *"B"* and *"m"* depend upon the type of flow, surface configuration, flow type and dimensions.

Ra is the Raleigh number and is given by the following equation,

$$Ra = Gr\,Pr \qquad \text{- [5-10]}$$

where, Pr is the Prandtl number (Equation 5-7), and *Gr* is known as the "Grashof number which is given by,

$$Gr = \frac{gL^3 \beta \Delta T}{v^2} \qquad \text{- [5-11]}$$

Here, g = acceleration due to gravity

β = coefficient of thermal expansion for the fluid

ΔT = temperature difference between fluid and solid surface

v = relative viscosity of the fluid

In the case of TAS models, the simulations were conducted for natural convection whereby arrays were modeled for the thermal properties of air.

5.4 Radiation

In the case of radiative heat transfer there exists the phenomena of absorptivity α, reflectivity ρ and transmissivity τ that represent the fractions of incident thermal radiation that a body absorbs, reflects and transmits, respectively.

$$\alpha + \rho + \tau = 1 \qquad \text{- [5-12]}$$

A blackbody is a perfect emitter of heat. The total amount of thermal radiation emitted by a blackbody is given by,

$$E_b = \sigma T^4 \qquad \text{- [5-14]}$$

where, σ = Stefan-Boltzmann constant = $5.67 x 10^{-8}$ W/ m^{2}K^4

T = absolute temperature in K.

For analytical purposes, the radiant thermal exchange between two blackbodies as shown in Figure 5.3, can be calculated on the basis of the following equation,

$$d \dot{Q}_{dA1 \to dA2} = E_{b1} \frac{\cos \theta_1 \cos \theta_2}{\pi r^2} dA_1 dA_2$$

where, dA_1 and dA_2 are areas of radiating and receiving surfaces respectively,

θ_1 and θ_2 are the respective angles,

E_{b1} is the thermal radiation per unit surface of A_1

r is the distance between the two surfaces.
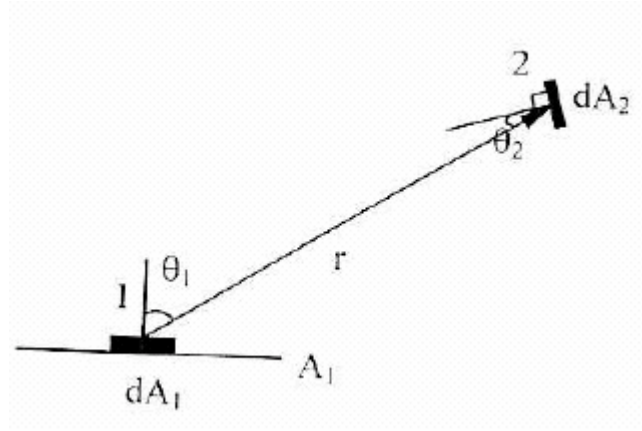
Figure 5.3 Radiant heat exchange between a finite and infinitesimal area [22], Chapter 6, p 181

5.4.1 *View Factor*

As shown in Figure 5.3, consider two surfaces A1 and dA2 where A1 is the emitting surface. The total thermal radiation from A1 to dA2 is given by,

$$Q_{A1-dA2} = \int \left(\frac{E_{b1} \cos \theta_1 \cos \theta_2}{\prod r^2} \right) d_{A1} d_{A22} = \Phi E_{b1} dA_2 \qquad \text{- [5-15]}$$

The configuration factor or view factor, Φ represents the fraction of thermal radiation from A_1 to dA_2. The configuration or view factor has a maximum value of 1.0, and it is additive in nature. For the case of a complex structure, individual view or configuration factors can be found for different elements broken down into smaller parts. The resultant view or configuration factor can then be obtained by summation of all the corresponding factors. The factor "Φ" plays an important role in numerical modeling of heat transfer as it determines the overall thermal response of structure. Radiation plays a key role as the amount of heat that is emitted from a surface contributes towards the overall fire event, and thus the temperature rise within supporting members.

6   TAS SIMULATIONS

6.1   TAS Models

This section provides an introduction to TAS modeling and the methodology behind the model development process. A model was developed for a W 12*x*27 steel beam which was the same as considered by Professor Bletzacker **[1]** for his experiments. The first step was to develop a steel model for a W 12*x*27 section by using TAS. Time dependent properties for steel were modeled as arrays for systematic simulations which helped in generating the results. The next step was to increase the complexity of the models by introducing additional elements such as concrete slab, vermiculite spray-applied insulation, and gypsum board insulation. Time-temperature data predicted by the models was compared with Professor Bletzacker's experimental results, which served as a benchmark for this thesis.

6.2   Objectives of TAS models

The objective of TAS modeling was to understand the finite element techniques and then to analyze the sensitivity of the model in terms of conduction, convection, and radiation by providing a comparison with Bletzacker's experimental results **[1]**. The objectives can be elaborated as below,

- ➢ To understand the techniques of finite element software and the features associated with TAS.

- ➢ To proceed in a step by step manner from simpler models to more complex configurations by the introduction of additional elements such as concrete slab, vermiculite, and gypsum board insulation. Different fire curves (eg. ASTM E-119 and ENV) were also considered to study their important characteristics and contribution from the view point of modeling and designing.

- ➢ To investigate and understand the nature of thermal properties of materials at elevated temperatures.

- ➢ Study analytical methods to determine their significance and evaluate the sensitivity of results in comparison with TAS models.

TAS is a user friendly and versatile model which allows the user to facilitate the design process by specifying the initial layout of nodes and then developing the brick elements. Heat was supplied to the beam through external sources in the form of convection and radiation. For all the models heat was supplied at five different locations which are described in the following section. Some of the important aspects to consider for designing a model are also described below.

6.3 Model Development

6.3.1 *Boundary nodes*

Specifying boundary nodes is a very important aspect of a model in TAS. Note, that boundary nodes are very different from boundary conditions which essentially mean displacement conditions. Boundary nodes are important in a model from the view point of heat conduction through the cross-section of the beam, and to get a sense of the stress, strain, and displacement picture in the form of color plots. For the case of a steel beam model, if no boundary nodes are specified then no heat conduction occurs and as a result the entire beam remains at a constant ambient temperature of 20°C. The reason for this is that the model behaves as if the radiative and convective heating effects occur in space with no connectivity to the steel beam. Thus, if a constant value is used, then the maximum temperature would be achieved at the first time-step without any iterative process. In this case the values were modeled as arrays based on the information obtained from standardized time-temperature curves like ASTM E-119 and ENV. For the case of steel beam protected with fire proofing material, the boundary nodes were defined at the underside face of the insulating material located in the bottom flange. Alternatively, Bletzacker's results [1] were implemented for the cases of bare steel model, and bare steel model with concrete whereby the boundary nodes were defined at the underside face of the bottom flange of unprotected steel.

6.3.2 *Run Time*

Before executing the TAS model it is very necessary that the user checks the model and corrects any errors that are identified. TAS has a built-in capability for checking the model, which is simply initiated done by clicking on the **"Check Model"** option. The run time for the model depends on the number of elements and nodes, and also on the time

step interval that has been adopted for the model through analytical calculations. The models were run on a Pentium IV processor with 512 MB RAM and 333 MHz processor speed. Large numbers of elements and nodes in a model increase the simulation time. For instance, approximately 6 to 8 hours were required for the simulation of a steel I-beam with vermiculite coating, a 4-inch thick concrete slab, and heat supplied from a total of five directions.

6.3.3 *Output*

TAS has a post-processor that compiles the results for a particular model. The results are generated in the format of a text file with an ".out" extension. This output file contains temperature data of all the nodes in the model at each time step.

6.3.4 *Plotting results*

In order to plot the results of temperature changes over time, the region of the model or nodes of interest are first selected; the results are then plotted. By double clicking the graph line, all the data points that were used for plotting can be accessed. This data similarly can be copied to different software tools for further data analyses and comparisons.

6.3.5 *Limitations*

TAS has significant limitations in terms of modeling imposed or distributed loads. The only loads that can be defined for a model are those related to gravity in three respective directions. As far as generating stress, strain and deformation results, TAS can only provide a range of minimum and maximum values for a particular time interval. TAS has the capability of generating these results through a unique solver known as GCG solver. Only color diagrams can be obtained for stress, strain and deformation results, and so it is very difficult to use TAS as an explicit tool for predicting and evaluating structural behavior at elevated temperatures. TAS was the only low-cost tool that was available for exploring the problem of thermal analyses. As an alternative use, other software such as SCINDIA or ABAQUS may help in generating fairly accurate stress results that would aid in the development of appropriate plots for the required parameters.

6.3.6 *Important Locations for study*

Throughout the thesis four locations were considered for analyzing time-temperature relationships within the steel beam. Figure 6.1 presents these different locations.
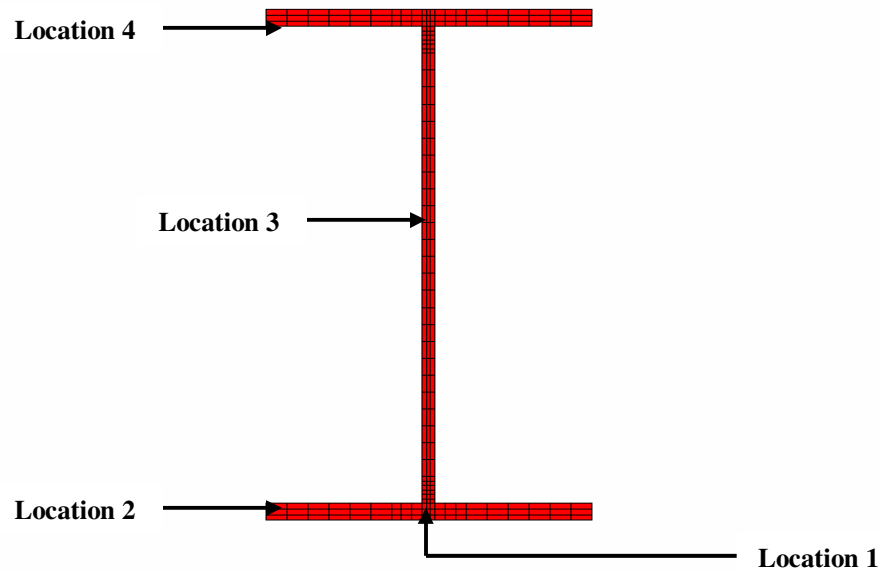
Figure 6.1 Locations in the beam

Location 1 was the region within the middle portion of the bottom flange, which has a width of *6.5″*. The thickness of the region was around *0.5″*.

Location 2 encompassed the outer face of the flange depth. Therefore, the thickness of this location was the same as the thickness of flange, which was *0.24″*.

Location 3 was referenced to the mid-height of the web from the bottom flange. The region consisted of a thickness of *0.25″ to 0.30″*.

Location 4 was the depth of the top flange. The thickness of location 4 was the same as the depth of the top flange, which in this case was *0.24″*.

6.4 Bare steel model

6.4.1 Introduction

A bare steel model was developed using finite element software TAS. The size and the dimensions for the model (Table 6-1) were the same as used by Professor Bletzacker for his experiments, which have been discussed earlier in the background literature section. The model was subjected to a time-temperature history directly from Professor Bletzacker's results **[1]** for temperatures within the bottom flange for the steel section. This initial model was analyzed solely for the purpose of observing and understanding the conduction phenomenon occurring through the section of the beam. The important parameters that were considered include the thermal conductivity and specific heat of steel, and these were modeled on the basis of the Eurocode equations **(section 4.3.4).** As previously described in **section 6.3.6**, in all TAS models, locations 1, 2, 3, 4, (Figure 6.1) were the focal points for comparing the finite element results with Bletzacker's experimental results. Figures 6.2 and 6.3 present different views for the bare steel model developed by using TAS.

Table 6-1 Sectional properties for W 12x27

BEAM PROPERTIES FOR W 12x27 SECTION								
$A\ (in^2)$	$d\ (in)$	$bf\ (in)$	$tf\ (in)$	$tw\ (in)$	$I_{xx}\ (in^4)$	$S_{xx}\ (in^3)$	$I_{yy}\ (in^4)$	$S_{yy}\ (in^3)$
7.95	11.96	6.497	0.4	0.237	204	34.2	18.30	5.63

Figure 6.2 Cross-sectional view of 2-D Steel beam(W 12x27) developed using TAS
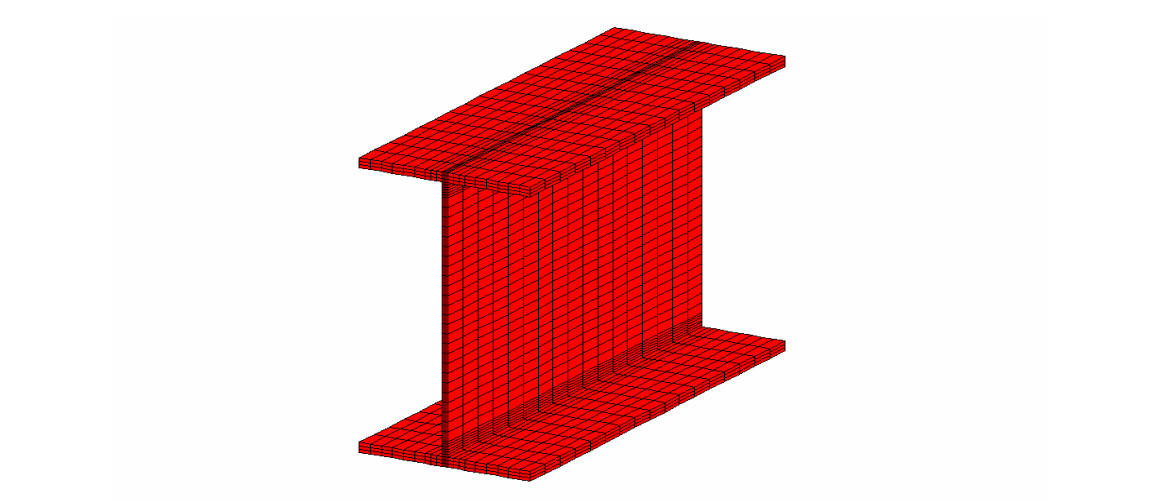
Figure 6.3 Ismoetric view of 3-D Steel beam(W 12x27) developed using TAS

6.4.2   *TAS model results*

Figures 6.4 and 6.5 present temperature Vs time graphs for different locations through the beam. These results were obtained by varying the thermal conductivity and specific heat of the steel in accordance with temperature. Figure 6.6 presents the results for all four locations on a single graph.
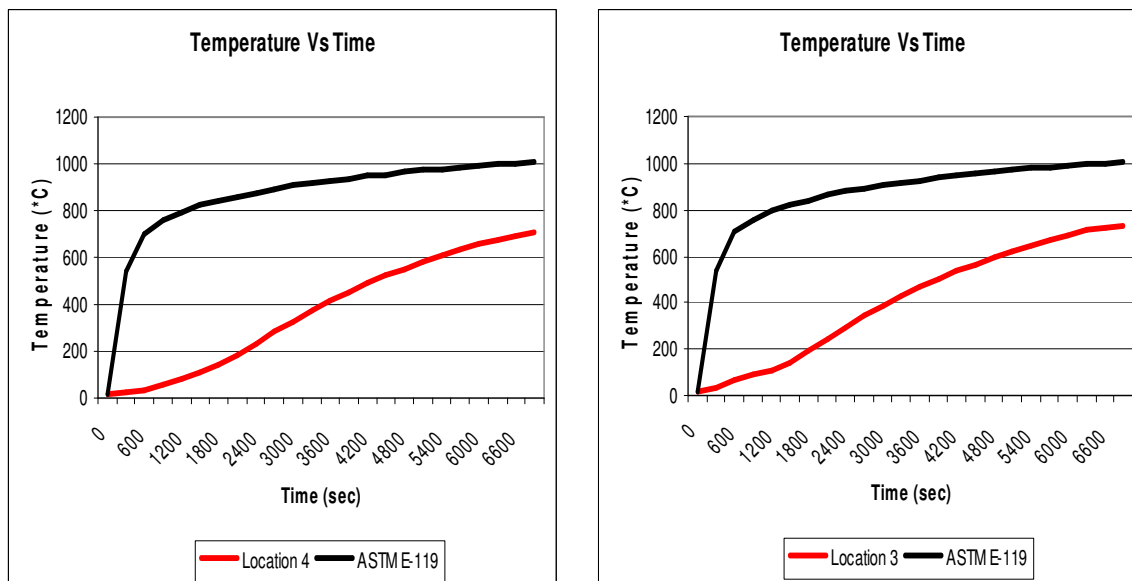
Figure 6.4 Temperature Vs Time graph for Locations 4 & 3
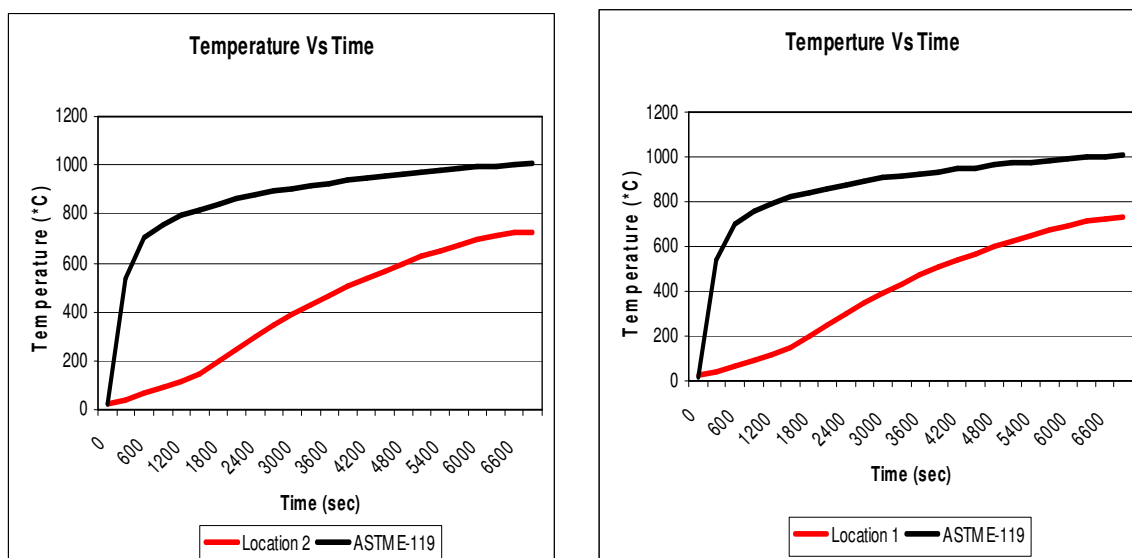
Figure 6.5 Temperature Vs Time graph for Locations 2 & 1
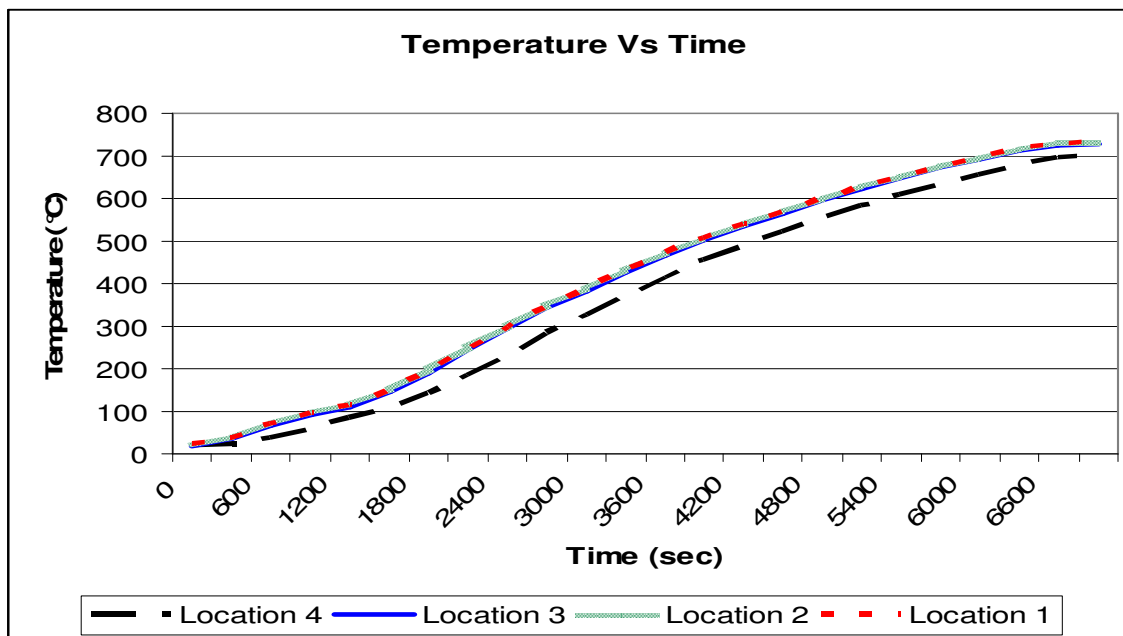
Figure 6.6 Temperature Vs Time graph for all Locations (Bare Steel Model)

6.4.3 *Results summary*

From Figures 6.4 and 6.5, it can be concluded that the model showed pretty good temperature distribution results throughout the beam when compared to the trend for ASTM E-119 curve. High temperature results were obtained for all locations, as expected due to the case of a bare steel model without any fire protection insulations. Figure 6.6 presents the results for all four locations. It was observed that there was a temperature lag between location 4 and other locations due to the fact that conduction that takes to transfer the heat from the bottom flange (location 1) towards the top flange (location 4).

6.5 Bare steel model with concrete slab

6.5.1 *Introduction*

In this case, the previous model of bare steel was extended to include a 4″ thick concrete slab over the top flange. Figure 6.7 presents an isometric view of the model with a 4″ thick concrete slab. Concrete, due to its thermal characteristics has the capability of absorbing a significant amount of heat that is directed towards the top flange of the steel section. For this reason concrete slab is also known as a "Heat Sink". The temperature of the top flange was expected to reduce drastically compared to the bare steel model, due to

the provision of the concrete slab. The reduction in the temperature of steel section reduces the thermal stresses and also improves the structural rigidity and strength of the material. The data for the time-temperature history and change of thermal conductivity and specific heat for steel remained the same as for the bare steel model. Thermal conductivity and specific heat of concrete were treated as constants for each model. The properties of concrete that were adopted for the model are shown in Table 6-2

Table 6-2 Properties of Concrete, [1], [22]

Width (ft)	Thickness (in)	Thermal Conductivity W/mK	Specific Heat J/kgK	Density Kg/m³
3	4	1.5 – 1.95	1000 -1260	2200
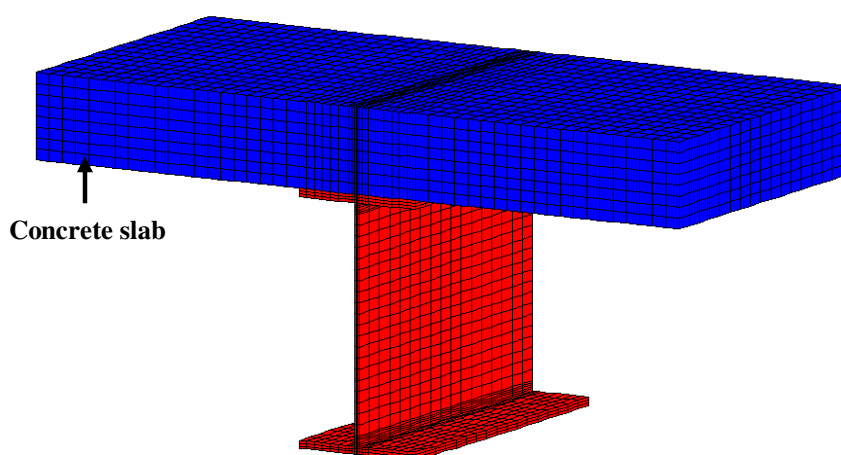
Concrete slab

Figure 6.7 Isometric view of 3-D Steel beam(W 12x27)model with 4"thick concrete slab developed using TAS

6.5.2   *TAS model results*

Figures 6.8 and 6.9 present the plots for a specific case, where the values for thermal conductivity and specific heat of concrete are 1.95W/mK and 1260J/kgK respectively.
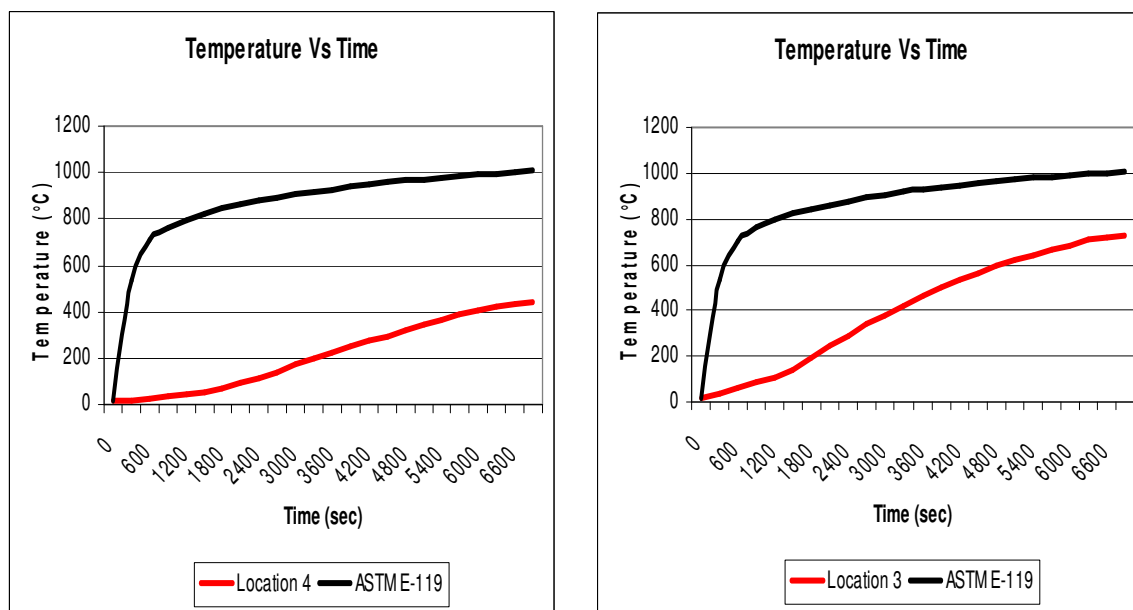
Figure 6.8 Temperature Vs Time graph for Locations 4 & 3 with 4" thick concrete slab
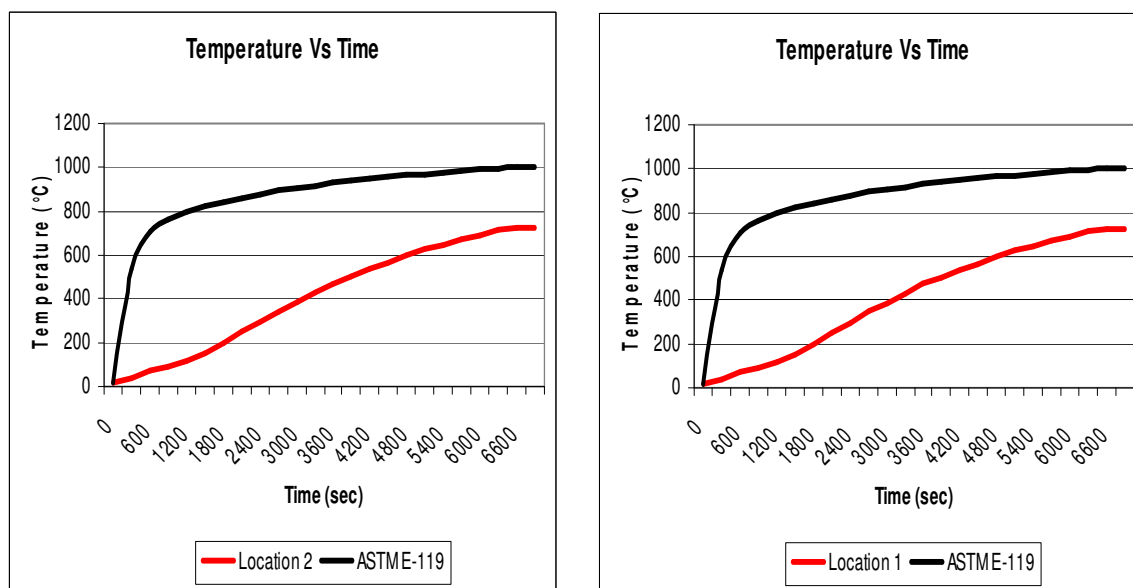
Figure 6.9 Temperature Vs Time graph for Locations 2 & 1 with 4" thick concrete slab

6.5.3 *Comparison of TAS model with Bletzacker's Experiments*

Table 6-3 provides a comparison between the results from Bletzacker's experiments **[1]** and those from the bare steel model with a 4″ thick concrete slab. Figure 6.10 presents a comparison of the results obtained from different models while Figures 6.11 and 6.12

present a comparison between Bletzacker's experimental results **[1]** and the results from bare steel with 4″ concrete slab model.

Table 6-3 Temperature data for different Locations

Location	Bletzacker's data (°C)	TAS model temperature (°C)
Location 4	465.55	443.53
Location 3	698.88	724.05
Location 2	748.88	727.64
Location 1	729.44	729.44
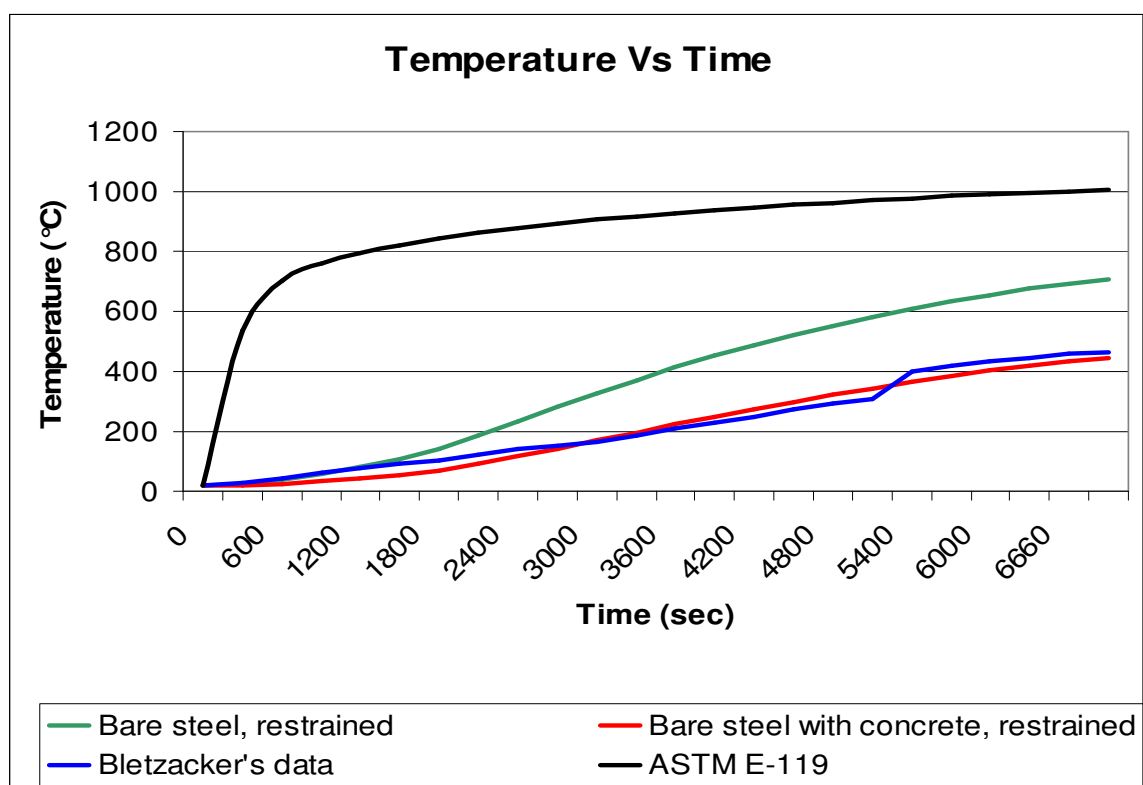
Figure 6.10 Temperature Vs Time graph for Location 4
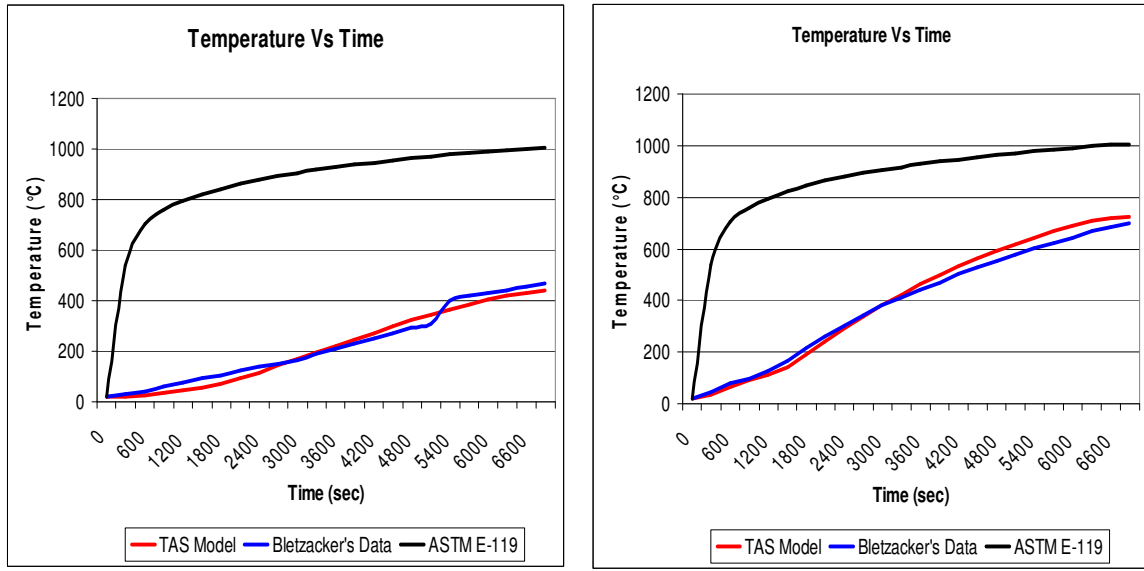
Figure 6.11 Temperature Vs Time graph for Locations 4 (left) & 3 (right)
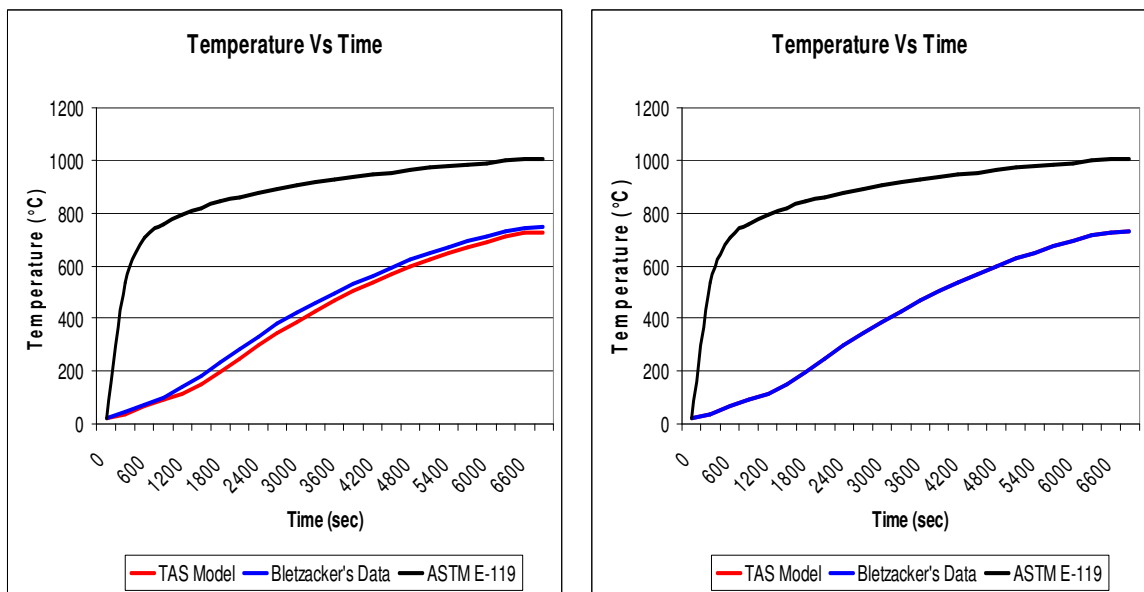
Figure 6.12 Temperature Vs Time graph for Locations 2 (left) & 1 (right)

6.5.4   *Results summary*

As, shown in Figure 6.10, the temperature for the top flange (location 4) reduces about **240°C** due to the 4″ thick concrete slab. A large amount of heat that is conducted towards the top flange of the beam gets absorbed mainly due to the thermal properties of concrete.

Also, the data obtained for location 4 shows a good correlation with Bletzacker's data **[1]**. Figures 6.11 and 6.12 present the time-temperature relationship for all locations. At all locations, the model showed good agreement with Professor Bletzacker's experimental results **[1]**. These results suggest that the overall conduction, convection and radiation within the steel beam and concrete slab were adequately modeled and suitable for further study.

6.6   Different values for Thermal conductivity

6.6.1   *Introduction*

Models were developed and simulated for different values of thermal conductivity for concrete to study the sensitivity of the temperature in the steel. As shown in Table 6-4, each case dealt with a constant value of thermal conductivity for the concrete. These constant values were selected on the basis of articles and journals that have been published and also by engineering judgment.

Table 6-4 Different values of Thermal conductivity for concrete

Case	Thermal Conductivity (W/mK)	Location 4 temperature (°C) from TAS model
Case A	1.95	443.56
Case B	1.7	455.61
Case C	1.6	460.92
Case D	1.5	466.54

6.6.2   *TAS model results*

Figure 6.13 presents the temperature Vs time plot for location 4 due to different constant values for the thermal conductivity of concrete.
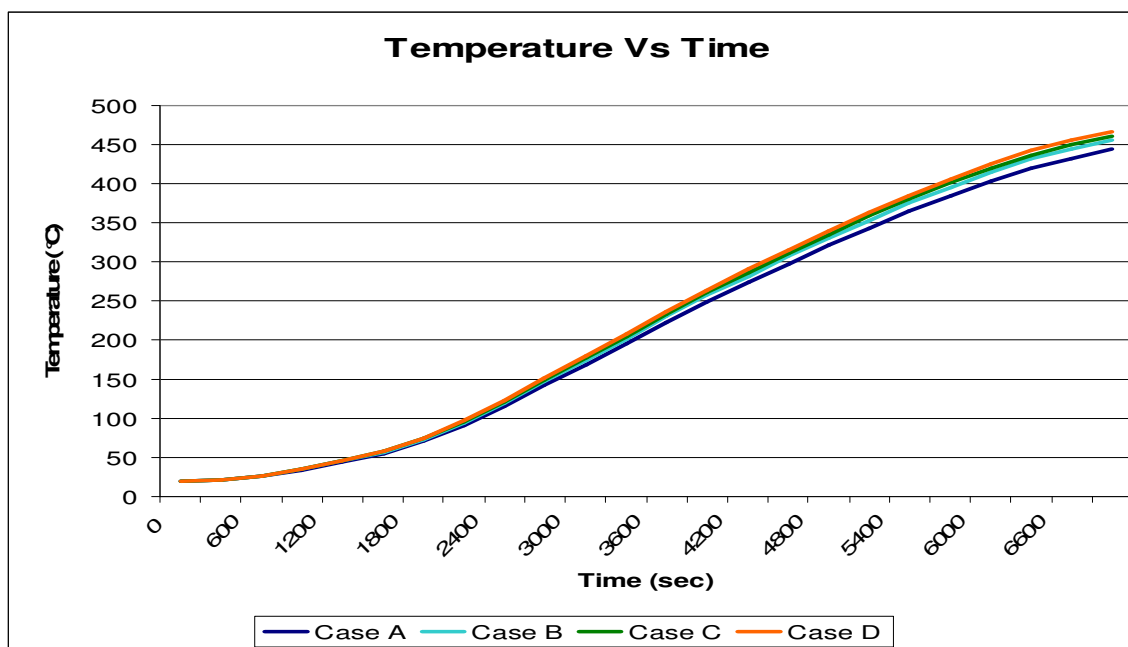
Figure 6.13 Temperature Vs Time for Location 4 due to different constant values for the thermal conductivity of concrete

6.6.3 *Results summary*

As shown in Figure 6.13, there is not much change in the top flange temperature due to different values of thermal conductivity of concrete. It was observed that a percentage change of **5.8% to 13%** for the values of thermal conductivity of concrete resulted in a **1.1% to 2.8%** change in the temperature results at location 4. From these results, it can be concluded that the temperature profile is not that sensitive due to the variation of thermal conductivity of concrete in the range of **1.5 to 1.95 W/mK**. The results were only analyzed for location 4 as the top flange was in direct contact with the slab.

6.7 Different values for Specific Heat

6.7.1 *Introduction*

The model was further exposed to study the effect of different constant values of specific heat of concrete. Again, the changes in the value of temperature for location 4 were studied. The results obtained for location 4 due to the changes made in specific heat are tabulated in Table 6-5.

Table 6-5 Different values of Specific heat for concrete

Case	*Specific heat* (**J/kgK**)	*Location 4 temperature* (°C) *from TAS model*
Case A	1023	454.30
Case B	1085	450.45
Case C	1200	443.55
Case D	1260	460.92

6.7.2 TAS model results

Figure 6.14 presents the temperature Vs time plot for location 4 due to different constant values for the specific heat of concrete.
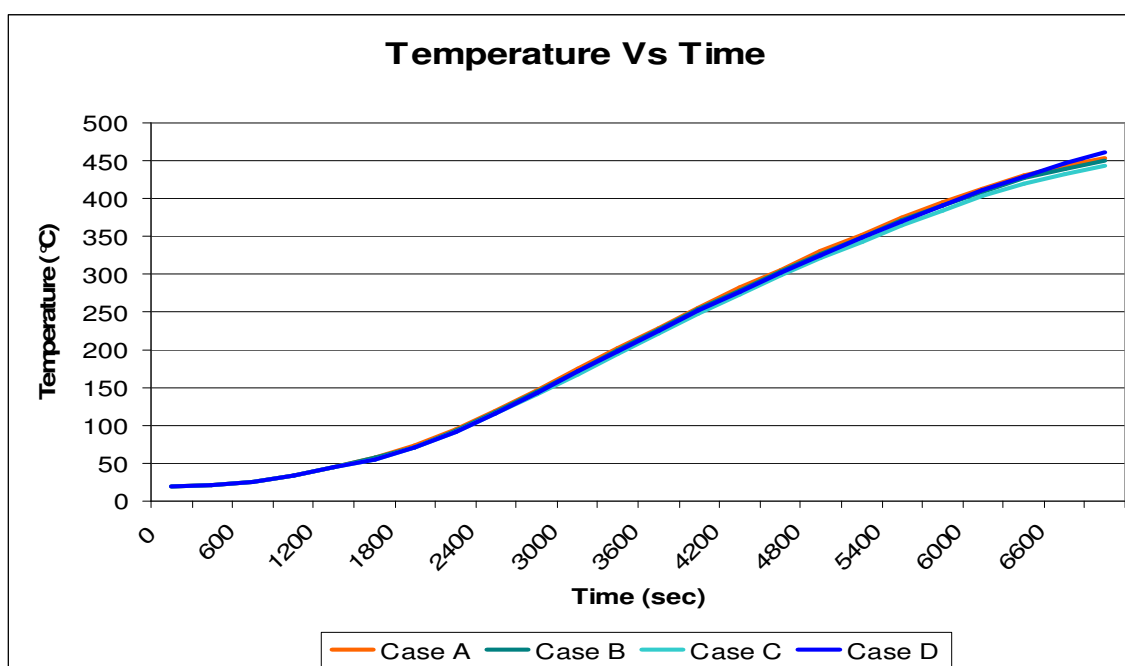
Figure 6.14 Temperature Vs Time at Location 4 due to different constant values for the specific heat of concrete

6.7.3 Results summary

As shown in Figure 6.14 there is not much change in the temperature range for location 4 due to the different values of specific heat. It was observed that a percentage change of **5.7% to 9.5%** for the values of specific heat resulted in a **1% to 4%** change for the temperature results for location 4. It can thus be concluded that the temperature profile is not that sensitive when subjected to a change in specific heat change of concrete over the range of **1023 to 1260 J/kgK**.

6.8   W12x27 steel beam with 0.5″ thick vermiculite coating

6.8.1 Introduction

The model of the W12x27 steel section with a 4″ concrete slab was extended to include a 0.5″ thick protective layer of spray-applied vermiculite coating. The first step towards simulating the performance was to use values for thermal properties of vermiculite. The next step was to conduct simulations with variable properties to investigate the sensitivity of the results and to provide a comparison with the results obtained from Bletzacker's experiments **[1]**. More details of the model development are listed in parts A and C of the Appendix.

6.8.2 W12x27 steel beam with 0.5″ thick vermiculite coating (constant thermal properties)

6.8.2.1 Introduction

The first step was to analyze the model with constant thermal properties for the vermiculite and to provide a comparison with Bletzacker's data **[1]** to estimate the lag between the two temperature- time curves. This study would aid to understand the influence of variable thermal properties which are discussed in the next section. The thermal properties of steel were the same as for the previous models while for concrete constant values of 1.95 W/mK and 1023 J/kg K were used for thermal conductivity and specific heat respectively. Figure 6.15 presents an aerial view of the model developed in TAS.
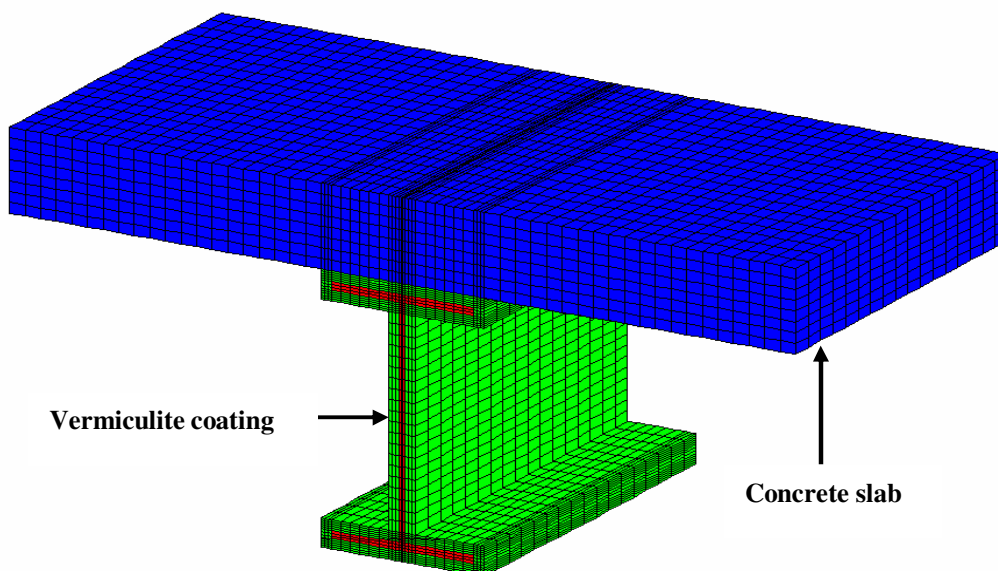
Figure 6.15 Isometric view of W 12x27 steel beam with 0.5″ thick vermiculite coating and 4″ thick concrete slab

6.8.2.2 *TAS model results*

Figures 6.16 and 6.17 present the temperature Vs time plots for W12*x*27 steel beam protected with 0.5″ thick vermiculite coating having constant thermal properties.
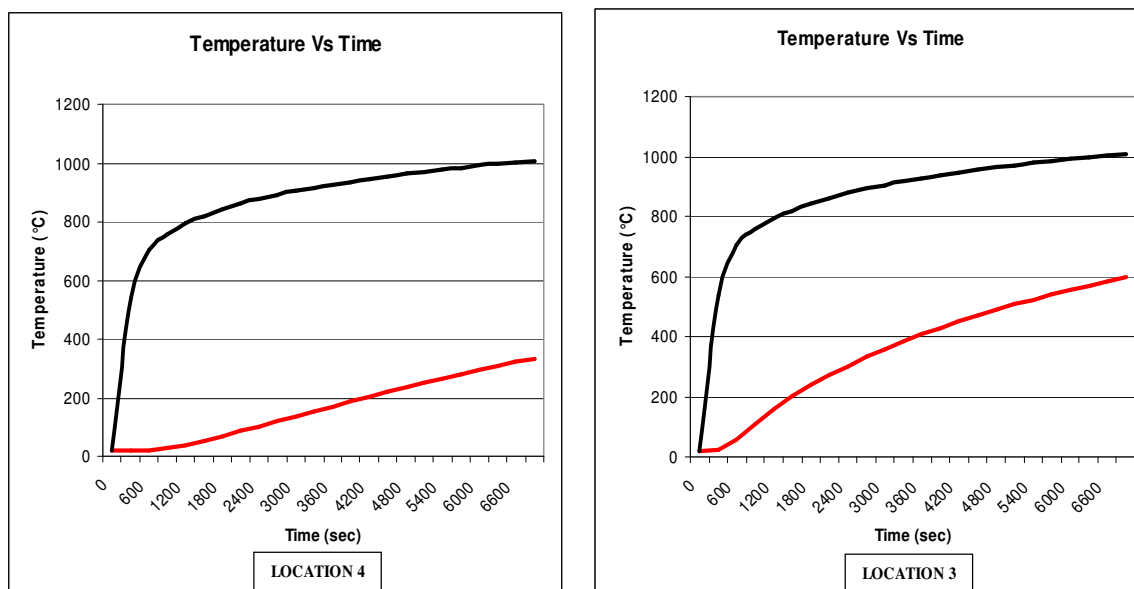
Figure 6.16 Temperature Vs Time graph for Locations 4 (left) & 3 (right)
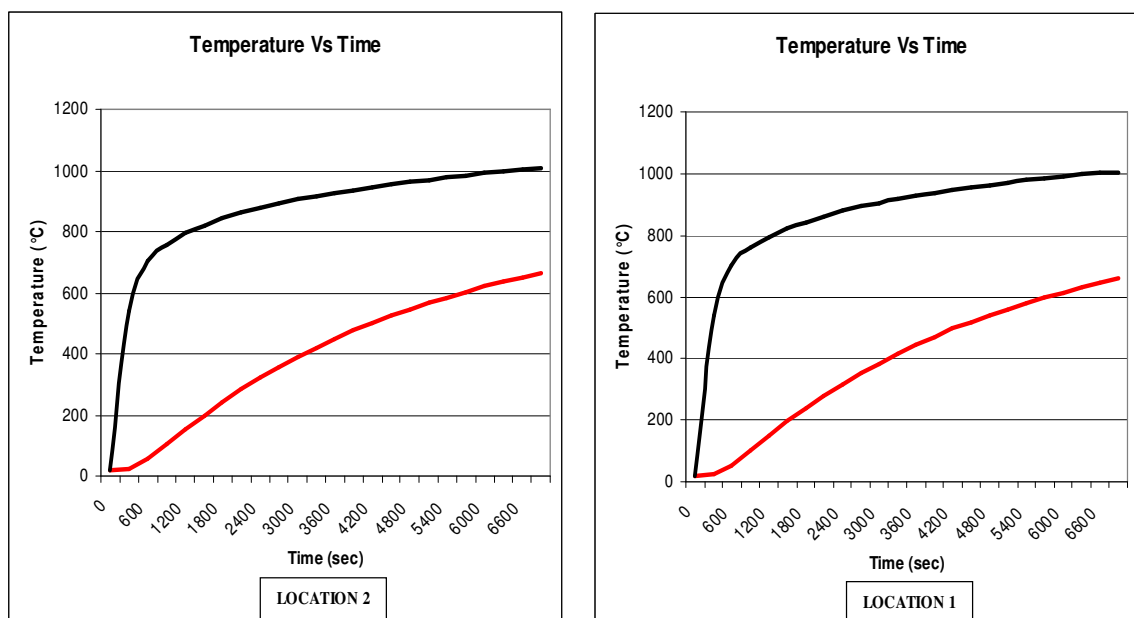
Figure 6.17 Temperature Vs Time graph for Locations 2 (left) & 1 (right)

6.8.2.3 *Comparison of results obtained from TAS model and Bletzacker's Data*

Figures 6.18 and 6.19 present the comparison of results from Bletzacker's data **[1]** and TAS model for vermiculite coating.
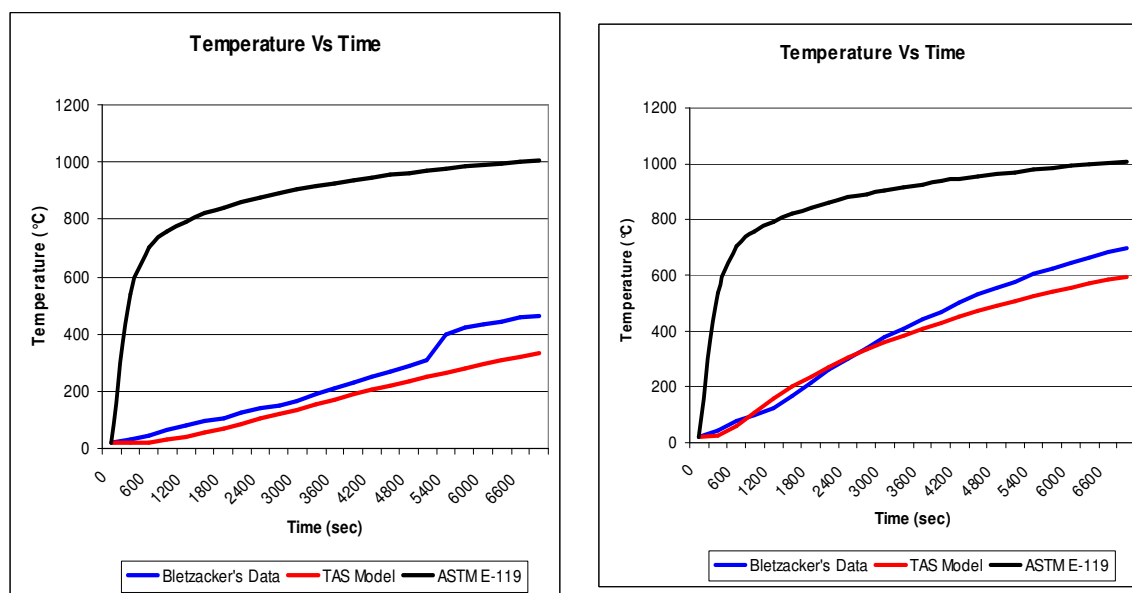
Figure 6.18 *Comparison of Temperature Vs Time data from different models for Locations 4 (left) & 3 (right)*
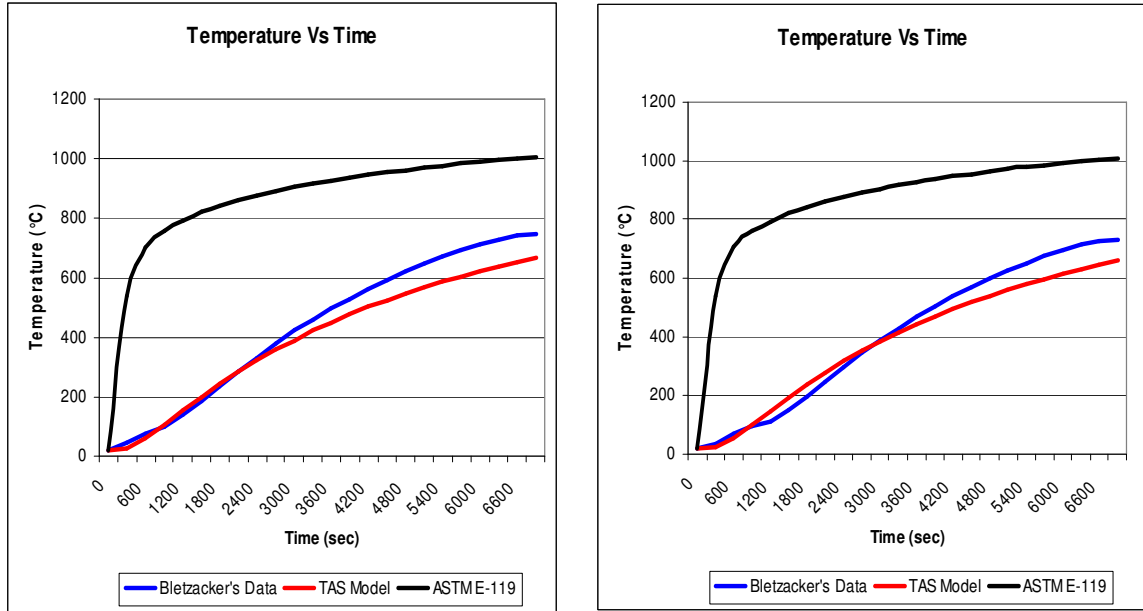
***Figure 6.19 Comparison of Temperature Vs Time data from different models for
Locations 2 (left) & 1 (right)***

6.8.2.4 *Results summary*

From Figures 6.18 and 6.19 it was observed that there was a temperature lag between the
results from TAS model with constant thermal properties for vermiculite and
Bletzacker's results **[1].** This was mainly due to the constant thermal properties for
vermiculite which is not the case in real life. It can be mentioned at this point that it
becomes very important to model thermal properties of vermiculite as an array in order to
achieve reasonable results.

6.8.3 *W12x27 steel beam with 0.5" thick vermiculite coating (variable thermal properties)*

6.8.3.1 *Introduction*

The basic model was the same as for the previous case involving constant thermal
properties of vermiculite, the only difference being that the thermal properties of
vermiculite were input as a temperature-dependent. The thermal properties of steel were
the same as for the initial model of bare steel while for concrete constant values of 1.95

W/mK and 1023 J/kg K were used for thermal conductivity and specific heat respectively. As previously described in **Chapter IV, section 4.5.3.3**, for vermiculite the results from the tests were only available up to a temperature limit of **400°C to 450°C**. For further assessment of thermal properties beyond this temperature limit, the technique of curve fitting was adopted. Different arrays were modeled to have a sense of the impact that would occur due to the changes in thermal characteristics for vermiculite. The thermal properties data for vermiculite have been discussed and presented in parts A and C of the Appendix.

6.8.3.2 *TAS model results*

Figures 6.20 and 6.21 present the results for a W 12*x*27 steel beam with 0.5″ thick vermiculite coating having variable thermal properties.
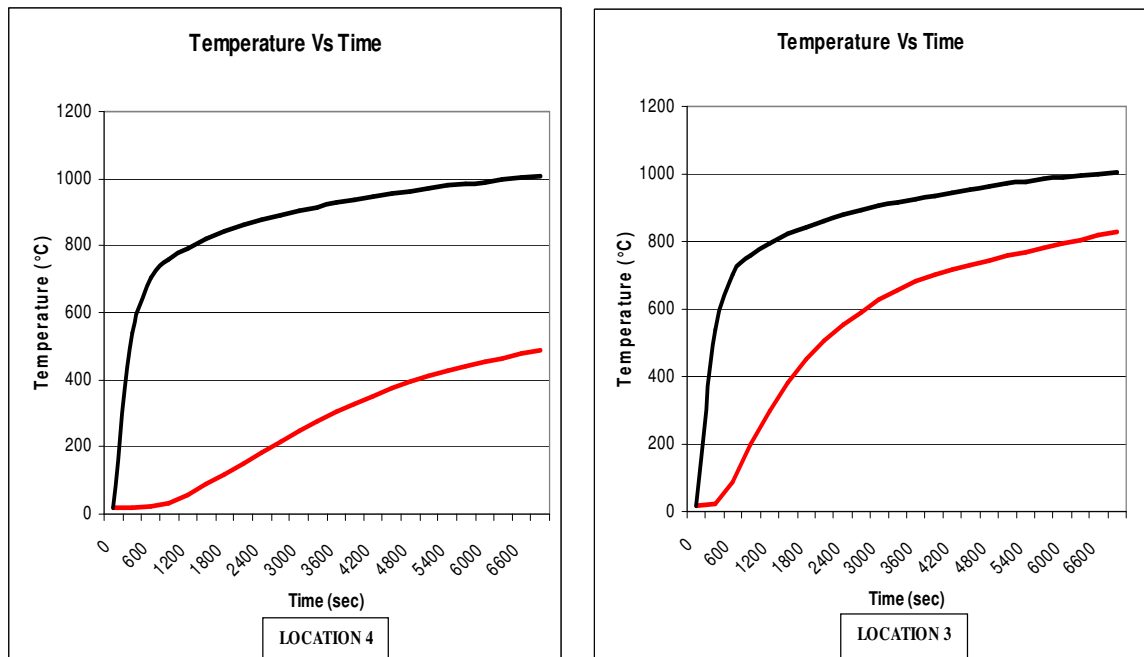
Figure 6.20 Temperature Vs Time for Locations 4 (left) & 3 (right)
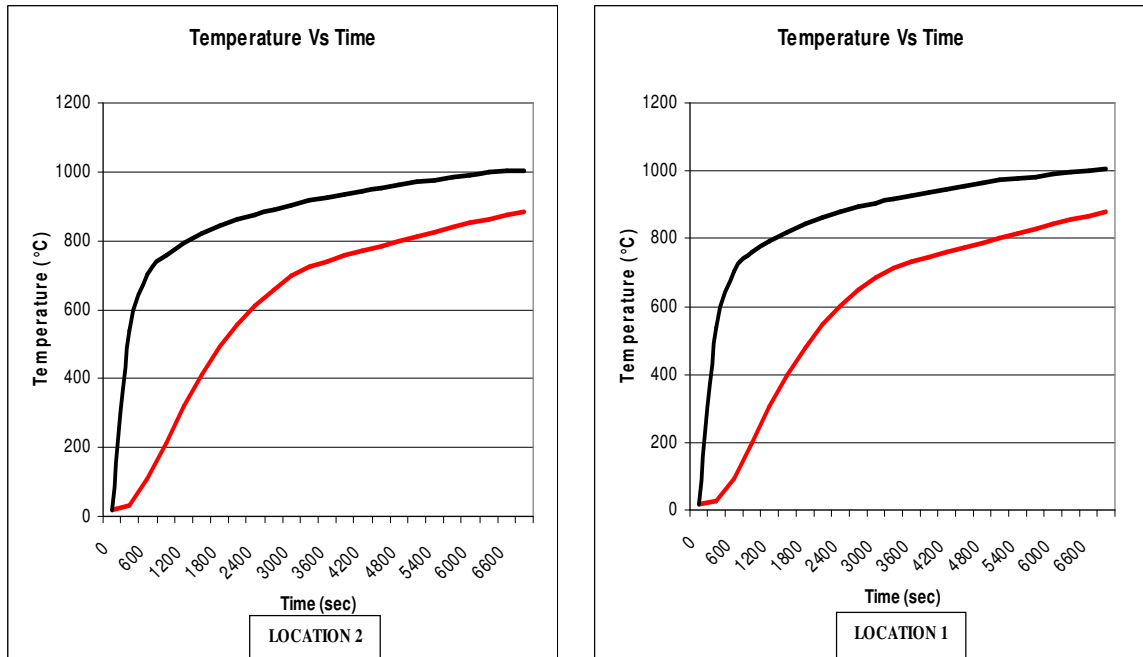
Figure 6.21 Temperature Vs Time for Locations 2 (left) & 1 (right)

6.8.3.3 Comparison of results from different models
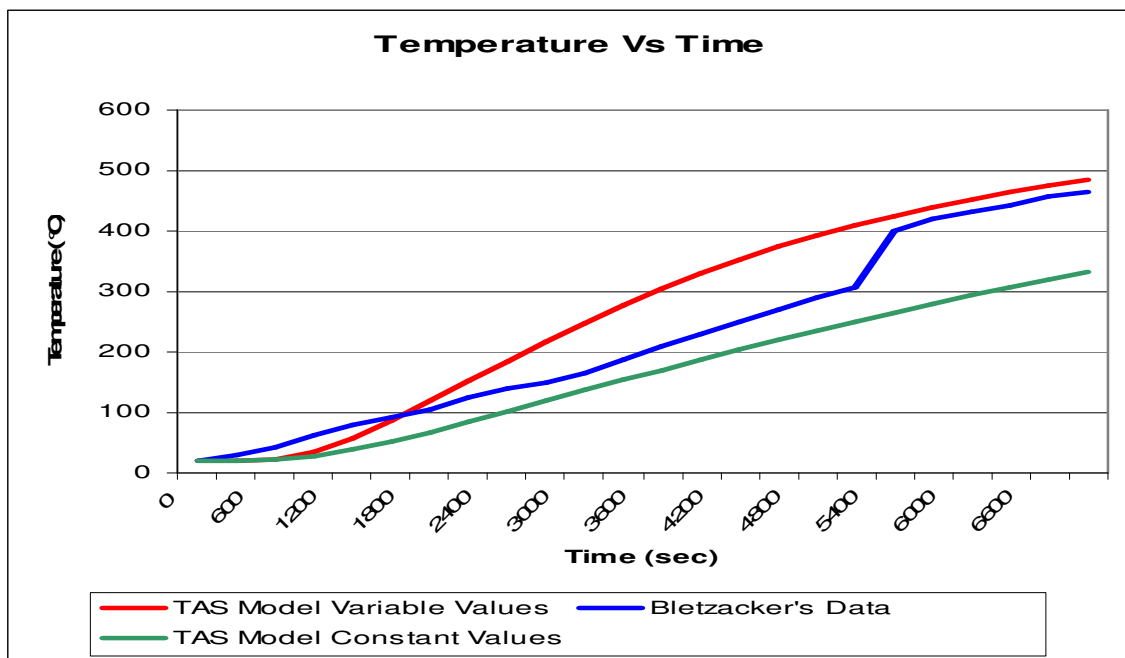
Figure 6.22 Comparison of Temperature Vs Time data from different models for Location 4
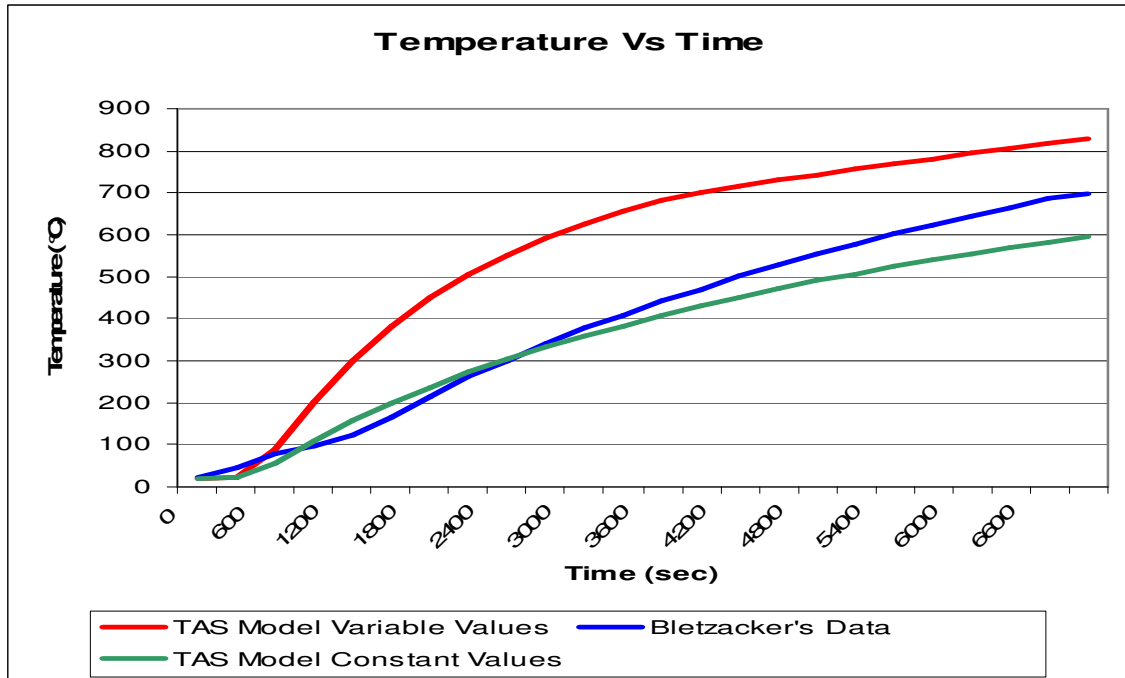
Figure 6.23 Comparison of Temperature Vs Time data from different models for Location 3
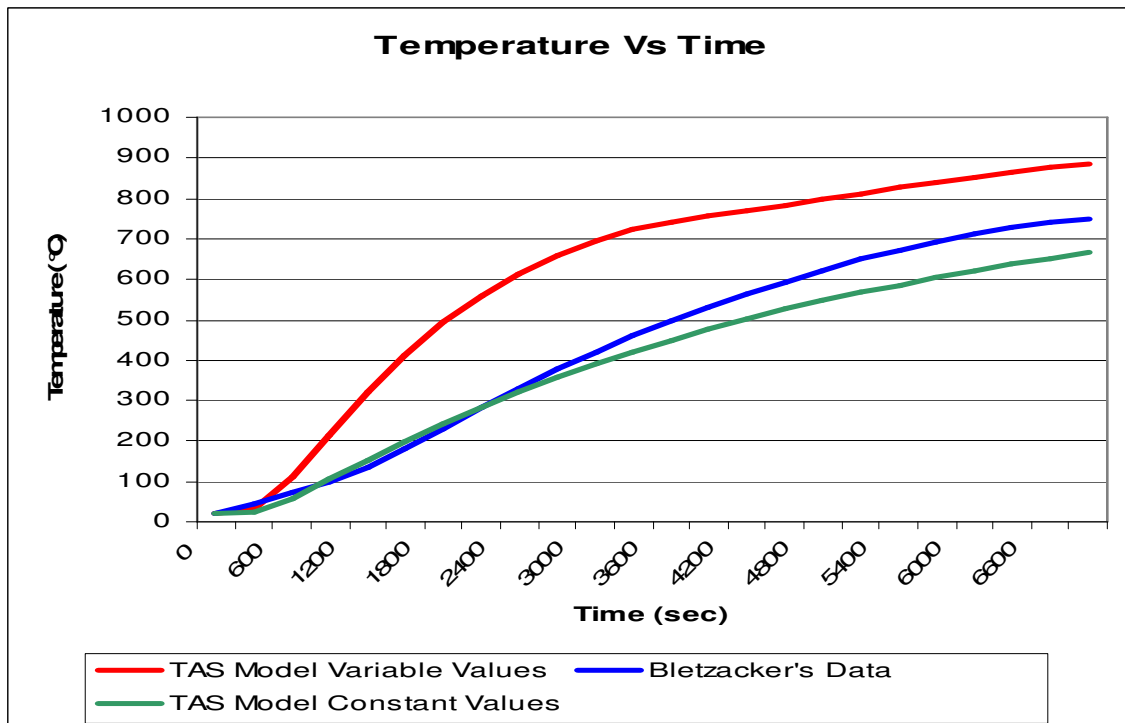
Figure 6.24 Comparison of Temperature Vs Time data from different models for Location 2

Temperature Vs Time
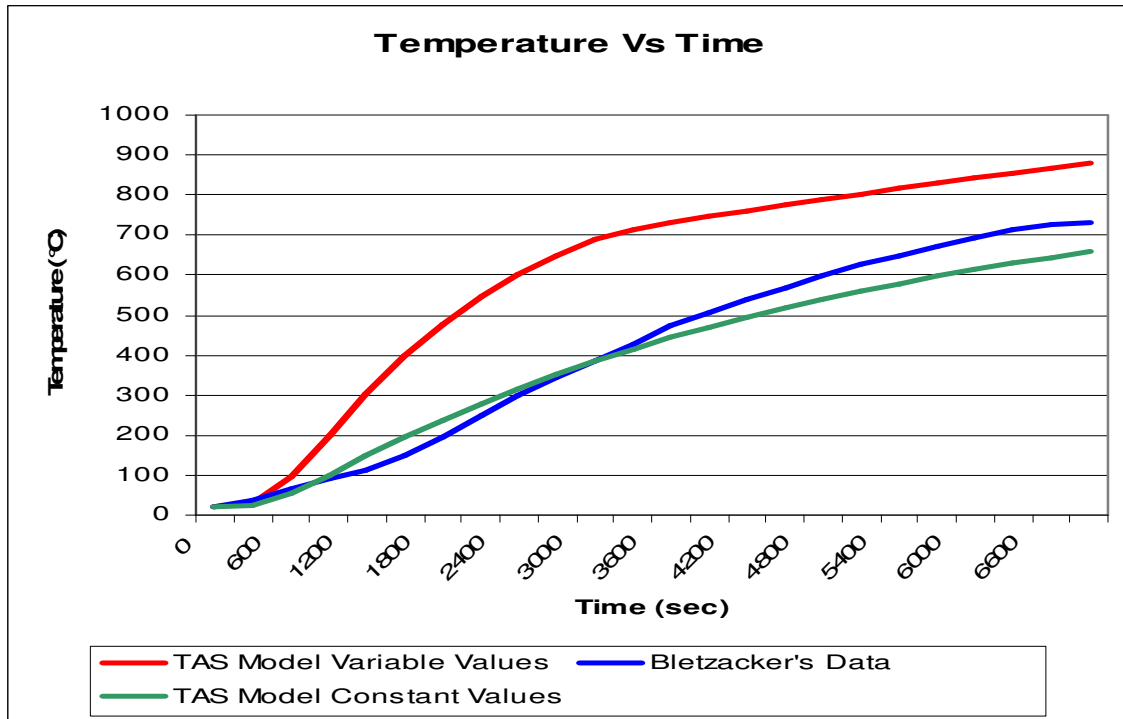
Figure 6.25 Comparison of Temperature Vs Time data from different models for Location 1

6.8.3.4 *Results summary*

Figures 6.20 and 6.21 present the time-temperature plots for the rise in steel temperature for different locations. A better understanding can be obtained from Figures 6.22 to 6.25 which present a comparison with Bletzacker's data **[1]**. From Figures 6.24 and 6.25, it can be concluded that for locations 1 and 2 the temperature rise in steel was pretty high as compared to Bletzacker's data **[1]** which could be attributed to the non-availability of thermal properties data above 450°C. If the thermal properties for vermiculite are established for higher temperatures then the results might be different from those that were obtained for this model. Thermal characteristics might show a non-linear behavior above 450°C unlike the assumption of linear interpolation above 450° C. It can also be suggested at this point that more research is needed on thermal properties of vermiculite due to its variable composition of cementitious material which makes it more difficult to estimate concrete results for the purpose of finite element modeling. These results may show a lot of variation due to the fact of quality standards and mix that are used by a particular manufacturer.

6.9   W12x27 steel beam with 5/8″ thick gypsum board coating

6.9.1   *Introduction*

The W12*x*27 steel section was modeled along with a 5/8″ thick protective enclosure of gypsum board. The thermal properties of steel were the same as for the initial model of bare steel while for concrete constant values of 1.95 W/mK and 1023 J/kg K were used for thermal conductivity and specific heat respectively. The first step towards modeling a W12*x*27 beam with gypsum enclosure was to simulate the TAS model with constant thermal values for gypsum through out the entire run time of the simulation. The next step was to simulate the model with variable thermal properties for gypsum, to investigate the sensitivity of the results and to provide a comparison with the results obtained from Bletzacker's experiments [1]. More details of the model development are listed in parts A and D of the Appendix.
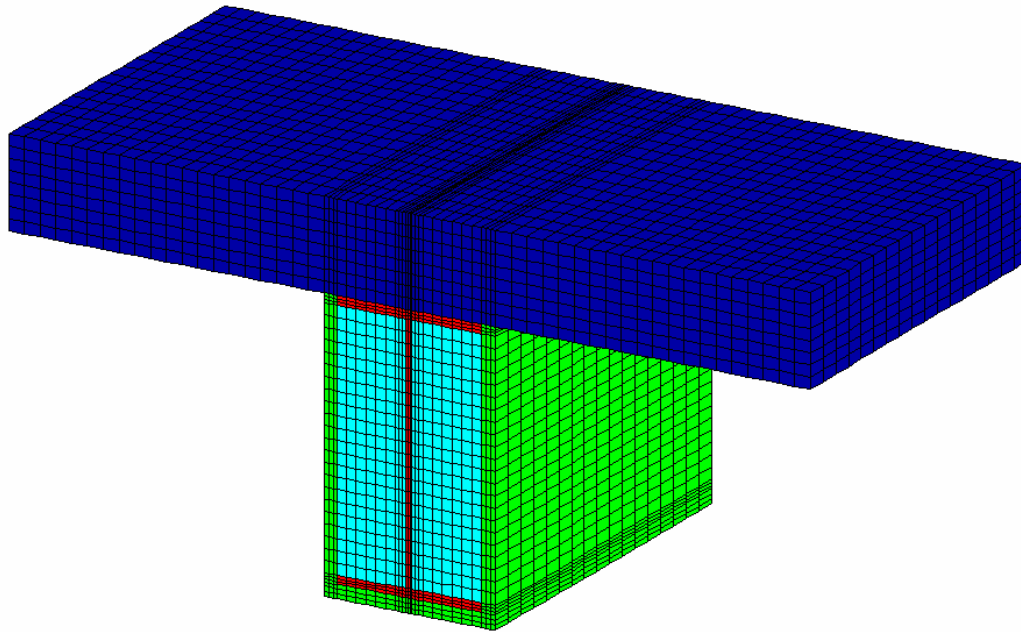
Figure 6.26 Isometric view of W 12x27 steel beam with 5/8" thick gypsum board enclosure and 4" thick concrete slab

6.9.2 *W12x27 Steel beam with 5/8" thick Gypsum Board Enclosure (constant thermal properties)*

6.9.2.1 *Introduction*

The first step was to analyze the model with constant thermal properties for the gypsum insulation. This study would aid to provide a comparison between models with constant against variable properties which is discussed in the next section.

6.9.2.2 *TAS model results*

Figures 6.27 and 6.28 present the results from TAS model for gypsum with constant thermal properties.
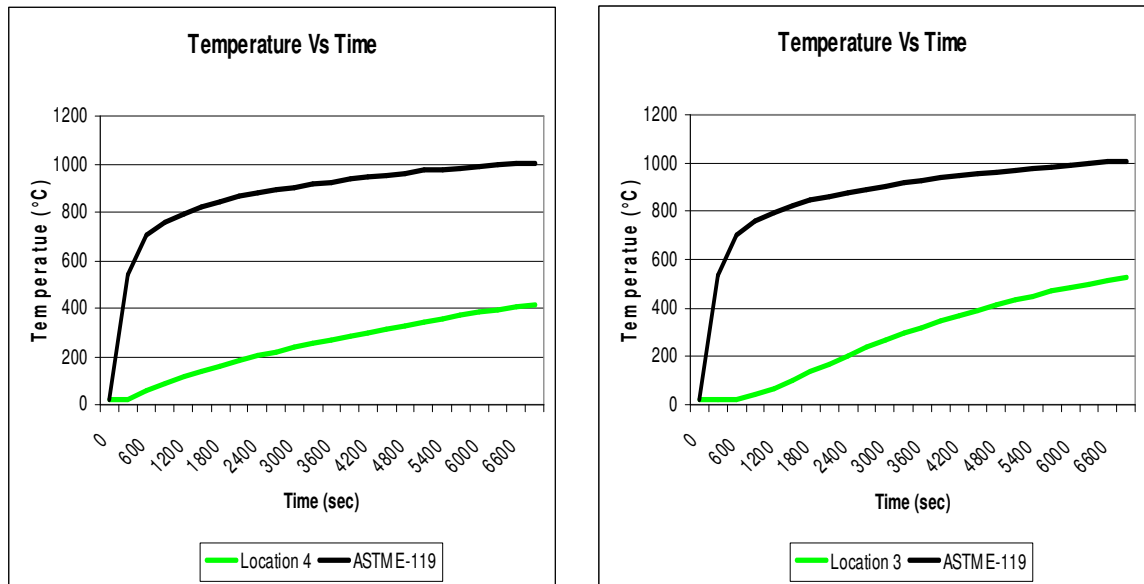
Figure 6.27 Temperature Vs Time for Locations 4 (left) & 3 (right)
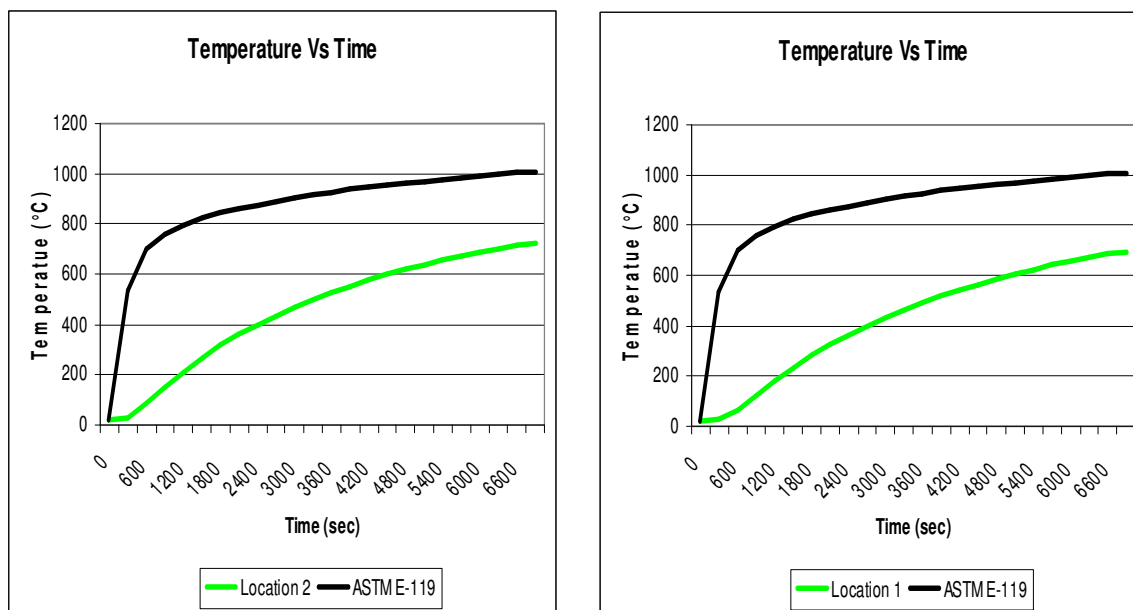
Figure 6.28 Temperature Vs Time for Locations 2 (left) & 1 (right)

6.9.3 W12x27 steel beam with 5/8″ thick gypsum board enclosure (variable thermal properties)

6.9.3.1 Introduction

The basic model was the same as for the previous case of constant properties of gypsum, the only difference being that the thermal properties of the insulated board were temperature dependent. The thermal properties of steel were the same as for the initial model of bare steel while for concrete constant values of 1.95 W/mK and 1023 J/kg K were used for thermal conductivity and specific heat respectively. The thermal properties that were used for gypsum board are contained in parts A and D of the Appendix.

6.9.3.2 TAS model results

Figures 6.29 and 6.30 present the temperature Vs time plots for the case of W12x27 steel beam protected with a 5/8″ thick gypsum board enclosure having constant thermal properties.
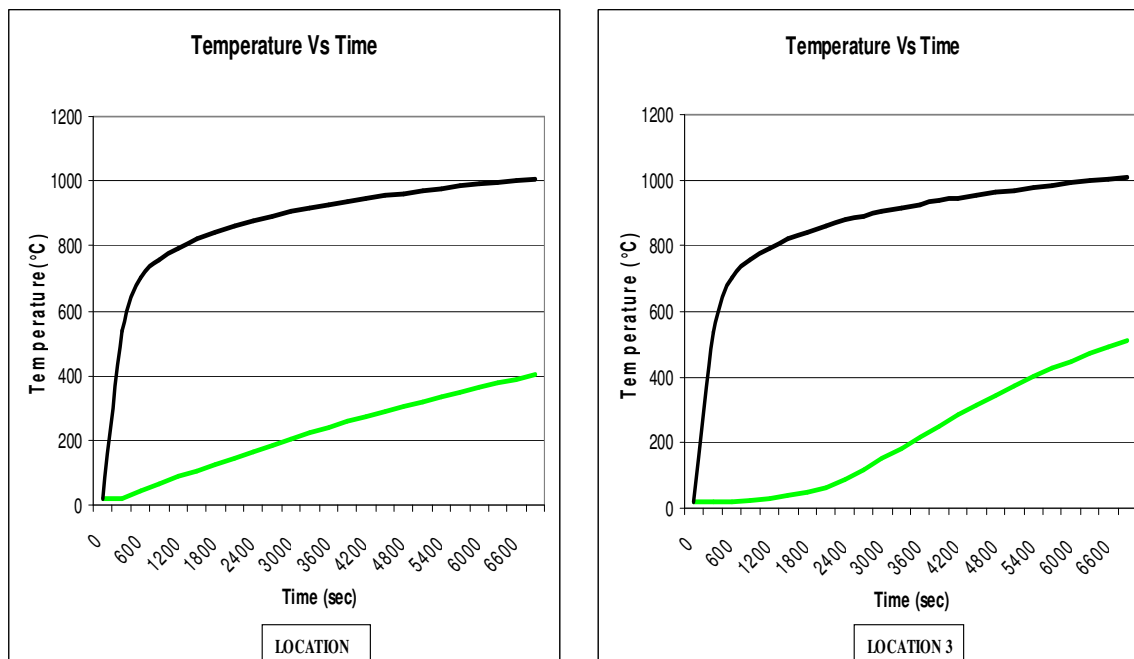
Figure 6.29 Temperature Vs Time for Locations 4 (left) & 3 (right)
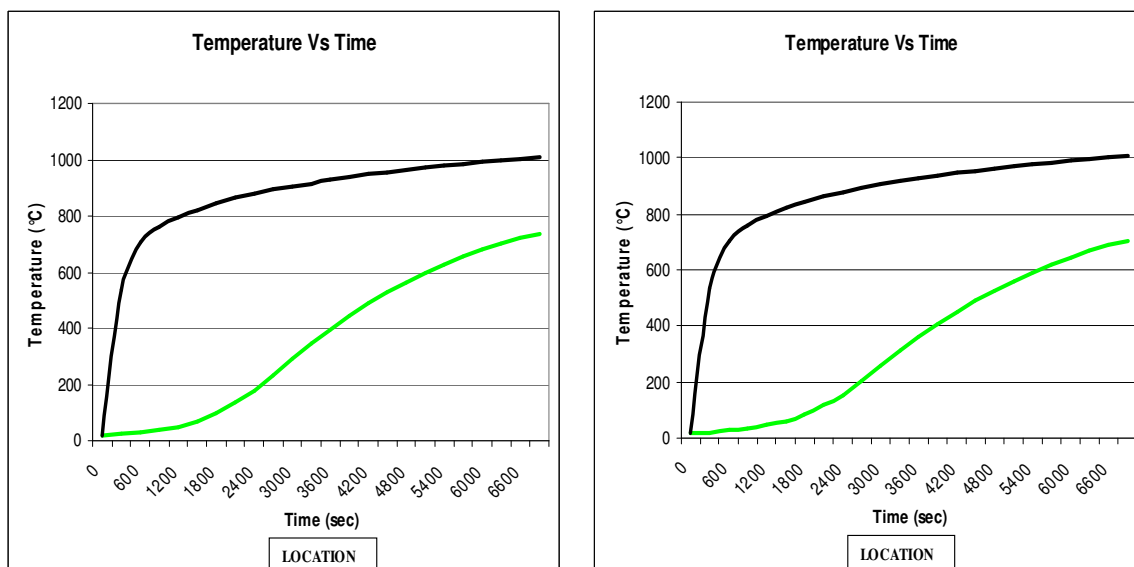
Figure 6.30 Temperature Vs Time for Locations 2 (left) & 1 (right)

6.9.3.3 *Comparison of results from different models*

Figures 6.31 to 6.34 present the comparison of results from vermiculite coating and gypsum board enclosure for a W 12*x*27 beam and their significance in comparison with Bletzacker's data.
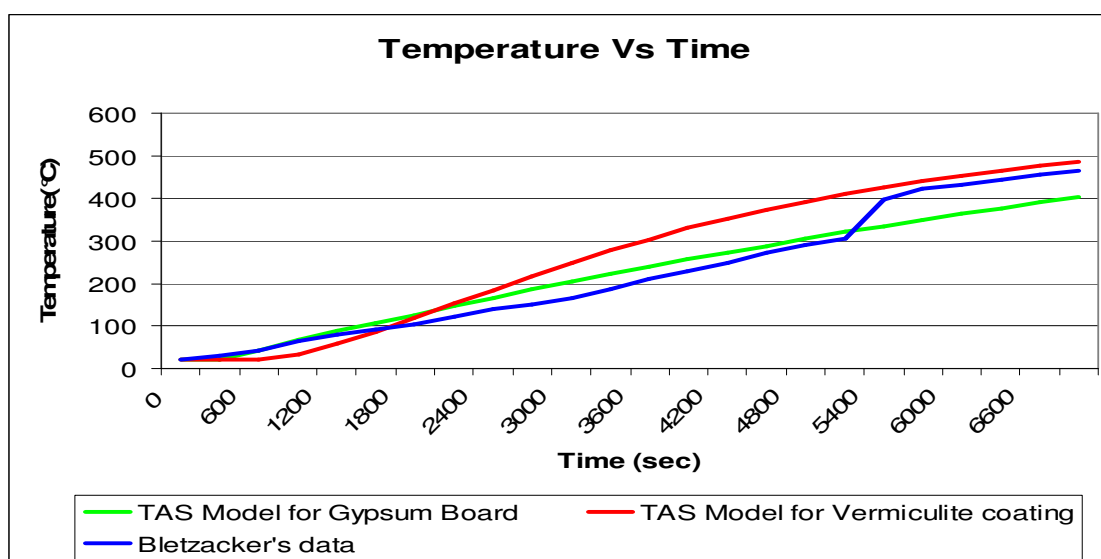
Figure 6.31 Comparison of Temperature Vs Time data from different models for Location 4
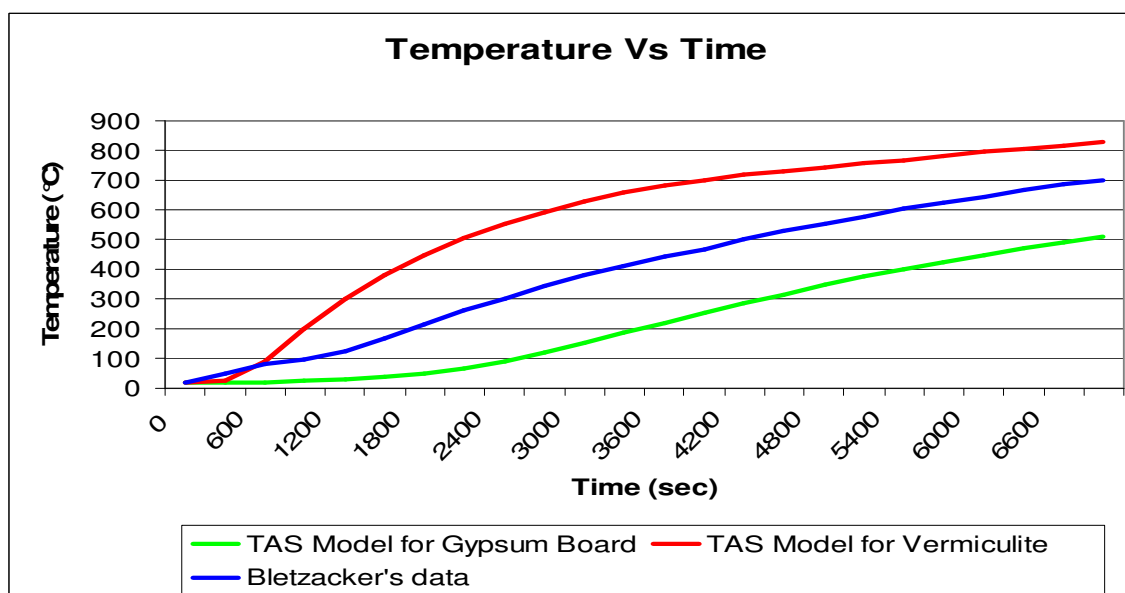
Figure 6.32 Comparison of Temperature Vs Time data from different models for Location 3
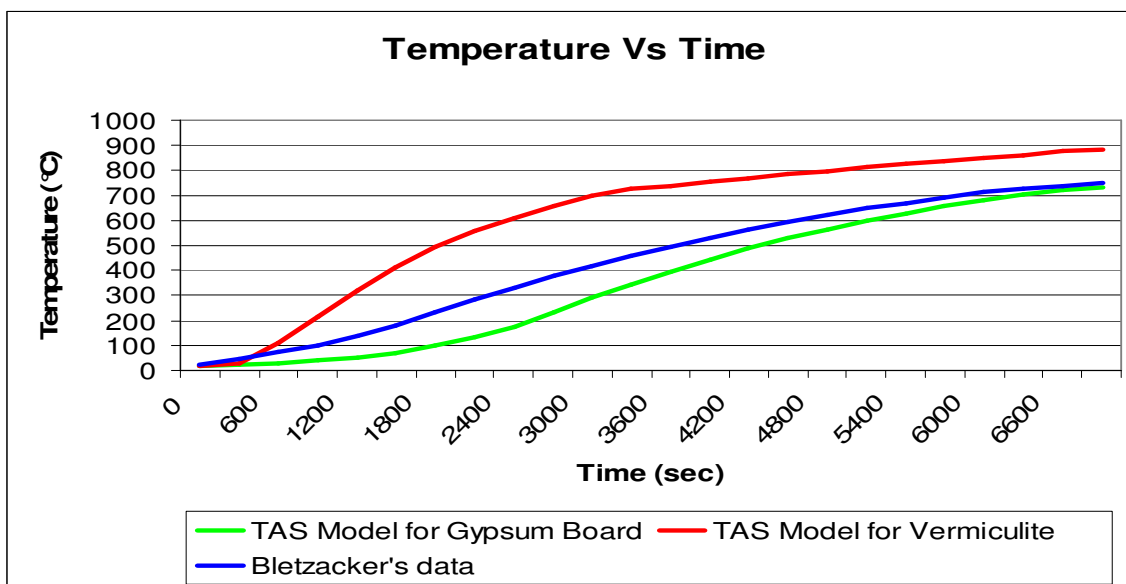
Figure 6.33 Comparison of Temperature Vs Time data from different models for Location 2
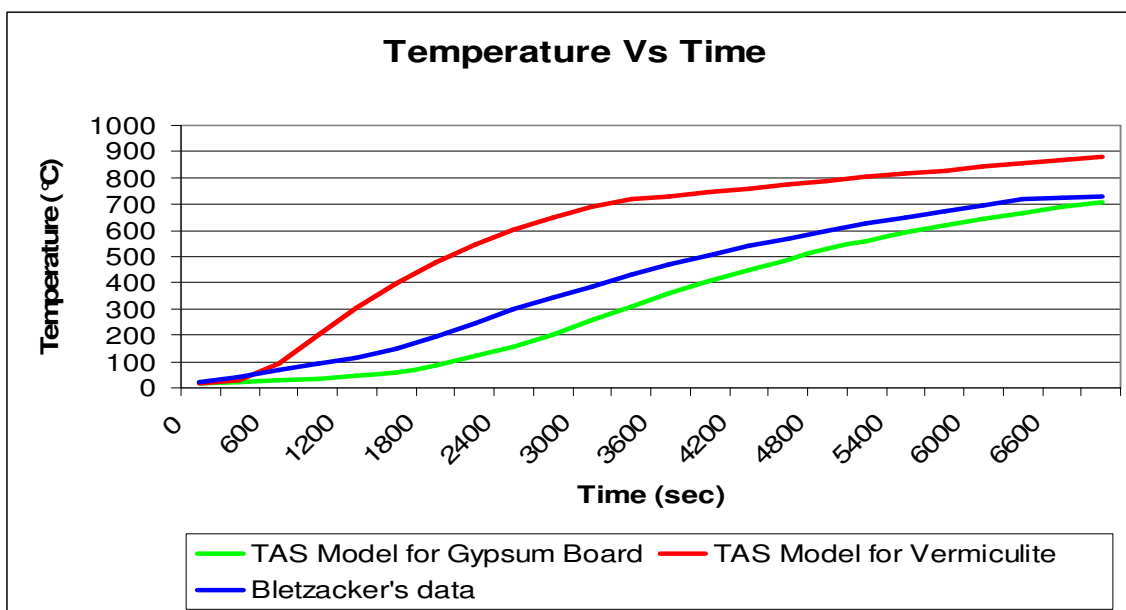
Figure 6.34 Comparison of Temperature Vs Time data from different models for Location 1

6.9.3.4 *Results summary*

From Figures 6.29 and 6.30, it is readily seen that there is a decrease in temperature of steel when gypsum board is used as a fire protective material. Further, Figures 6.31 to 6.34 present a comparison between results obtained from the gypsum model, vermiculite model and Bletazacker's data **[1]**. The temperature profile in the steel for gypsum board is about **20% to 30%** lower as compared to the steel temperature when vermiculite coating is used. These comparisons help in concluding that gypsum board gives a better performance as compared to vermiculite. Also, one should understand that the thermal properties of gypsum board have been defined for temperatures upto the range of **1300°C to 1500°C [4],** which makes it easier to model the high temperature performance of gypsum board as compared to vermiculite.

6.10 W12*x*27 steel beam with 0.5″ thick vermiculite coating subjected to ENV fire curve

6.10.1 *Introduction*

The model developed previously for the case of 0.5″ thick vermiculite coating was subjected to ASTM E-119 fire curve. In an actual fire the time-temperature curve is defined mainly by two phases, known as growth phase and decay phase. The ASTM E-119 curve shows a steep increase in temperature with time, while the ENV curve illustrates both a growth and a decay period for the fire. It is thus essential to study the behavior of steel when subjected to different fire curves in order to determine the sensitivity of the thermal response to the temperature profile for the environment. For this reason, the TAS models were analyzed through application of the ENV time-temperature history. As listed below, three different scenarios were studied with the ENV curve,

Case 1: Maximum fire temperature of 892°C occurring at 56 minutes
Case 2: Maximum fire temperature of 850.95°C occurring at 35.35 minutes
Case 3: Maximum fire temperature of 947.84°C occurring at 102 minutes

The three cases for fire curves were established by varying the opening factor "F" within the range of 0.055 to 0.068. The formulas that were used for determining the necessary parameters have been described in **Chapter 3, section 3.5.** A detailed time-temperature history has been presented in part E of the Appendix.

6.10.2 *TAS model results*

Figures 6.35 and 6.36 present the results for Case 1, where the maximum fire temperature of 892° C occurred at 56 minutes.
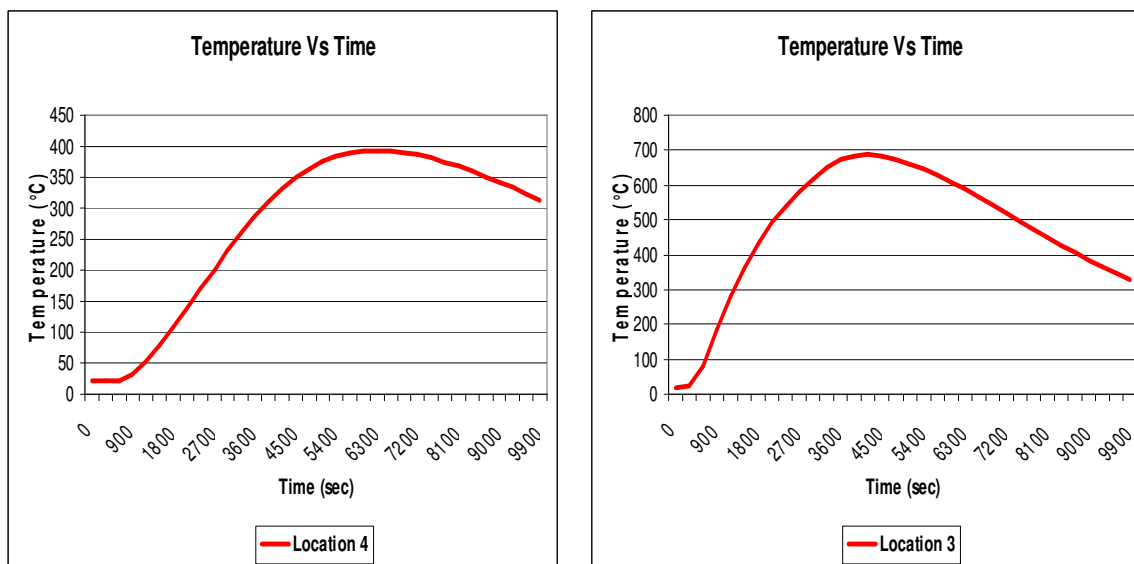
Figure 6.35 Temperature Vs Time for Locations 4 (left) & 3 (right)
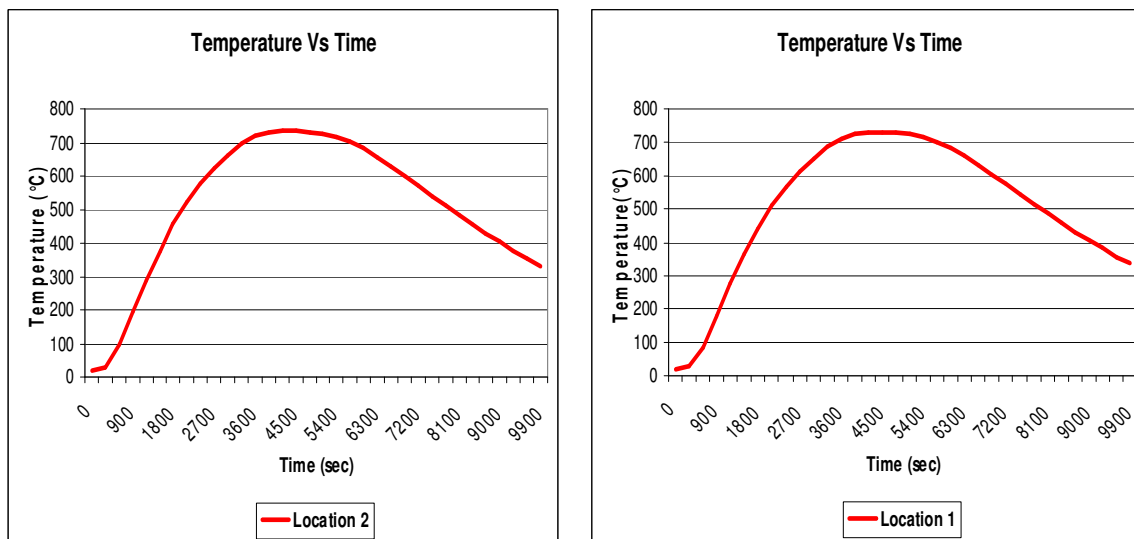
Figure 6.36 Temperature Vs Time for Locations 2 (left) & 1 (right)

6.10.3 *Comparison of temperature results for different fire intensities*

Figures 6.37 and 6.38 present the comparison of temperature results for the major locations of study when subjected to different fire intensities. Due to very lengthy simulation times, the analyses for cases 2 and 3 were restricted to a time limit of 6900 seconds, which took 60 hours.
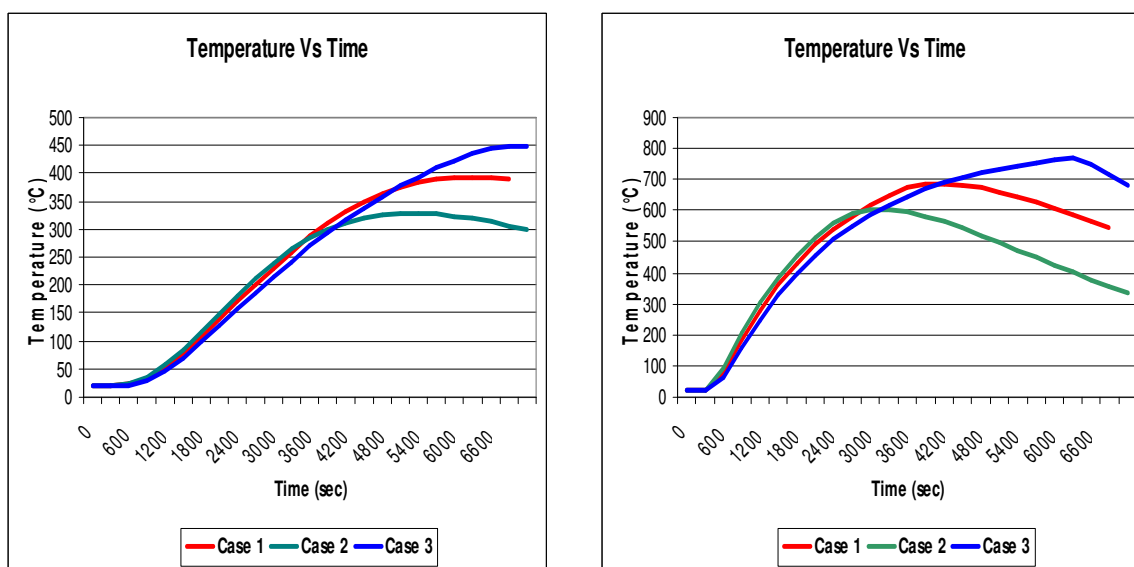
Figure 6.37 Temperature Vs Time for Locations 4 (left) & 3 (right)
from different cases
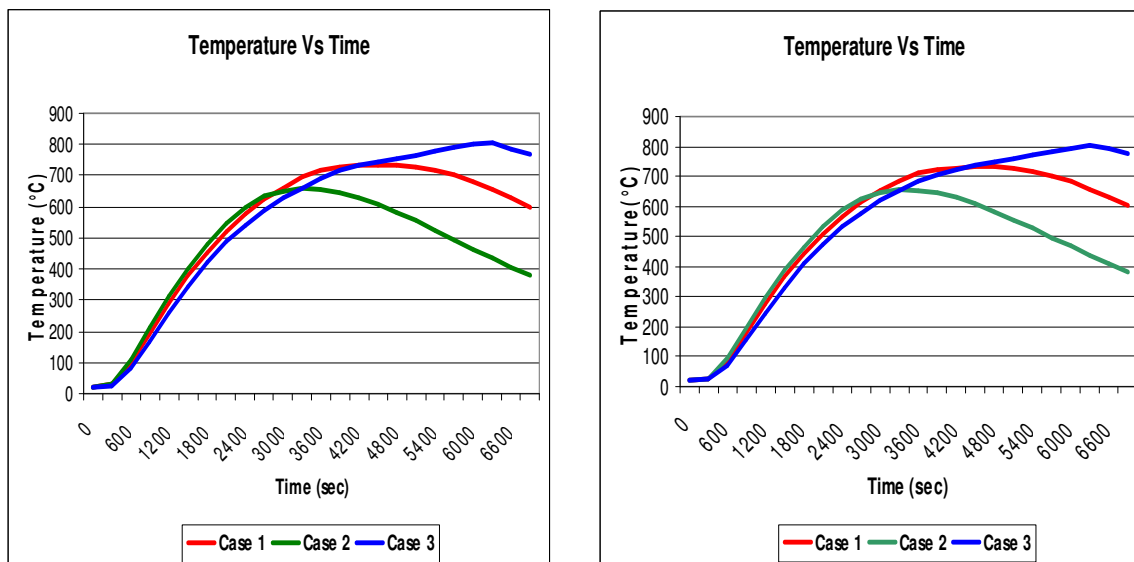
Figure 6.38 Temperature Vs Time for Locations 2 (left) & 1 (right)
from different cases

6.10.4 *Comparison of results from ENV curve and ASTM E-119*

Figures 6.39 and 6.40 present a comparison of the temperature profile for different locations from ENV and ASTM E-119 fire curves.
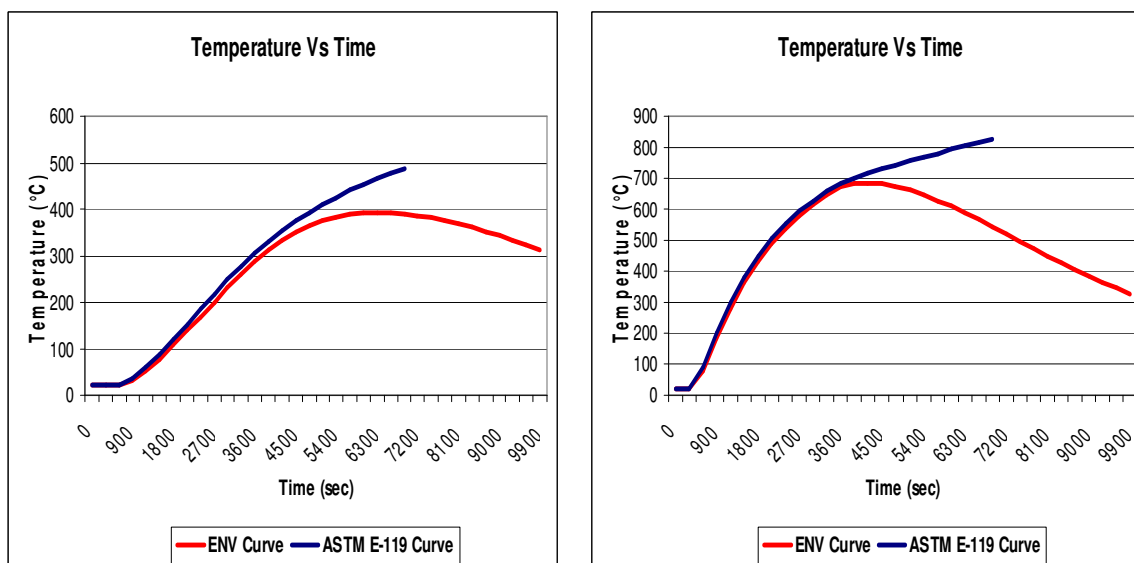
Figure 6.39 Temperature Vs Time for Locations 4(left) & 3(right)
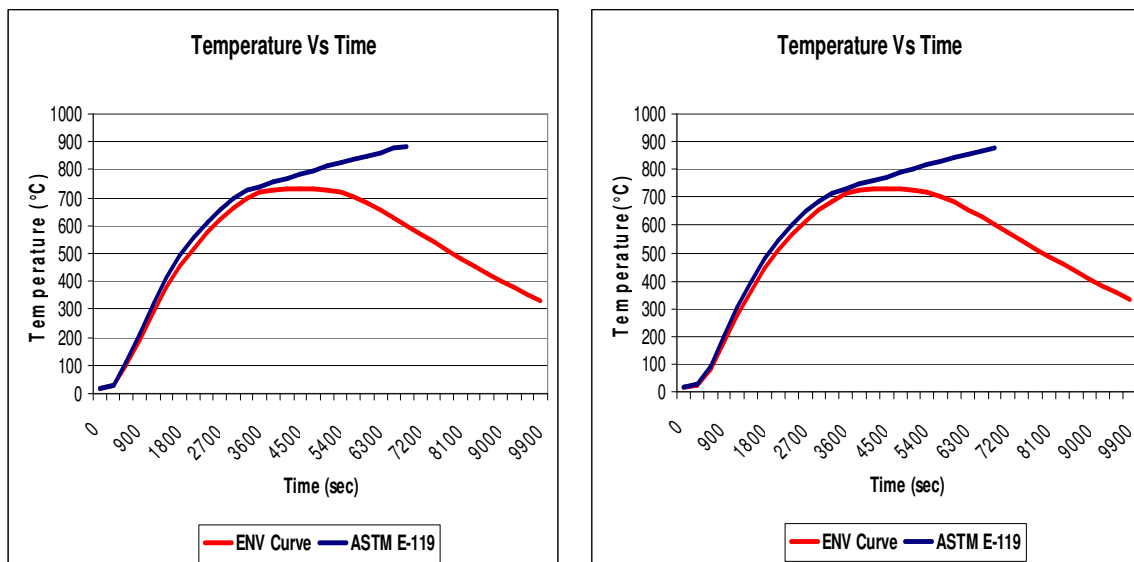
Figure 6.40 Temperature Vs Time for Locations 2(left) & 1(right)

6.10.5 *Results summary*

As shown in Figures 6.35 and 6.36 for the case of W12*x*27 beam subjected to ENV fire curve, there is a rise in temperature for sometime, and after a peak temperature is reached, the temperature drops down. The period for the temperature rise is known as Heating Phase, while the period for temperature decrease is known as Cooling Phase**.** Figures 6.37 and 6.38 present a comparison for different cases due to the different fire scenarios and fire intensities. As seen from the graphs the temperature in steel for all the location varies significantly with the change in fire intensities and the respective heating and cooling periods. It becomes very essential to study the sensitivity of results due to variation of opening factors and thus the fire intensity for a room. From these three cases, the temperature profile for all locations was found to vary in the range of 100° to 200° C. Further, Figures 6.39 and 6.40 provide a comparison of the temperature profiles obtained for different locations due to the formulations from ASTM E-119 curve and the ENV curve. From comparison of the steel temperatures resulting from the two different curves, one can observe that there is good agreement between both responses for the initial fire growth period but after a time of 4200 seconds the curves follow a different trajectory. The ASTM E-119 curve continues to grow, while the ENV curve shows a decrease in temperature due to the fire load properties and the room conditions.

6.11 W12x27 steel beam with 5/8″ thick gypsum board enclosure subjected to ENV fire curve

6.11.1 *Introduction*

The model which was earlier developed to investigate 5/8″ thick gypsum board (section section 6.9.2) was previously subjected to the ASTM E-119 fire curve. The model was subsequently subjected to the ENV time-temperature history formulated in the Eurocode. The gypsum board simulation was studied for the case when the maximum fire intensity occurred at 55 minutes **(Case 1, section 6.10.16.10.1).**

6.11.2 *TAS model results*

Figures 6.41 and 6.42 present the results obtained for the model of W 12*x*27 beam with 0.5″ thick gypsum board protection. All the properties and basic modeling remained the same as for the previous model of gypsum board which was subjected to a time-temperature profile based on ASTM E-119 curve.
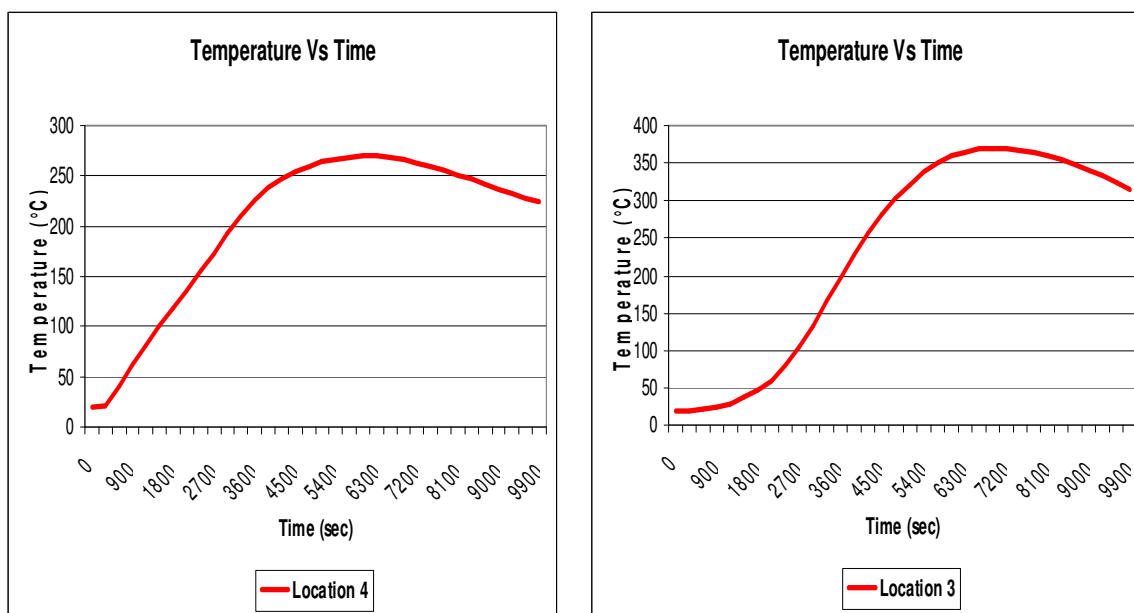
Figure 6.41 Temperature Vs Time data for Locations 4 (left) & 3 (right)
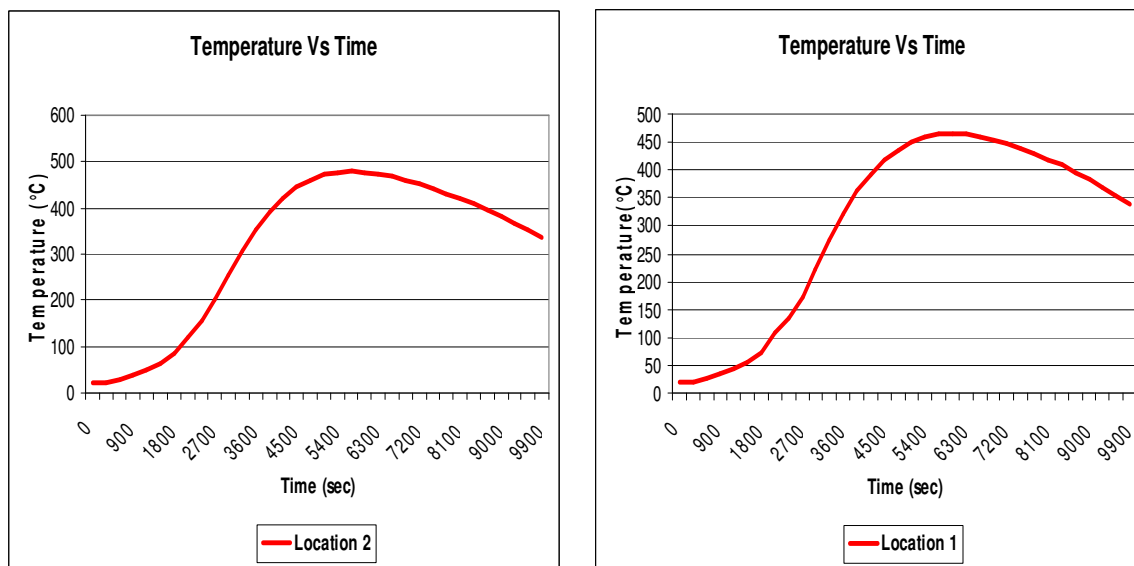
Figure 6.42 Temperature Vs Time data for Locations 2 (left) & 1 (right)

6.11.3 Comparison between results obtained for different locations from ENV curve and ASTM E-119

Figures 6.43 and 6.44 present a comparison of the temperature profile for different locations from ENV and ASTM E-119 fire curves.
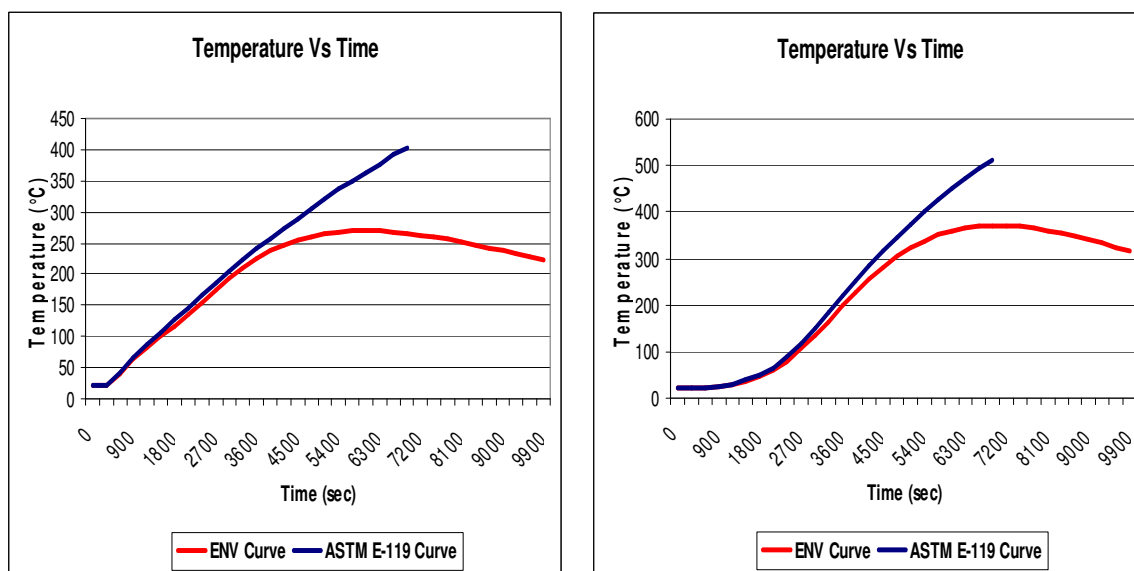
Figure 6.43 Comparison of Temperature Vs Time data from different models for Locations 4 (left) & 3 (right)
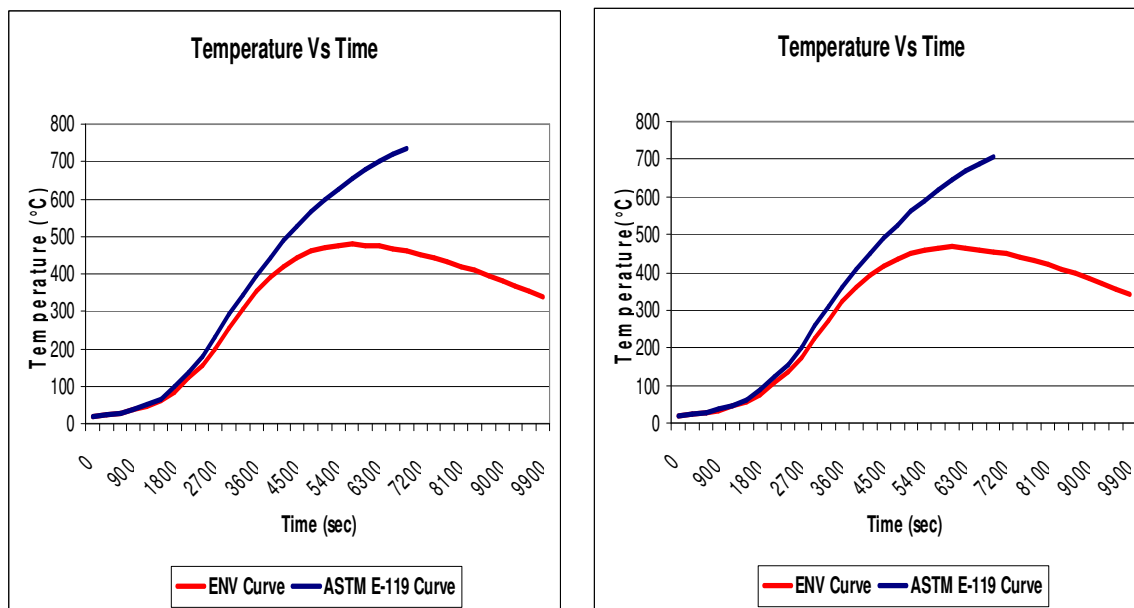
Figure 6.44 Comparison of Temperature Vs Time data from different models for Locations 2 (left) & 1 (right)

6.11.4 *Results summary*

As shown in Figures 6.43 and 6.44, comparison of the steel temperatures resulting from the ASTM E-119 and the ENV curves, one can conclude that there is a good agreement between both the curves for the fire growth period. But, after a time of 4200 seconds, the responses follow a different trajectory. The ASTM E-119 curve continues to grow, while the ENV curve shows a decrease in temperature due to the fire load properties and the room conditions.

6.12 Comparison of results between Vermiculite and Gypsum models subjected to ENV fire curve

Figure 6.45 presents a comparison between results obtained by subjecting the vermiculite and gypsum model to the time-temperature profile based on ENV fire curve. Comparison was made for **Case 1**, where the maximum fire temperature of **892°C** occurred at **56 minutes**.
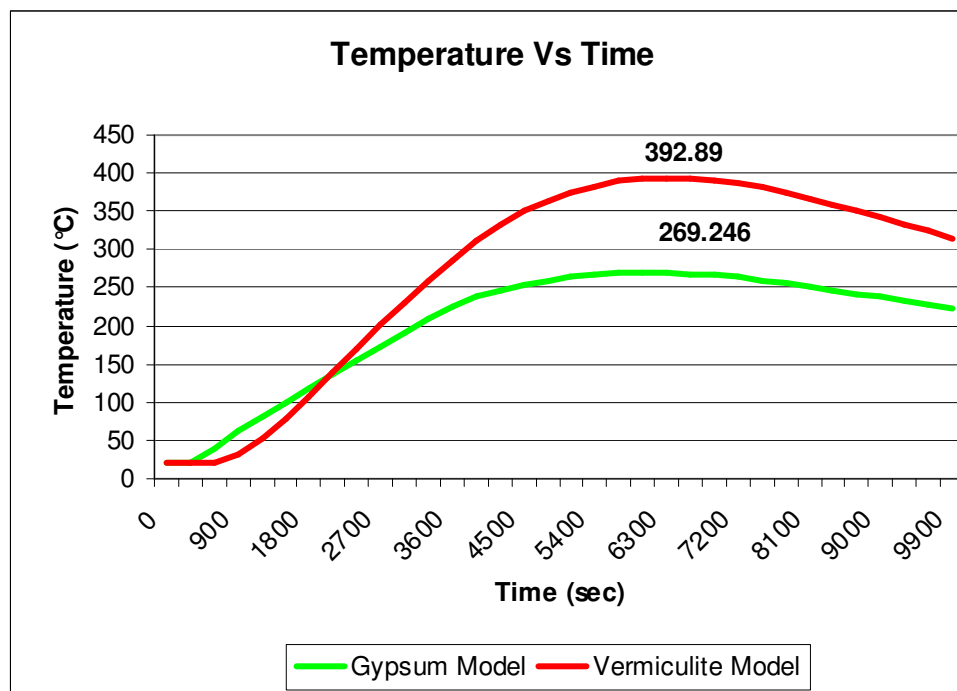
Figure 6.45 Temperature Vs Time graph for location 4

6.12.1 *Results summary*

As observed from Figure 6.45**,** for location 4, when the steel beam was protected with vermiculite coating, the maximum temperature was **392.14°C** at **6600 seconds**, and the maximum temperature was **269.62°C** at **6000 seconds** when gypsum board was the fire resistance material. Thus there is a time lag (Δt) of 600 seconds when the maximum temperature in steel was reached. This indicates that gypsum proved to be a better fire resistive material when the steel beam was subjected to a natural fire as described by the ENV fire curve.

7 LUMPED MASS PARAMETER METHOD

7.1 Introduction

Depending on the type of building and its importance, it may not be always feasible to adopt a rigorous numerical modeling or finite element modeling technique to assess structural performance during a fire event. In many cases it may happen that an approximate analytical method would suffice for design and decision making. Analytical calculations are much simpler as compared to the complex finite element models due to the omission of temperature gradients that may occur across a steel section. There are many methods to predict temperature rise in case of insulated steel members, viz. ECCS method, ENV 1993-1-2 approach, etc. The method that was adopted in this thesis project was the Lumped Parameter Method based on the ECCS method [12]. The method suffers the limitation of not taking into consideration the thermal or temperature gradients that exist through the steel section. Thus, it would tend to predict a higher range of temperature for the entire steel section. Also, the analytical method cannot handle the effects and interaction between two different materials, viz. steel and concrete. The analysis was done to represent the effectiveness and the limitations of an analytical approach. All the analyses were conducted through application of the ASTM E-119 time-temperature curve.

7.2 ECCS method

The ECCS formulations [12] provide closed-form equations to predict the temperature of steel at different time intervals. The first step in this method is to predict the heat capacity of the insulation. In order to determine this value for the insulating material, the parameter "Φ" is calculated from the following equation,

$$\Phi = \left(\frac{c_p \rho_p}{C_{ps} \rho_s} \right) d_p \left(\frac{A_p}{V_i} \right) \qquad \text{-[8-1]}$$

where, Φ = insulation heat capacity factor

c_p = specific heat of gases

C_{ps} = specific heat of steel

ρ_p = density of insulation

ρ_a = density of structural steel

A_p = area of steel protection per unit length exposed to fire

V_i = volume of steel per unit length

d_p = insulation thickness

In the equation above if, the value of Φ exceeds 0.5 then the insulation is considered to have substantial heat capacity and the heat flow for the enclosed steel is given by equation 8-2, while for insulating members with negligible heat capacity, the heat flow is given by equation 8-3.

$$\Delta\theta_{a,t} = \left(\frac{\frac{\lambda_p}{d_p}}{C_{ps}\rho_s}\right)\left(\frac{A_p}{V_i}\right)\frac{(\theta_a - \theta_{a,t})\Delta t}{(1+\frac{\Phi}{2})} - \frac{\Delta\theta_t}{1+\frac{2}{\Phi}} \qquad \text{-[8-2]}$$

$$\Delta\theta_{a,t} = \left(\frac{\frac{\lambda_p}{d_p}}{C_{ps}\rho_s}\right)\left(\frac{A_p}{V_i}\right)(\theta_t - \theta_{a,t})\Delta t \qquad \text{-[8-3]}$$

where, λ_p = thermal conductivity of protection material

θ_a = structural steel temperature

$\theta_{a,t}$ = structural steel temperature at time t
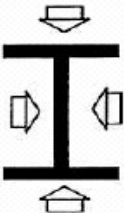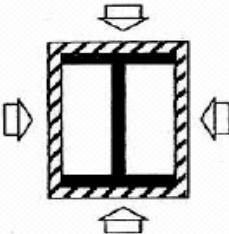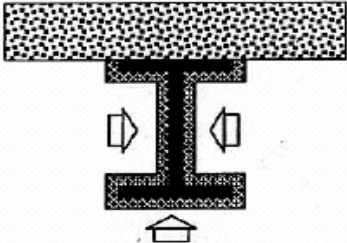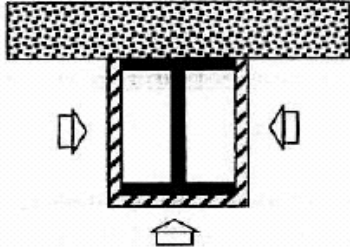
$\Delta\theta_t$ = incremental increase in steel temperature

To determine the time step, the following equation has been suggested by ECCS,

$$\Delta t \leq \frac{25000}{\frac{A_p}{V_i}} \qquad \text{-[8-4]}$$

Here, "V" is the cross sectional area of the steel section that is used for design purposes, and this value can be directly obtained from the *AISC Manual of Steel Construction*. A_p is the heated perimeter of the steel section, which would depend upon the type and layout of the insulating material. Usually, the value for A_p can be calculated based on the expressions that have been established for different configurations. Table 7-1 presents the perimeter expressions A_p/V_i for some common cases.

Table 7-1 Perimeter expressions for some particular cases of steel, [21], Ch 6, p 191

Fire exposure situation	A_p/V
Unprotected steel section exposed to fire exposure around all sides	$\dfrac{2(2B - t_w + D)}{A_s}$
Fire exposure on all sides of board protection	$\dfrac{2(B + D)}{A_s}$
Fire protection on three sides: profile protection	$\dfrac{2(B - t_w) + B + 2D}{A_s}$
Fire protection on three sides: board protection	$\dfrac{2D + B}{A_s}$

Once the time step is determined, the temperature of steel is calculated at each interval for the duration of the proposed fire event, and a curve of steel temperature Vs time is plotted. Also, based on the values of the steel temperature at each time interval, corresponding values for the reduced Young's modulus and yield strength can be calculated from the following relationships suggested by Eurocode [12], [22]

Yield Stress:

For $0 \leq T \leq 600$ °C
$$F_{yT} = \left(1 + \frac{T}{900 \ln\left(\frac{T}{1750}\right)}\right) F_{y0}$$
-[8-5]

For $600° \, C < T \leq 1000°$ C
$$F_{yT} = \left(\frac{340 - 0.34T}{T - 240}\right) F_{y0}$$
-[8-6]

where, F_{y0} = initial Yield strength at 20°C

F_{yT} = Yield strength at time T

T = temperature

Young's Modulus:

For $0 \leq T \leq 600$ °C
$$E_T = \left(1 + \frac{T}{2000 \ln\left(\frac{T}{1100}\right)}\right) E_0$$
-[8-7]

For $600°C < T \leq 1000°$ C
$$E_T = \left(\frac{690 - 0.69T}{T - 53.5}\right) E_0$$
-[8-8]

where, E_0 = initial Young's modulus at 20°C

E_T = Young's modulus at time T

T = temperature

7.3   Vermiculite Model

7.3.1   *Introduction*

Analytical analysis using the ECCS method applied to the model configuration that was developed using TAS for the study of vermiculite insulation, as described in section 6.8. The purpose of the study was to analyze the effectiveness of the analytical method. The analysis was conducted in a step-by-step manner, starting with constant thermal properties for steel and vermiculite, and then developing an array of temperature-dependent values to explore the sensitivity of the results.

7.3.2   *Comparison between results from different models*

Figure 7.1 presents a comparison between the results obtained from the ECCS method for variable and constant thermal properties of steel and vermiculite. Further, Figures 7.2 and 7.3 enable a comparison between the results obtained from analytical modeling and those obtained from TAS modeling and Bletzacker's experiments **[1]**. Location 4 data from TAS model was not included for comparison purposes due to the fact that the concrete slab and its respective properties could not be incorporated within the analytical methods. The results suggest that the analytical techniques are highly conservative in comparison to finite element models. Also, a temperature increase was observed which accounted for **3% to 8%** hike in temperature results that were obtained from analytical method.
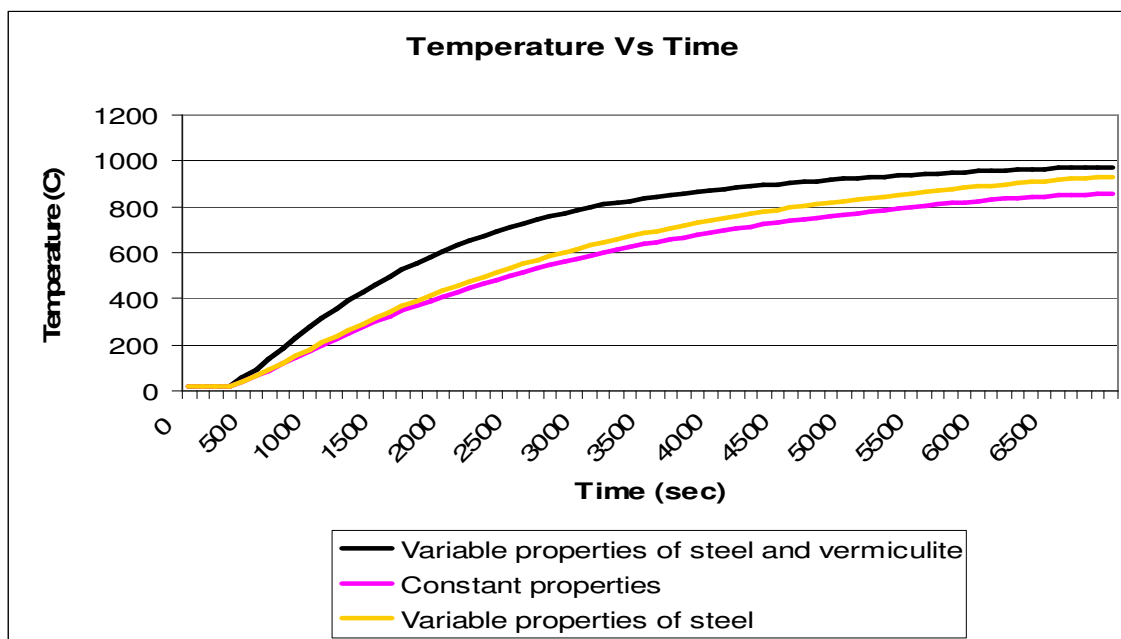
Figure 7.1 Temperature Vs Time comparison between results from different analytical models
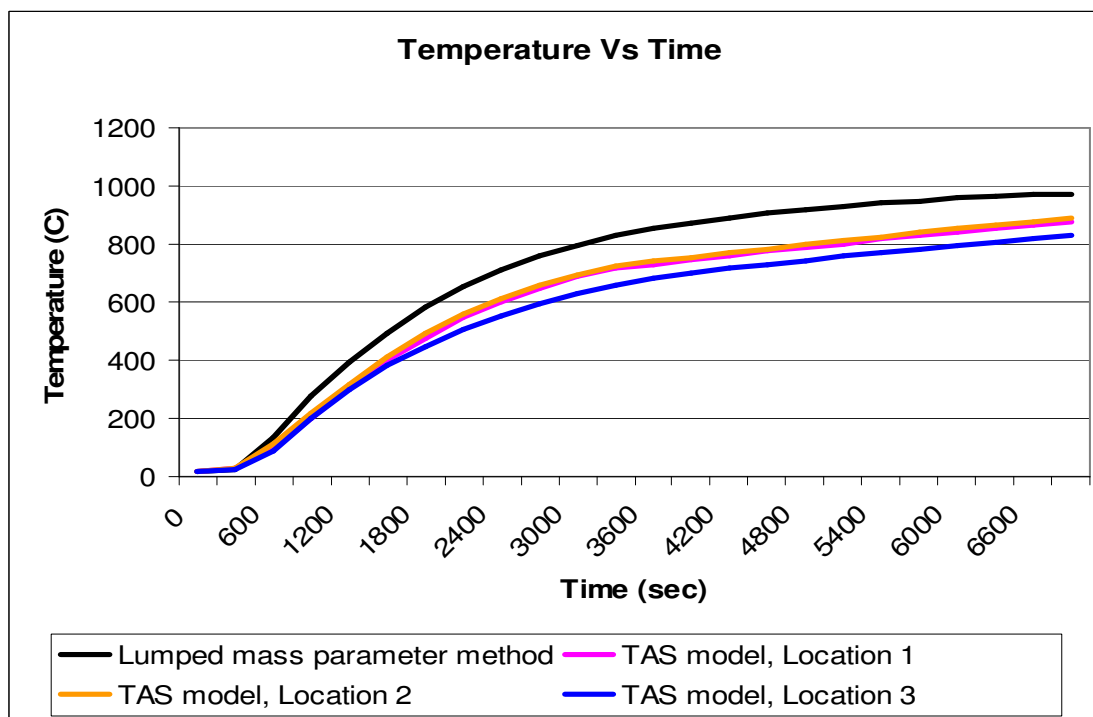
Figure 7.2 Temperature Vs Time comparison between results from analytical method and TAS modeling
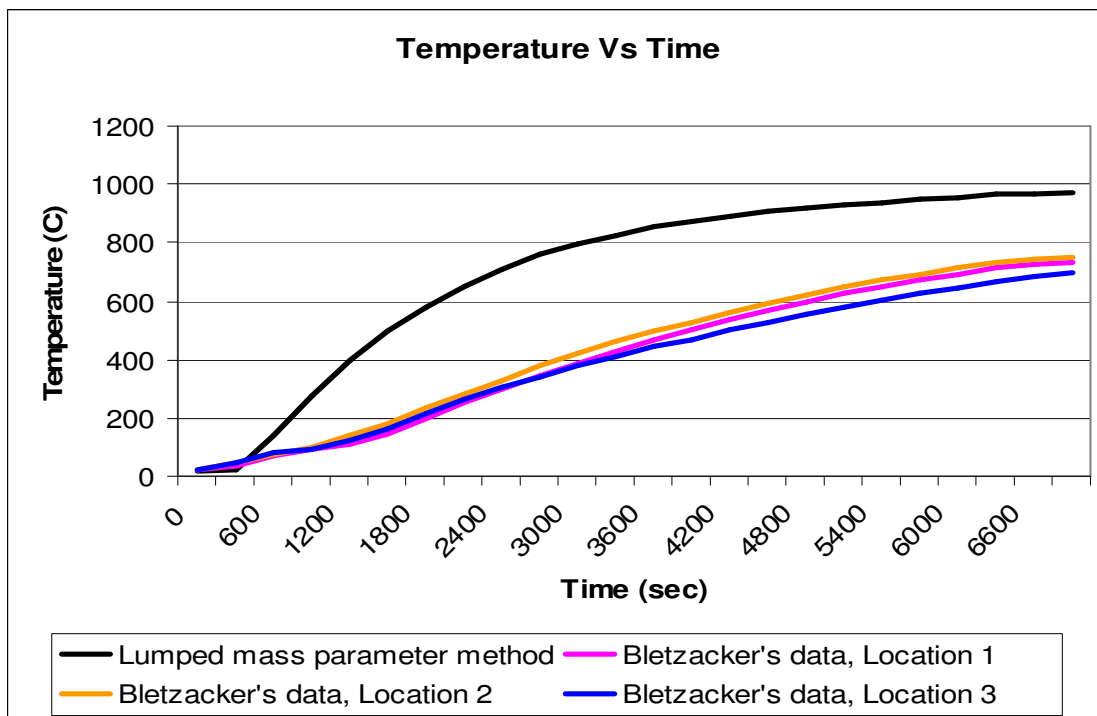
Figure 7.3 Temperature Vs Time comparison between results from analytical method and Bletzacker's data

7.4 Gypsum Board Model

7.4.1 *Introduction*

Analytical analysis was performed using the ECCS method applied to the model configuration that was developed using TAS for the study of gypsum board insulation as described in section 7.9. The purpose of the study was to analyze the effectiveness of the ECCS method for modeling the contribution of gypsum board insulation. The analysis was carried out in a step-by-step manner, starting with constant thermal properties for steel and gypsum board, and then developing an array of temperature-dependent thermal properties to explore the sensitivity of the results.

7.4.2 *Comparison between results from different models*

Figure 7.4 presents a comparison between the results obtained from ECCS method for variable thermal properties of steel and vermiculite and those obtained from TAS modeling.
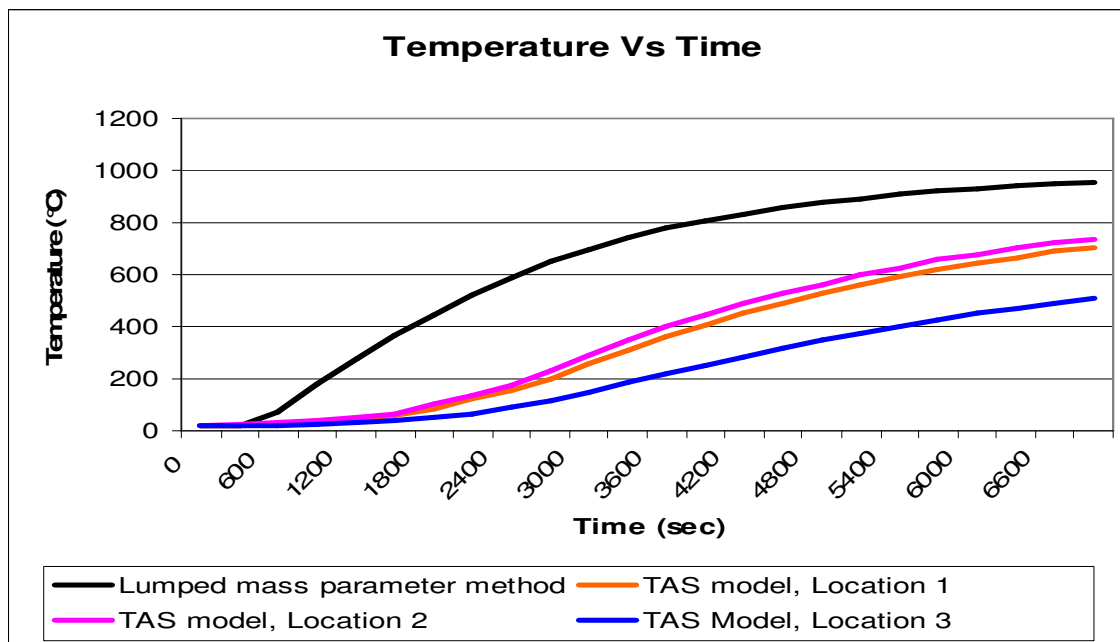
Figure 7.4 Temperature Vs Time comparison analytical methods and TAS models

7.5 Mechanical Properties of Steel

7.5.1 *Mechanical properties of steel from vermiculite model*
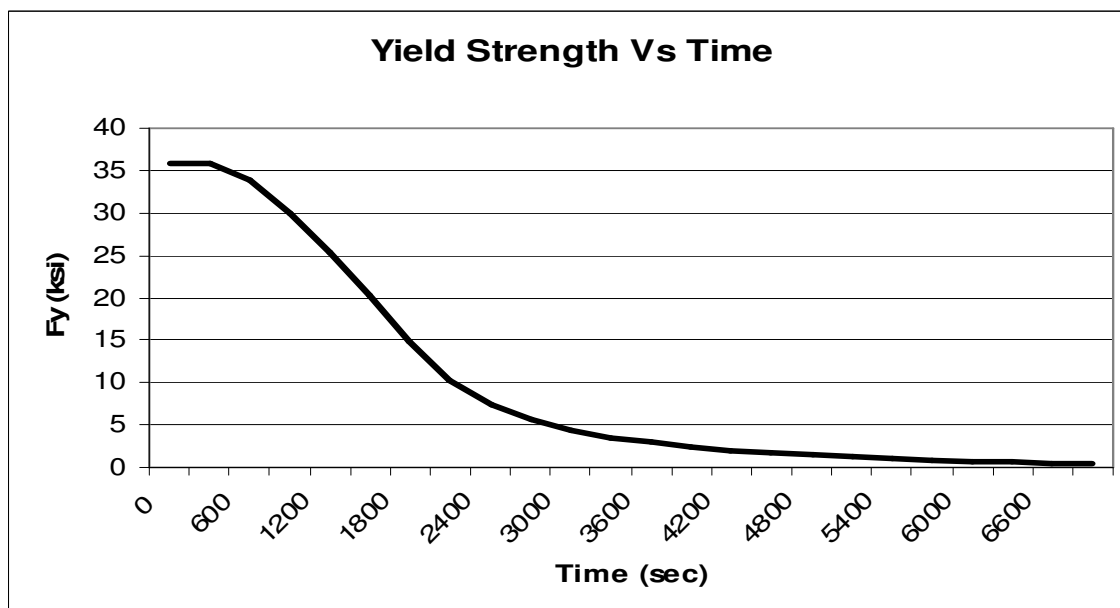
Figure 7.5 Yield Strength Vs Time for 0.5" thick vermiculite model

Modulus of Elasticity Vs Time
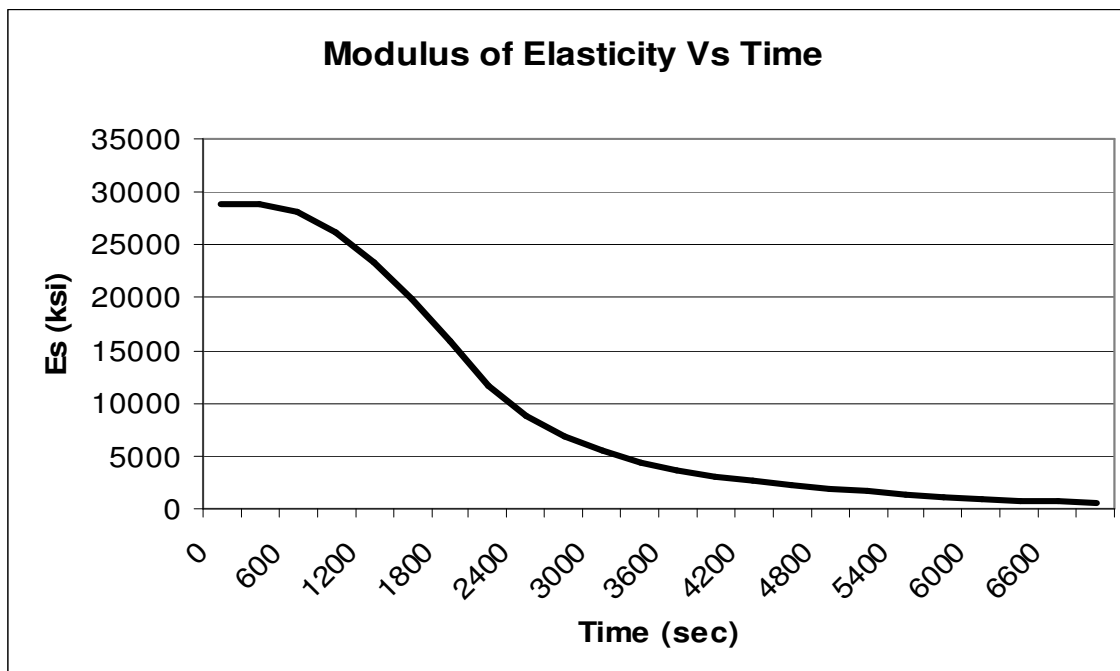
Figure 7.6 Modulus of Elasticity Vs Time for 0.5" thick vermiculite model

7.5.2 *Mechanical properties of steel from gypsum model*

Yield Strength Vs Time
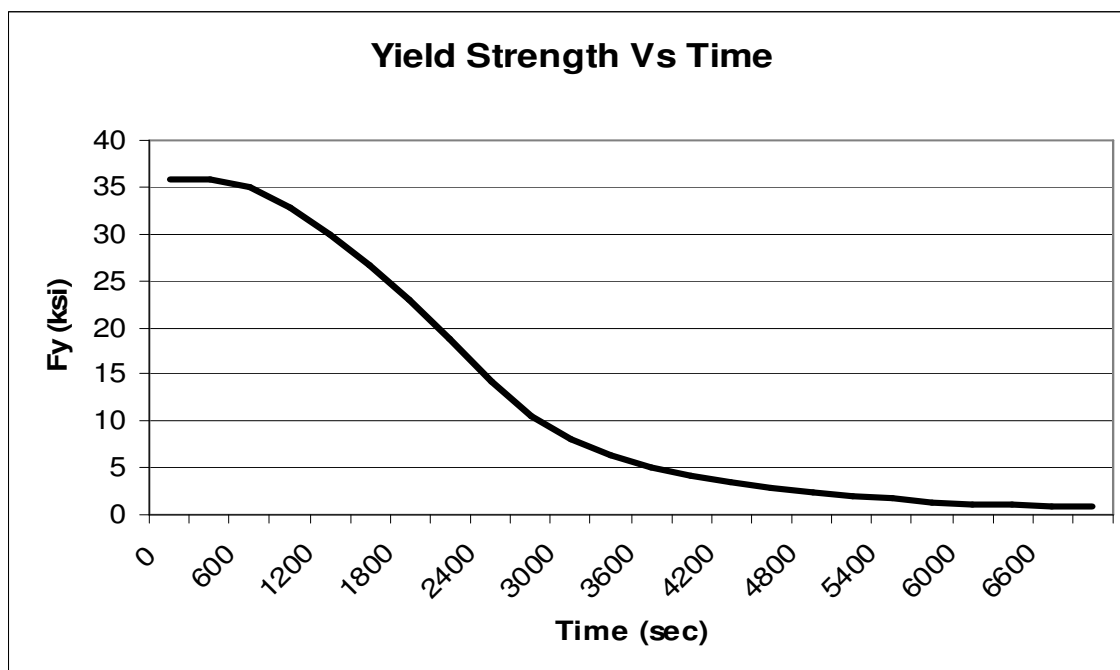
Figure 7.7 Yield Strength Vs Time for 5/8" thick gypsum board model

Modulus of Elasticity Vs Time
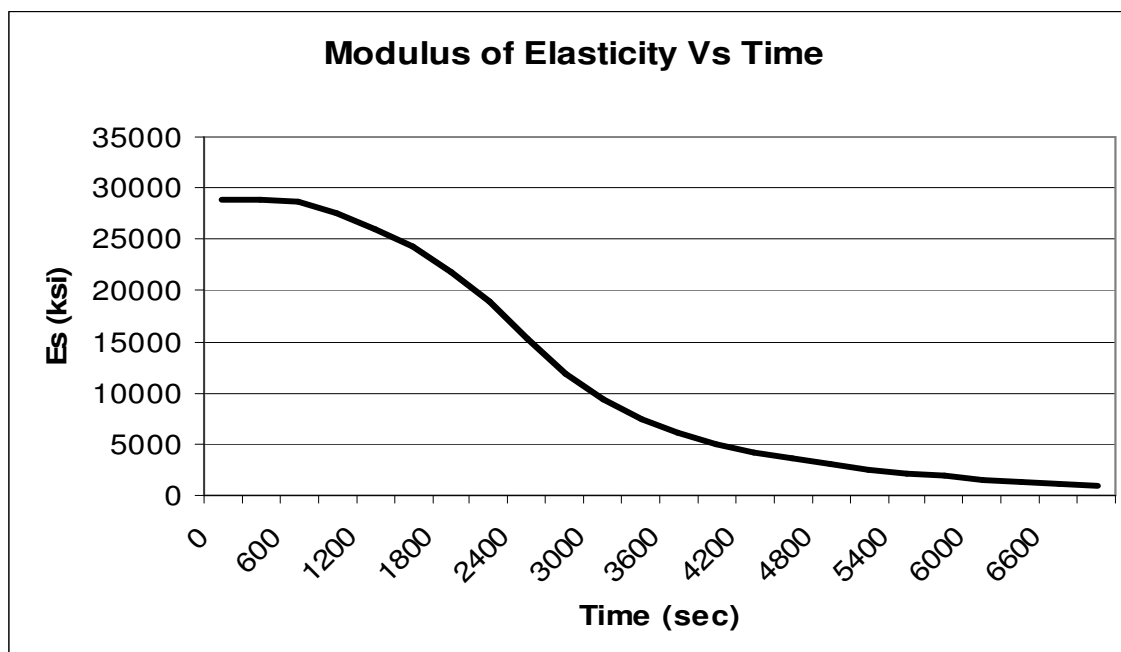
Figure 7.8 Modulus of Elasticity Vs Time for 5/8" thick gypsum board model

7.5.3 *Results summary*

From Figures 7.1 to 7.4 it can be concluded that the analytical model showed a steep increase in temperature when compared to TAS model results and Bletzacker's experimental results. The results from analytical models were compared with temperature profiles for locations 1,2, and 3 only, due to the fact that it is not possible to incorporate the effect of the concrete slab interaction with the steel beam at location 4. The method is not that accurate due to the fact that analytical techniques cannot consider the effect of non-uniform temperature gradients that occur through the beam section. Further, Figures 7.5 to 7.8 represent the profile for the mechanical properties of steel. It was observed that the yield strength, and modulus of elasticity for steel decrease with an increase in temperature, and a stage is reached when the carrying capacity of the beam is nearly zero which results to a failure of the beam.

8   CONCLUSIONS

In this thesis, different aspects related to heat transfer mechanism for a W 12*x*27 steel beam section were studied in a comprehensive manner by the use of the finite element software, TAS. The scope of work included comparisons of the numerical results with published test data and results obtained from simpler analytical models. The conclusions for different models and overall observations are discussed below.

W 12x27 Bare Steel Model:

From the analysis of bare steel model, it was observed that the temperature rise was very high for the entire beam section with all the locations in the temperature range of **700° to 800°C**. The study of thermal properties and their variation with temperature helped to establish a model for conduction within the steel beam.

W 12x27 Bare Steel Model with 4" Thick Concrete Slab:

The simulations for this model showed that the temperature for the top flange, which is directly in contact with the slab, resulted in a significant decrease in the temperature, compared to the bare steel model. The difference was in the range of **300° to 350°C**. Different constant thermal properties for concrete were considered in order to test the sensitivity. The results suggested that there was not a significant change in temperature profile for the top flange when thermal conductivity and specific heat for concrete were varied within the range of **1.5 to 1.95 W/mK** and **1023 to 1260 J/kgK,** respectively.

W 12x27 Steel Beam with 4" thick Concrete slab and 1/2" thick Vermiculite Coating:

This model was a replica of the beam that was tested in a lab by Professor Bletzacker **[1]** in 1966. In order to test the sensitivity of the model, simulations were conducted for the cases of constant and variable thermal properties of vermiculite. The simulations for constant thermal properties resulted in a lag in the predicted temperature profile when compared with Bletzacker's data **[1].** The thermal properties of vermiculite are not well defined for temperatures above the limit of **450°C**. For this reason, the technique of curve

fitting was adopted. The properties are highly variable due to the presence of cementitious materials and other components. The results suggested that the temperature profile for location 4 showed good agreement with the experimental results from Professor Bletzacker's studies **[1]**. But, for locations 1, 2, and 3 the results obtained from the simulations showed a steep increase in temperature profile when compared with Bletzacker's experimental results **[1]**. According to the literature review, it was observed that the non-availability of thermal properties at high temperatures played a critical role towards the high temperature profile that was observed for this model. From the simulations it was observed that TAS modeling results were conservative with the margin of error in the range of **14% to 17%.**

W 12x27 Steel Beam with 4″ thick Concrete slab and 5/8″ thick Gypsum Board Insulation:

This model was developed with a 5/8″ thick gypsum board insulation which provided fire resistance. Simulations were conducted for the cases of constant and variable thermal properties for gypsum in order to explore the sensitivity of results. Thermal properties for gypsum are pretty well defined at high temperatures, and the use of test data from NIST helped the modeling and analysis. The simulation results indicated that gypsum proved to be a better fire protection material in comparison to vermiculite due to the fact that the temperature for all the locations within the steel section showed a drop of about **100° to 200°C**.

W 12x27 Bare Steel Model with 4″ thick Concrete slab and 1/2″ thick Vermiculite Coating subjected to ENV fire curve:

The model for 1/2″ thick vermiculite model, as mentioned before, was subjected to a parametric design fire curve, known as the ENV fire curve. Simulations were carried out for different fire intensities viz. 55 minutes, 35.35 minutes, and 102 minutes durations with corresponding maximum fire temperatures of 891°C, 800°C, and 900°C, respectively. From the simulations, it was observed that a fire curve consists of two different phases, namely heating and cooling phases which depend up on the characteristics of the room. Characteristics such as opening factor and fire load play a

critical role for the peak temperature that occurs during a fire event. The opening factors for these simulations were varied in the range of 0.058 to 0.068. The resultant fire intensity and duration were dependent on opening factor. The resulting maximum temperature for location 4 from the ENV fire curve was in the range of **325° to 370°C** as compared to **485° to 500°C** from ASTM E-119 simulations.

W 12x27 Bare Steel Model with 4" thick Concrete slab and 5/8" thick Gypsum Board Insulation subjected to ENV fire curve:

The gypsum board model was subjected to the ENV fire curve with a fire intensity of 892°C occurring at 56 minutes. The results suggested that the highest temperature for location 4 when gypsum board was used was **269.24°C** in comparison to a temperature of **392.89°C** when vermiculite was used as a fire resistant material. It was also observed that there was a time lag of 600 seconds between the occurrence of these peak temperatures in the gypsum board and vermiculite models. This 10 minutes time difference may be of critical importance for the safety of the occupants and the responders in case of a fire event.

Lumped Mass Parameter Method for W 12x27 Beam Model with 1/2" thick Vermiculite Coating:

Analytical analysis was done using the Lumped Mass Parameter Method. Analysis of the W 12*x*27 beam protected with 1/2″ vermiculite coating subjected to ASTM E-119 time-temperature profile was performed. The results showed a maximum temperature of **972° C** for the steel section as compared to **886°C** and **748.88°C** from TAS modeling results and Blezacker's experimental results **[1].** Analytical techniques suffer from the drawback of not taking into consideration the effect of temperature gradients that occur throughout the cross-section of the beam. Also, the contribution of the concrete slab could not be modeled as there has not been much advances in analytical techniques that can handle different materials to determine their interrelationships.

Lumped Mass Parameter Method for W 12x27 Beam Model with 5/8″ thick Gypsum Board Insulation:

Analytical analysis of a configuration with gypsum board insulation was done using the Lumped Mass Parameter Method. Analysis of W 12x27 beam protected with 5/8″ gypsum board subjected to ASTM E-119 time-temperature profile was carried out. The results showed a maximum temperature of **952.85° C** for the steel section as compared to **734°C** from TAS modeling results. The analytical results again proved that gypsum gave a better performance when compared to vermiculite with the temperature difference being about 20°C between the two materials.

Overall Observations:

The overall observation that could be made from this project was that TAS proved to be a very sophisticated yet user friendly tool to analyze time-temperature relationships for an assembly. It was also seen that TAS model results showed good agreement with physical test results from Professor Bletzcaker's results [**1].** The only drawback to the use of TAS at this time is that it does not have good capabilities for analyzing stress results. The results suggest that TAS or similar finite element analyses could provide a cost-effective supplement or alternative to physical tests by combining its results with other stress analysis tools in the field of Fire Protection.

9   RECOMMENDATIONS FOR FUTURE WORK

A number of questions arised from this project. Some of them are,

➢ What is the behavior of concrete when subjected to high temperatures? This issue becomes very important when buildings have a significant volume of concrete as the basic construction material and less steel is involved. Explicit equations need to be developed for modeling thermal characteristics in order to determine the key areas contributing towards high temperatures and failures within concrete.

➢ What would be the behavior of a steel frame or bay when modeled and subjected to high temperatures using TAS? This would lead to an understanding for the behavior of connections when subjected to a fire event. Further, the sensitivity of failure with regard to the location of fire within a room could be explored.

➢ How critical were fire loads and opening factors with respect to the temperature rise in steel?

➢ What is the behavior of vermiculite beyond the temperature limit of 450°C? This would help in a more accurate comparison of results with regard to Bletzacker's data.

➢ What would be the stress behavior of steel at high temperatures? The effects of restrained Vs partially restrained end conditions could be analyzed. The time-temperature results from these simulations could be used for analyzing stress results through application of finite element tools such as SCINDIA, ABAQUS, and others. The analyses would provide a more clear understanding to structural engineers regarding the concept of critical failure.

➢ How critical is the time difference when the maximum temperature is reached in steel, when vermiculite and gypsum are used separately as fire protective materials? This study would help in determining the structural performance of vermiculite and gypsum and thereby the performance of entire beam section.

➢ What is the significance of using different fire curves for the purpose of fire testing and fire modeling? A sensitivity analysis of fire curves could be done in order to understand their significance from the view point of design and critical condition.

10 BIBLIOGRAPHY

[1] Bletzacker R.W. "*Effect of Structural Restraint on the Fire Resistance of Protected Steel Beam Floor and Roof Assemblies",* Ohio State University, 1966.

[2] Bryant R., Womeldorf C., Johnsson E. and Ohlemiller T. "Radiative Heat Flux Measurement Uncertainty"*, Journal of Fire and Materials*, Vol. 27, pp. 209-222, 2003.

[3] Chitty R. and Foster J., "Application of Computer Modeling To Real Fire Incidents." Proceedings of the Ninth International Conference on Interflam, Edinburgh, Scotland, September 2001.

[4] Cooper L.Y., "*The Thermal Response of Gypsum-Panel/Steel Stud Wall Systems Exposed to Fire Environments – A Simulation for use in Zone – Type Fire Models*.", NIST, June 1997.

[5] Delichatsios M., Paroz B. and Bhargava A. "Flammability Properties for Charring Materials." *Journal of Fire Safety*, Vol. 38, pp 219-228, 2003.

[6] Halverson H., Bausano J., Case S. and Lesko J., *Simulation of Structural Response of Composite Structures under Fire Exposure*." Department of Engineering Science & Mechanics at Blacksburg, Virginia Tech.

[7] Hoben International, England (http://www.hoben.co.uk/vermiculite/specs.htm)

[8] Lane B, "Performance Based Design for Fire Resistance" Modern Steel Construction, December 2000.

[9] Lie T.T. "Fire Resistance of Structural Steel." *Engineering Journal*, Fourth Quarter, 1978.

[10] Podebradska J., Pavlik J., Toman J. and Cerny R. *Specific Heat Capacity of Cementitious Composites in High-Temperature Range*, Czech Technical University, Department of Structural Mechanics, Czech Republic.

[11] Poh K.W. *"*Stress-Strain-Temperature Relationship for Structural Steel." *Journal of Materials in Civil Engineering*, Vol. 38, No.5, pp. 371-379, September/October 2001.

[12] Purkiss J.A., *Fire Safety Engineering – Design of Structures*, Butterworth-Heinemann, 1996.

[13]   Ruddy J.L. and Ioannides S.A. "Thickness Determination for Spray-Applied Fire Resistive Materials." Proceedings of the NASCC, 2002

[14]   Sakumoto Y. "Research on New Fire-Protection Materials and Fire-Safe Design." *Journal of Structural Engineering*, Vol. 125, No. 12, pp. 1415-1422, December 1999.

[15]   "The Future of Fire Engineering." Modern Steel Construction, July 1998.

[16]   The Schundler Company, New Jersey, USA (www.schundler.com)

[17]   Thomas G. "Thermal Properties of Gypsum Plasterboard at High Temperatures." *Journal of Fire and Materials*, Vol. 26, pp. 37-45, 2002.

[18]   Tide R.H.R. "Integrity of Structural Steel after Exposure to Fire." *Engineering Journal*, First Quarter, pp. 26-38, 1998.

[19]   Toh W.S., Tan K.H. and Fung T.C. "Strength And Stability of Steel Frames in Fire: Rankine Approach." *Journal of Structural Engineering*, Vol. 127, No. 4, pp. 461-469, April 2001.

[20]   Toman Jan, Cerny Robert, *et. al.*, "*Specific Heat Capacity of Cementitious Composites in High Temperature Range",* Czech Technical University.

[21]   Vila Real P.P.M., Lopes N., Simoes da Silva L., Piloto P. and Franseen J.-M. " "Numerical modeling of steel beam-columns in case of fire-comparison with Eurocode 3." *Fire Safety Journal*, Vol. 39, pp. 23-29, 2004.

[22]   Wang Y.C. *Steel And Composite Structures – Behavior and Design for Fire Safety,* Spon Press, 2002.

[23]   Wong M.B. and Ghojel J.I., "Sensitivity Analysis of Heat Transfer Formulations for Insulated Structural Steel Components." *Journal of Fire Safety*, Vol. 38, pp. 187-201, 2003.

[24]   www.astm.org **-** American Institute of Standards and Materials.

[25]   www.harvardthermal.com - TAS (Thermal Analysis Software)

[26]   www.sirtrade.com/default0.htm - SAFIR

[27]   www.webmineral.com/data/Vermiculite.shtml – Vermiculite Information

[28]   Yuen W.W. "The Effect of Thermal Radiation on the Dynamics of Flashover in a Compartment Fire." The 6th ASME-JSME Thermal Engineering Joint Conference, March 16-20, 2003.

11 APPENDIX

A BLETZACKER'S DATA

A.1 Time-Temperature Data

In this thesis, the data from Professor Bletzacker's study was used as a benchmark for all the TAS models. Table A-I presents the temperature data at different locations for W12*x*24 section. This data was recorded by the use of thermocouples placed within the steel section.

Table A-I Temperature results for different locations from Bletzacker's experiments

Bletzacker's Data (Temperature results when heat is applied at mid-span)											
Location			**Location 1**			**Location 2**			**Location 3**		**Location 4**
Time	*Time*		*Temperature*			*Temperature*			*Temperature*		*Temperature*
min	*sec*		°F	°C		°F	°C		°F	°C	°F	°C
0	0		70	21.11		70	21.111		70	21.11	70	21.11
5	300		100	37.78		115	46.111		115	46.11	85	29.44
10	600		155	68.33		165	73.889		175	79.44	110	43.33
15	900		200	93.33		210	98.889		205	96.11	145	62.78
20	1200		235	112.78		280	137.778		255	123.89	175	79.44
25	1500		300	148.89		360	182.222		330	165.56	200	93.33
30	1800		385	196.11		450	232.222		420	215.56	220	104.44
35	2100		480	248.89		540	282.222		505	262.78	255	123.89
40	2400		570	298.89		625	329.444		575	301.67	285	140.56
45	2700		655	346.11		715	379.444		645	340.56	300	148.89
50	3000		730	387.78		790	421.111		715	379.44	330	165.56
55	3300		805	429.44		860	460.000		770	410.00	370	187.78
60	3600		880	471.11		925	496.111		830	443.33	410	210.00
65	3900		940	504.44		985	529.444		875	468.33	445	229.44
70	4200		1000	537.78		1045	562.778		935	501.67	480	248.89
75	4500		1055	568.33		1100	593.333		985	529.44	520	271.11
80	4800		1110	598.89		1150	621.111		1030	554.44	555	290.56
85	5100		1160	626.67		1200	648.889		1070	576.67	585	307.22
90	5400		1200	648.89		1240	671.111		1120	604.44	750	398.89
95	5700		1245	673.89		1280	693.333		1155	623.89	790	421.11
100	6000		1280	693.33		1315	712.778		1190	643.33	810	432.22
105	6300		1320	715.56		1345	729.444		1230	665.56	830	443.33
110	6600		1340	726.67		1365	740.556		1265	685.00	855	457.22
114	6840		1345	729.44		1380	748.889		1290	698.89	870	465.56

A.2 **Properties of Materials**

A.2.1 *Steel Properties*

Properties like density and emissivity, for steel, were constant, and their values were 7850 kg/m^3 and 0.8 respectively. Temperature dependant properties like thermal conductivity and specific heat were calculated based on the equations given below.

Thermal conductivity

$$k_s = 54 - \left(\frac{T_s}{300}\right) \qquad \text{for } 20°C < T \leq 800°C \qquad \text{-[A-1]}$$

$$k_s = 27.3 \qquad \text{for } T_s > 800°C \qquad \text{-[A-2]}$$

Specific Heat

$$C_s = 425 + 0.733T_s + 0.000169T_s^2 + 2.22x10^{-6}T_s^3 \qquad \text{-[A-3]}$$

$$\text{for } 20°C \leq T_s \leq 600°C$$

$$C_s = 666\left(\frac{13002}{T_s - 738}\right) \qquad \text{-[A-4]}$$

$$\text{for } 600°C < T_s \leq 735°C$$

$$C_s = 545 - \left(\frac{17820}{T_s - 731}\right) \qquad \text{-[A-5]}$$

$$\text{for } 735°C < T_s \leq 900°C$$

$$C_s = 650 \qquad \text{for } T_s > 900°C \qquad \text{-[A-6]}$$

Thermal properties of steel were calculated based on the temperature results from Bletzacker's data. For all the models, temperature data for Location 1 was taken into consideration for evaluating thermal properties of steel.

Table A-II summarizes the thermal properties that were calculated based on Bletzacker's experimental data **[1].** These values were eventually used as arrays for the TAS models.

Table A-II Thermal Properties of Steel

Time	Time		Temperature		Thermal Conductivity (k_s)	Specific Heat (C_s)
					Steel Properties	
min	*sec*		*°F*	*°C*	*W/mK*	*J/kgK*
0	0		70	21.11	53.934	440.587
5	300		100	37.78	53.869	451.910
10	600		155	68.33	53.772	470.639
15	900		200	93.33	53.686	484.230
20	1200		235	112.78	53.622	493.867
25	1500		300	148.89	53.504	509.955
30	1800		385	196.11	53.342	528.341
35	2100		480	248.89	53.170	546.930
40	2400		570	298.89	52.998	564.342
45	2700		655	346.11	52.848	582.139
50	3000		730	387.78	52.708	600.074
55	3300		805	429.44	52.569	621.109
60	3600		880	471.11	52.429	646.206
65	3900		940	504.44	52.321	669.857
70	4200		1000	537.78	52.203	697.218
75	4500		1055	568.33	52.106	725.979
80	4800		1110	598.89	51.999	758.653
85	5100		1160	626.67	51.913	782.784
90	5400		1200	648.89	51.838	811.908
95	5700		1245	673.89	51.752	868.804
100	6000		1280	693.33	51.687	957.089
105	6300		1320	715.56	51.612	1245.297
110	6600		1340	726.67	51.580	1813.235
114	6900		1345	729.44	51.569	2185.715

A.2.2   *Properties of Vermiculite*

Table A-III summarizes the values obtained from the tests conducted by Schundler Company, Inc., which is a local company based in New Jersey, USA. The test was carried out for one meter thickness of vermiculite.

Table A-III Thermal Resistivity data from test done by Schundler Company Inc.

Mean Temp. ^0F (^0C)	4-Super Fine (Vermiculite) $^0F \cdot h \cdot ft^2/Btu$ $(K \cdot m^2/W)$
-199 (-84)	3.4 (0.59)
-58 (-50)	3.0 (0.52)
-13 (-25)	2.7 (0.48)
75 (24)	2.3 (0.40)
212 (100)	1.8 (0.32)
302 (150)	1.6 (0.28)
392 (200)	1.4 (0.25)
482 (250)	1.2 (0.22)
572 (300)	1.1 (0.19)
662 (350)	0.94 (0.17)
752 (400)	0.84 (0.15)
850 (454)	0.73 (0.13)

Thermal Conductivity

Thermal conductivity is defined as the inverse of thermal resistivity. The values presented in Table A-III were used along with the techniques of interpolation and curve fitting to estimate a reasonable performance of vermiculite at temperatures higher than **454°C** as specified in the table above. Table A-IV presents the values for thermal conductivity that were used for the TAS models.

Table A-IV Thermal Conductivity at different temperatures based on data from experimental tests & interpolations

Temperature	Thermal Resistance	Thermal Conductivity
(°C)	(Km^2/W)	(W/mK)
20	0.400	0.064
100	0.320	0.079
150	0.280	0.091
200	0.250	0.102
250	0.220	0.115
300	0.190	0.134
350	0.170	0.149
400	0.150	0.169
450	0.130	0.195
500	0.198	0.129
550	0.198	0.129
600	0.198	0.129
650	0.198	0.129
700	0.198	0.129
750	0.198	0.129
800	0.198	0.129
850	0.198	0.129
900	0.198	0.129
950	0.198	0.129
1000	0.198	0.129
1060	0.198	0.129

Specific Heat

The technique of curve fitting was implemented to establish the properties for specific heat of vermiculite. Figure A.1 presents the results obtained from the tests conducted by Toman Jan *et. al* [20] and those from the technique of curve fitting. Table A-V presents the values that were used for the purpose of modeling specific heat for vermiculite.
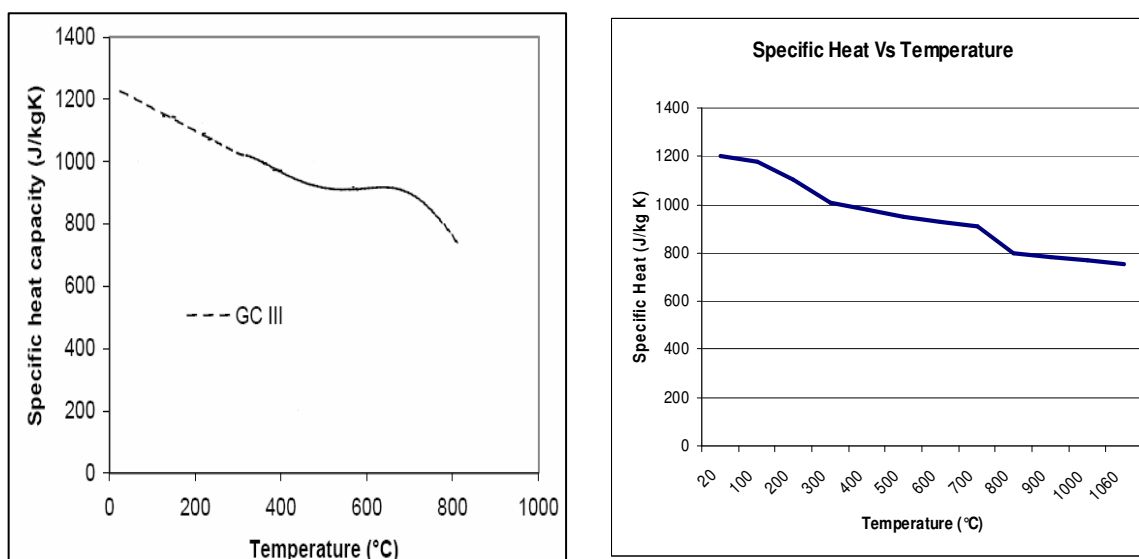
Figure A.1 Comparison of graph of Specific heat Vs Temperature obtained from test data,[16] and from the technique of curve fitting(Interpolation)

Table A-V Specific heat Vs Temperature data

Temperature (°C)	Specific heat (J/kgK)
20	1200
100	1180
200	1100
300	1010
400	980
500	950
600	925
700	910
800	800
900	780
1000	770
1060	755

A.2.3 *Thermal Properties of Gypsum*

The thermal properties of gypsum board are well established up to temperatures of 1200°C **[4]**. Tests were conducted by NIST to establish the behavior of thermal properties of gypsum at high temperatures.

Thermal Conductivity

Table A-VI presents the data for thermal conductivity from the tests done by NIST.

Table A-VI Thermal Conductivity data at different temperatures, NIST [4]

Temperature (°C)	Thermal Conductivity (W/mK)
20	0.25
100	0.12
200	0.12
300	0.12
400	0.12
500	0.17
600	0.22
700	0.27
800	0.27
900	0.4
1060	0.5

Specific Heat

Table A-VII presents the data for specific heat from the tests done by NIST.

Table A-VII Specific heat data at different temperatures, NIST [4]

Temperature (°C)	Specific heat (J/kgK)
20	1500
100	10000
125	18479
200	1500
300	700
400	650
500	625
600	550
650	3000
700	550
800	525
900	525
1060	525

B BARE STEEL MODEL WITH 4″ CONCRETE SLAB

Table B-I to B-VIII present the time-temperature data for the case of bare steel model with concrete slab simulated for different values of thermal conductivity and specific heat of concrete. This data was used to plot the graphs for different locations which have been presented in the thesis report.

Table B-I Time-Temperature data for bare steel model with constant thermal characteristics of concrete k_c = 1.95 W/mK, and C_{pc} =1200J/kgK

Location 1			Location 2			Location 3			Location 4	
Time	Temperature		Time	Temperature		Time	Temperature		Time	Temperature
(sec)	°C		(sec)	°C		(sec)	°C		(sec)	°C
0	21.1111		0	20		0	20		0	20
300	37.7754		300	37.4896		300	35.067		300	20.9902
600	68.3235		600	67.7168		600	63.3716		600	25.4532
900	93.3263		900	92.6947		900	88.6777		900	33.8731
1200	112.773		1200	112.162		1200	108.58		1200	43.8988
1500	148.881		1500	147.87		1500	142.969		1500	55.2042
1800	196.104		1800	194.706		1800	189.062		1800	70.6651
2100	248.88		2100	247.166		2100	241.232		2100	91.03
2400	298.873		2400	297.026		2400	291.275		2400	115.344
2700	346.105		2700	344.139		2700	338.546		2700	141.695
3000	387.773		3000	385.789		3000	380.481		3000	168.733
3300	429.437		3300	427.331		3300	422.013		3300	195.496
3600	471.1		3600	468.867		3600	463.505		3600	222.194
3900	504.44		3900	502.301		3900	497.319		3900	248.569
4200	537.774		4200	535.551		4200	530.557		4200	273.568
4500	568.327		4500	566.099		4500	561.218		4500	297.59
4800	598.882		4800	596.575		4800	591.663		4800	320.641
5100	626.661		5100	624.365		5100	619.578		5100	343.051
5400	648.887		5400	646.703		5400	642.208		5400	364.494
5700	673.887		5700	671.556		5700	666.881		5700	384.373
6000	693.331		6000	691.099		6000	686.662		6000	403.062
6300	715.55		6300	713.011		6300	708.108		6300	419.273
6600	726.663		6600	724.385		6600	719.971		6600	432.546
6900	729.44		6900	727.642		6900	724.055		6900	443.556

Table B-II Time-Temperature data for bare steel model with constant thermal characteristics of concrete k_c = 1.7 W/mK, and C_{pc} =1200J/kgK

Location 1			Location 2			Location 3			Location 4	
Time	Temperature		Time	Temperature		Time	Temperature		Time	Temperature
(sec)	°C		(sec)	°C		(sec)	°C		(sec)	°C
0	21.1111		0	20		0	20		0	20
300	37.7721		300	37.2514		300	35.0786		300	21.0249
600	68.3252		600	67.2083		600	63.4123		600	25.6759
900	93.3289		900	92.1647		900	88.7345		900	34.4682
1200	112.773		1200	111.651		1200	108.651		1200	44.9364
1500	148.876		1500	147.05		1500	143.067		1500	56.7075
1800	196.098		1800	193.61		1800	189.186		1800	72.7772
2100	248.874		2100	245.872		2100	241.382		2100	93.9293
2400	298.878		2400	295.684		2400	291.449		2400	119.164
2700	346.105		2700	342.785		2700	338.744		2700	146.481
3000	387.769		3000	384.488		3000	380.699		3000	174.468
3300	429.436		3300	426.022		3300	422.254		3300	202.121
3600	471.102		3600	467.556		3600	463.771		3600	229.657
3900	504.437		3900	501.113		3900	497.604		3900	256.822
4200	537.775		4200	534.383		4200	530.862		4200	282.521
4500	568.327		4500	564.987		4500	561.542		4500	307.168
4800	598.883		4800	595.485		4800	592.007		4800	330.777
5100	626.664		5100	623.335		5100	619.933		5100	353.693
5400	648.887		5400	645.773		5400	642.574		5400	375.585
5700	673.885		5700	670.615		5700	667.278		5700	395.832
6000	693.33		6000	690.252		6000	687.094		6000	414.821
6300	715.55		6300	712.149		6300	708.705		6300	431.233
6600	726.664		6600	723.744		6600	720.751		6600	444.599
6900	729.443		6900	727.164		6900	724.756		6900	455.619

Figures B.1 and B.2 present the comparison of time-temperature results from TAS model with a thermal conductivity value of 1.7 W/mK and the results from Bletzacker's experiments **[1].**
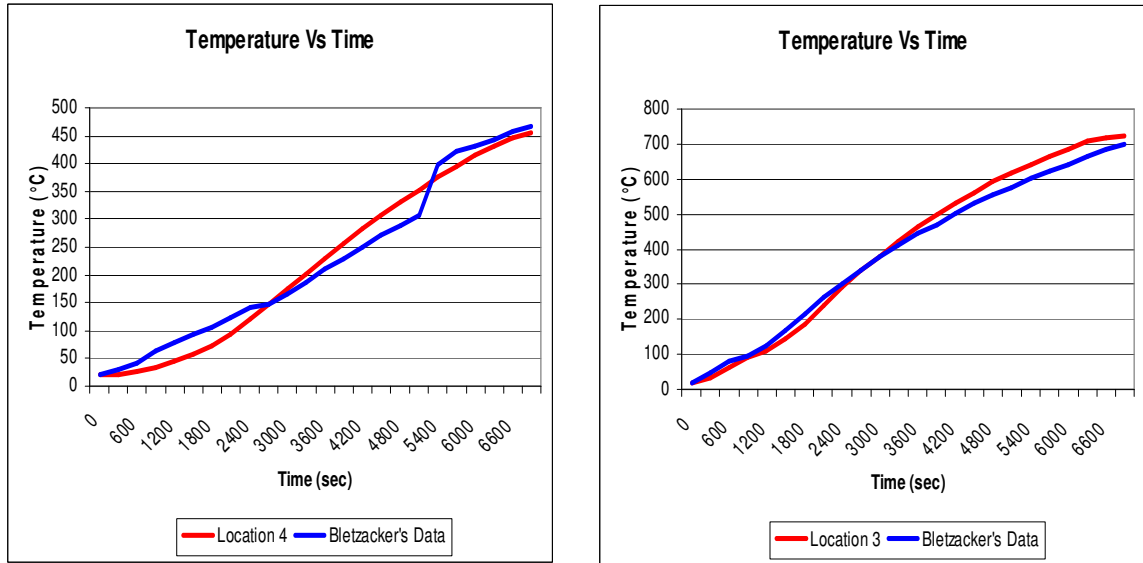
Figure B.1 Temperature Vs Time for Location 4 (left) and Location 3 (right)
[k=1.7 W/mK]
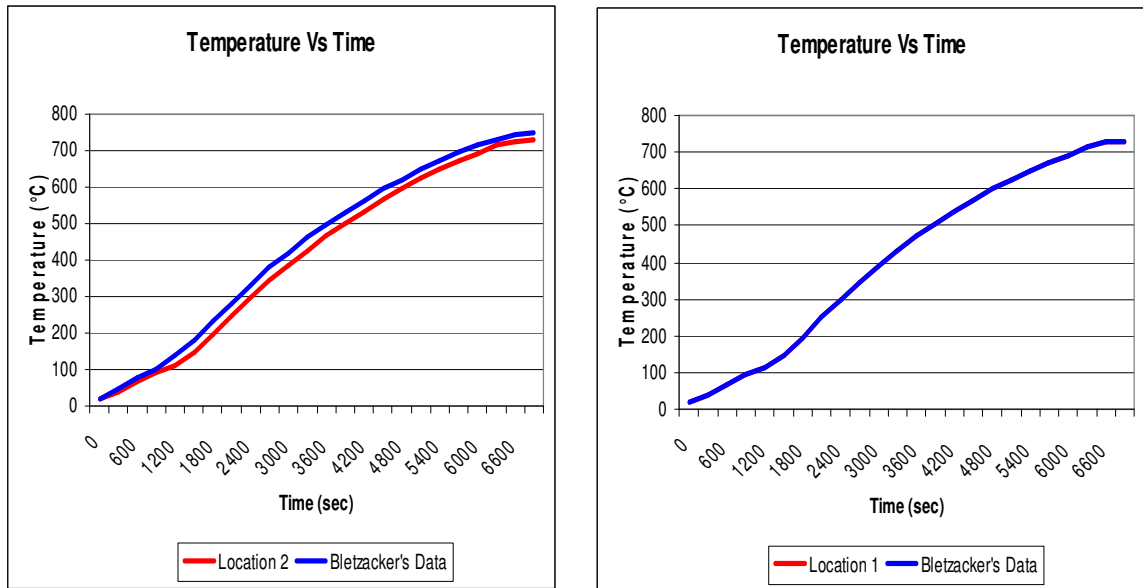
Figure B.2 Temperature Vs Time for Location 2 (left) and Location 1 (right)
[k=1.7 W/mK]

Table B-III Time-Temperature data for bare steel model with constant thermal characteristics of concrete, k_c = 1.6 W/mK, and C_{pc} =1200J/kgK

Location 1			Location 2			Location 3			Location 4	
Time (sec)	**Temperature °C**		**Time (sec)**	**Temperature °C**		**Time (sec)**	**Temperature °C**		**Time (sec)**	**Temperature °C**
0	21.1111		0	20		0	20		0	20
300	37.7721		300	37.2517		300	35.0802		300	21.0398
600	68.3252		600	67.2096		600	63.4189		600	25.7729
900	93.3289		900	92.1678		900	88.748		900	34.7291
1200	112.773		1200	111.656		1200	108.671		1200	45.3925
1500	148.885		1500	147.058		1500	143.093		1500	57.3684
1800	196.097		1800	193.621		1800	189.218		1800	73.7047
2100	248.872		2100	245.887		2100	241.422		2100	95.2015
2400	298.876		2400	295.703		2400	291.496		2400	120.84
2700	346.102		2700	342.808		2700	338.799		2700	148.58
3000	387.766		3000	384.515		3000	380.761		3000	176.982
3300	429.44		3300	426.053		3300	422.322		3300	205.023
3600	471.105		3600	467.59		3600	463.845		3600	232.925
3900	504.439		3900	501.15		3900	497.682		3900	260.434
4200	537.772		4200	534.422		4200	530.945		4200	286.439
4500	568.329		4500	565.029		4500	561.629		4500	311.361
4800	598.886		4800	595.528		4800	592.097		4800	335.215
5100	626.661		5100	623.379		5100	620.026		5100	358.354
5400	648.885		5400	645.818		5400	642.669		5400	380.445
5700	673.885		5700	670.661		5700	667.374		5700	400.856
6000	693.331		6000	690.299		6000	687.192		6000	419.981
6300	715.552		6300	712.195		6300	708.802		6300	436.485
6600	726.663		6600	723.79		6600	720.847		6600	449.896
6900	729.444		6900	727.212		6900	724.855		6900	460.925

Figures B.3 and B.4 present the comparison for the time-temperature results from TAS model with a thermal conductivity value of 1.6 W/mK and the results from Bletzacker's experiments **[1].**
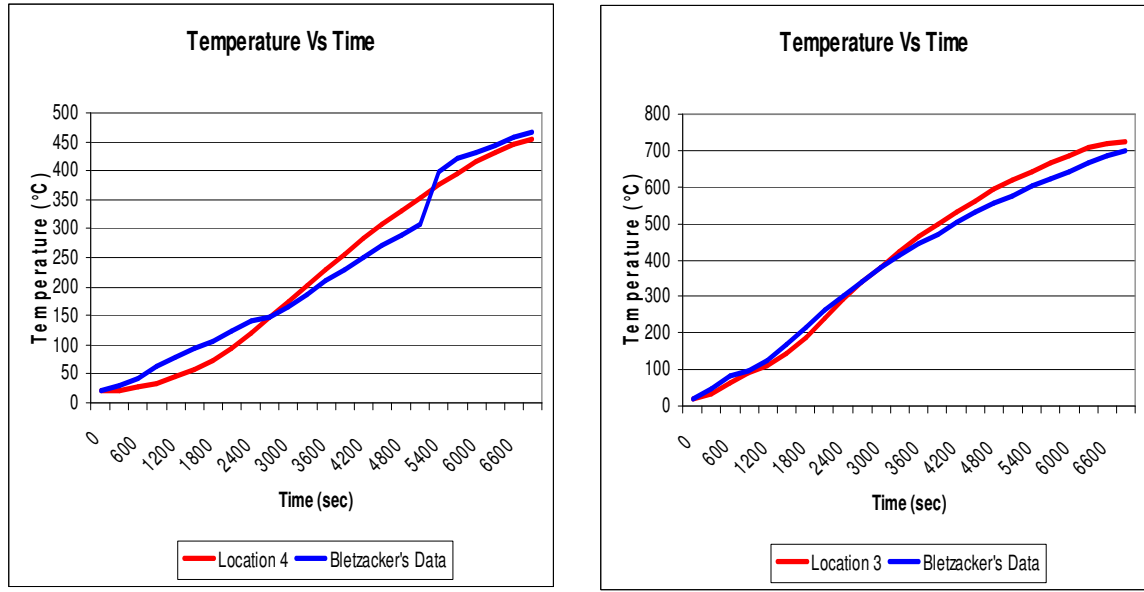
Figure B.3 Temperature Vs Time for Location 4 (left) and Location 3 (right)
[k=1.6 W/mK]
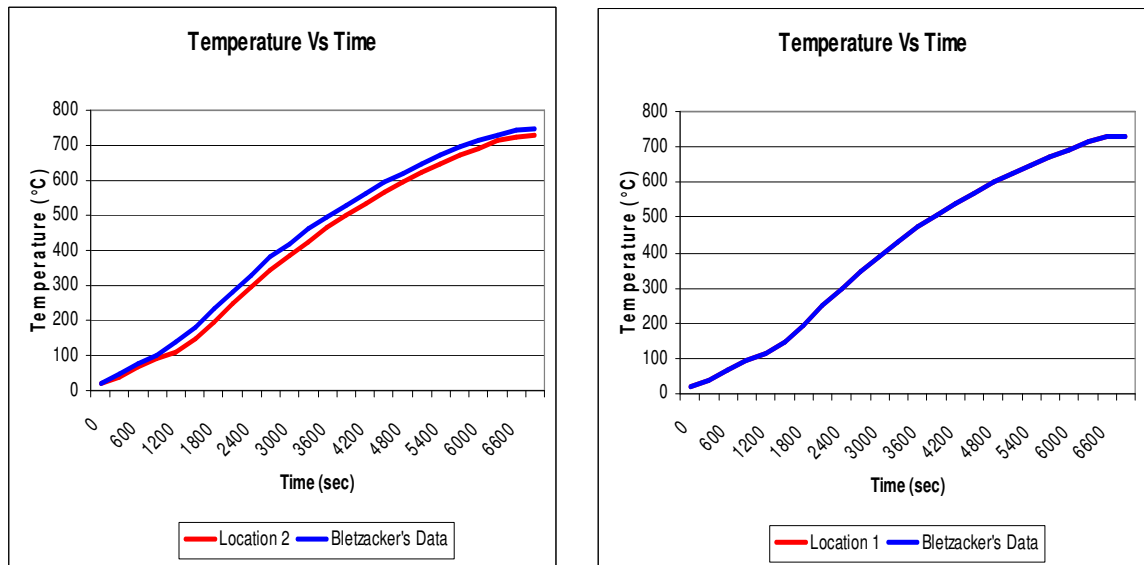
Figure B.4 Temperature Vs Time for Location 2 (left) and Location 1 (right)
[k=1.6 W/mK]

Table B-IV Time-Temperature data for bare steel model with constant thermal characteristics of concrete k_c = 1.5 W/mK, and C_{pc} =1200J/kgK

Location 1			Location 2			Location 3			Location 4	
Time	Temperature		Time	Temperature		Time	Temperature		Time	Temperature
(sec)	°C		(sec)	°C		(sec)	°C		(sec)	°C
0	21.1111		0	20		0	20		0	20
300	37.7721		300	37.252		300	35.0818		300	21.0553
600	68.3253		600	67.211		600	63.4257		600	25.875
900	93.329		900	92.171		900	88.7622		900	35.0049
1200	112.773		1200	111.661		1200	108.692		1200	45.8758
1500	148.884		1500	147.066		1500	143.12		1500	58.0688
1800	196.096		1800	193.632		1800	189.252		1800	74.6869
2100	248.871		2100	245.902		2100	241.464		2100	96.5479
2400	298.873		2400	295.723		2400	291.546		2400	122.613
2700	346.099		2700	342.832		2700	338.857		2700	150.799
3000	387.771		3000	384.544		3000	380.826		3000	179.64
3300	429.436		3300	426.085		3300	422.393		3300	208.091
3600	471.102		3600	467.626		3600	463.922		3600	236.379
3900	504.436		3900	501.189		3900	497.765		3900	264.251
4200	537.774		4200	534.463		4200	531.032		4200	290.579
4500	568.327		4500	565.072		4500	561.72		4500	315.79
4800	598.883		4800	595.573		4800	592.191		4800	339.903
5100	626.663		5100	623.426		5100	620.122		5100	363.277
5400	648.887		5400	645.866		5400	642.768		5400	385.58
5700	673.885		5700	670.709		5700	667.475		5700	406.166
6000	693.329		6000	690.348		6000	687.294		6000	425.437
6300	715.551		6300	712.244		6300	708.903		6300	442.041
6600	726.664		6600	723.838		6600	720.947		6600	455.501
6900	729.443		6900	727.261		6900	724.958		6900	466.543

Figures B.5 and B.6 present the comparison for the time-temperature results from TAS model with a thermal conductivity value of 1.6 W/mK and the results from Bletzacker's experiments **[1].**
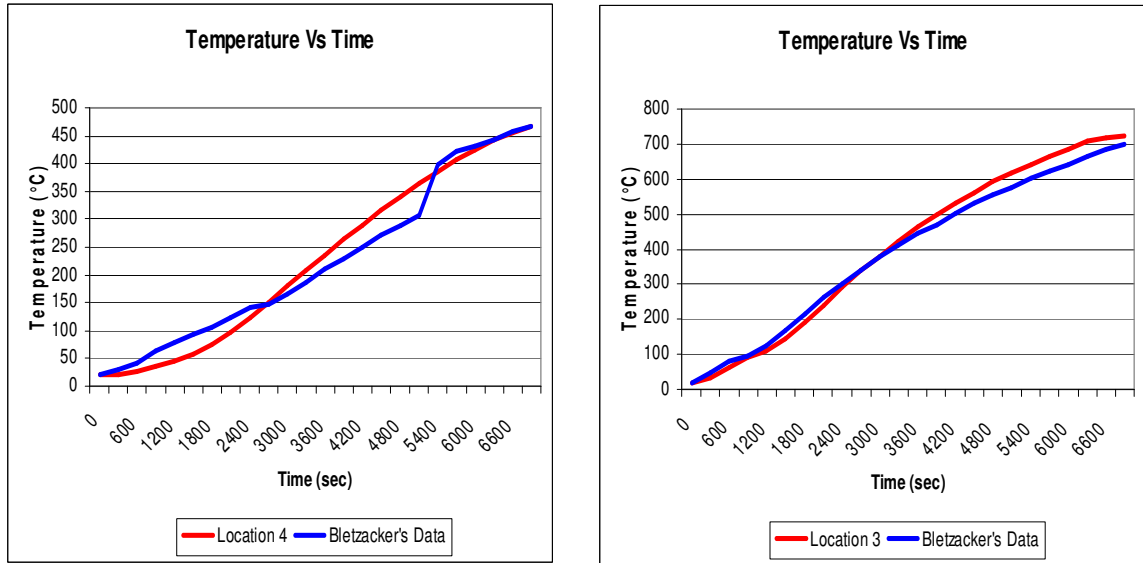
Figure B.5 Temperature Vs Time for Location 4 (left) and Location 3 (right)
[k=1.5 W/mK]
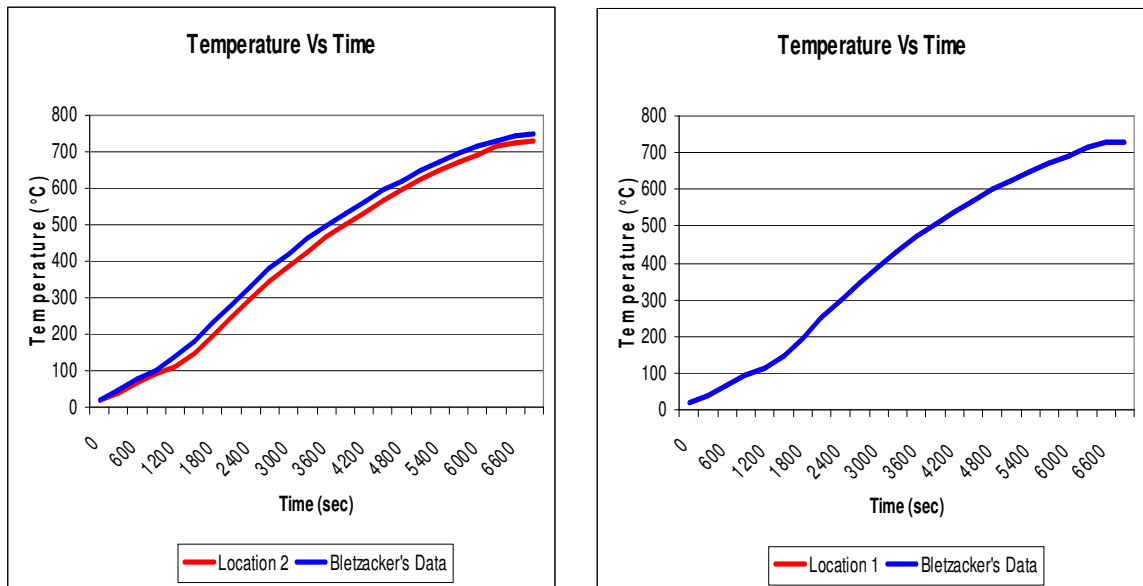
Figure B.6 Temperature Vs Time for Location 4 (left) and Location 3 (right)
[k=1.5 W/mK]

Table B-V Time-Temperature data for bare steel model with constant thermal characteristics of concrete k_c = 1.95 W/mK, and C_{pc} =1260 J/kgK

Location 1			Location 2			Location 3			Location 4	
Time (sec)	**Temperature °C**		**Time (sec)**	**Temperature °C**		**Time (sec)**	**Temperature °C**		**Time (sec)**	**Temperature °C**
0	21.1111		0	20		0	20		0	20
300	37.7721		300	37.49		300	35.0728		300	20.9795
600	68.3251		600	67.7186		600	63.3904		600	25.4737
900	93.3289		900	92.6963		900	88.6918		900	33.9732
1200	112.773		1200	112.163		1200	108.59		1200	44.038
1500	148.877		1500	147.873		1500	142.989		1500	55.4461
1800	196.1		1800	194.71		1800	189.088		1800	71.1794
2100	248.879		2100	247.172		2100	241.263		2100	91.9322
2400	298.874		2400	297.033		2400	291.307		2400	116.63
2700	346.103		2700	344.147		2700	338.581		2700	143.309
3000	387.77		3000	385.798		3000	380.517		3000	170.622
3300	429.437		3300	427.343		3300	422.055		3300	197.69
3600	471.104		3600	468.882		3600	463.557		3600	224.836
3900	504.439		3900	502.318		3900	497.376		3900	251.657
4200	537.772		4200	535.571		4200	530.623		4200	277.083
4500	568.329		4500	566.121		4500	561.293		4500	301.59
4800	598.885		4800	596.601		4800	591.75		4800	325.187
5100	626.663		5100	624.393		5100	619.668		5100	348.103
5400	648.885		5400	646.734		5400	642.304		5400	369.882
5700	673.887		5700	671.595		5700	667.003		5700	390.265
6000	693.331		6000	691.15		6000	686.817		6000	409.908
6300	715.551		6300	713.118		6300	708.429		6300	428.392
6600	726.665		6600	724.556		6600	720.478		6600	445.956
6900	729.444		6900	727.783		6900	724.475		6900	460.924

Figures B.7 and B.8 present the comparison for the time-temperature results from TAS model with a specific heat value of 1260 J/kgK and the results from Bletzacker's experiments **[1].**
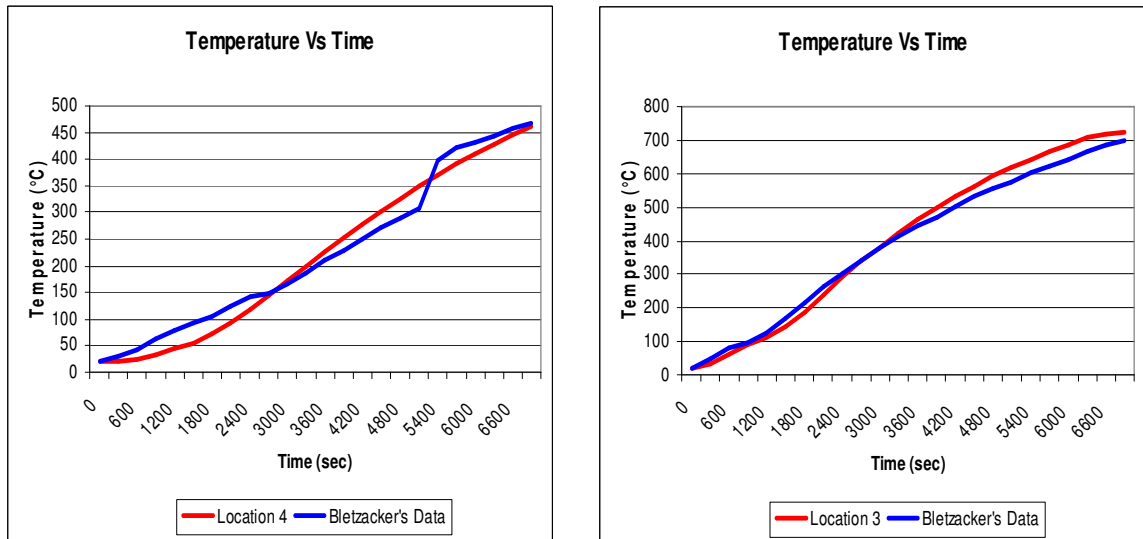
Figure B.7 Temperature Vs Time for Location 4 (left) and Location 3 (right)
$[C_{pc} = 1260 \ J/kgK]$
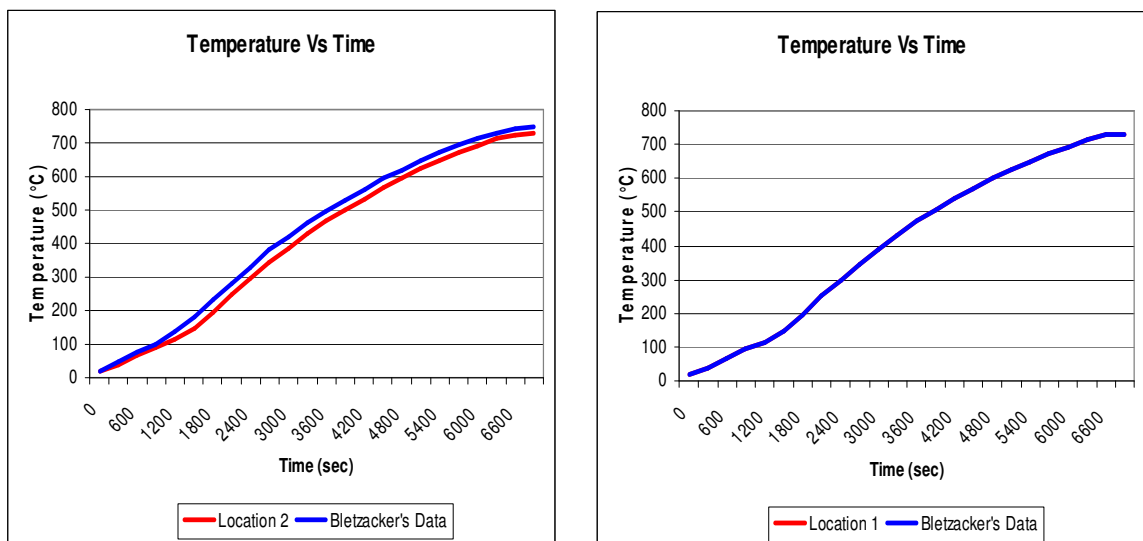
Figure B.8 Temperature Vs Time for Location 2 (left) and Location 1 (right)
$[C_{pc} = 1260 \ J/kgK]$

Table B-VI Time-Temperature data for bare steel model with constant thermal characteristics of concrete k_c = 1.95 W/mK, and C_{pc} =1200J/kgK

Location 1			Location 2			Location 3			Location 4	
Time	**Temperature**		**Time**	**Temperature**		**Time**	**Temperature**		**Time**	**Temperature**
(sec)	**°C**		**(sec)**	**°C**		**(sec)**	**°C**		**(sec)**	**°C**
0	21.1111		0	20		0	20		0	20
300	37.7721		300	37.4902		300	35.0752		300	20.9902
600	68.3252		600	67.7193		600	63.3978		600	25.4532
900	93.3289		900	92.6978		900	88.7047		900	33.8731
1200	112.773		1200	112.166		1200	108.607		1200	43.8988
1500	148.876		1500	147.876		1500	143.01		1500	55.2042
1800	196.099		1800	194.715		1800	189.115		1800	70.6651
2100	248.877		2100	247.179		2100	241.295		2100	91.03
2400	298.883		2400	297.041		2400	291.345		2400	115.344
2700	346.101		2700	344.157		2700	338.623		2700	141.695
3000	387.767		3000	385.81		3000	380.563		3000	168.733
3300	429.435		3300	427.356		3300	422.104		3300	195.496
3600	471.102		3600	468.896		3600	463.609		3600	222.194
3900	504.437		3900	502.333		3900	497.43		3900	248.569
4200	537.77		4200	535.587		4200	530.68		4200	273.568
4500	568.327		4500	566.139		4500	561.352		4500	297.59
4800	598.883		4800	596.62		4800	591.81		4800	320.641
5100	626.661		5100	624.412		5100	619.73		5100	343.051
5400	648.887		5400	646.753		5400	642.366		5400	364.494
5700	673.884		5700	671.616		5700	667.067		5700	384.373
6000	693.331		6000	691.171		6000	686.881		6000	403.062
6300	715.551		6300	713.139		6300	708.493		6300	419.273
6600	726.663		6600	724.577		6600	720.542		6600	432.546
6900	729.444		6900	727.805		6900	724.541		6900	443.556

Table B-VII Time-Temperature data for bare steel model with constant thermal

characteristics of concrete $k_c = 1.95W/mK$, and $C_{pc} =1085 \, J/kgK$

Location 1			Location 2			Location 3			Location 4	
Time	Temperature		Time	Temperature		Time	Temperature		Time	Temperature
(sec)	°C		(sec)	°C		(sec)	°C		(sec)	°C
0	21.1111		0	20		0	20		0	20
300	37.7721		300	37.4906		300	35.0794		300	21.0429
600	68.3252		600	67.7208		600	63.412		600	25.6845
900	93.3289		900	92.7007		900	88.7296		900	34.3797
1200	112.773		1200	112.17		1200	108.641		1200	44.6785
1500	148.876		1500	147.882		1500	143.052		1500	56.2782
1800	196.098		1800	194.724		1800	189.167		1800	72.1451
2100	248.875		2100	247.191		2100	241.357		2100	93.0175
2400	298.879		2400	297.057		2400	291.416		2400	117.885
2700	346.097		2700	344.176		2700	338.704		2700	144.775
3000	387.771		3000	385.832		3000	380.651		3000	172.308
3300	429.438		3300	427.381		3300	422.199		3300	199.513
3600	471.104		3600	468.924		3600	463.71		3600	226.623
3900	504.439		3900	502.363		3900	497.536		3900	253.374
4200	537.772		4200	535.619		4200	530.789		4200	278.695
4500	568.329		4500	566.172		4500	561.465		4500	303.011
4800	598.885		4800	596.655		4800	591.926		4800	326.334
5100	626.662		5100	624.449		5100	619.849		5100	349.007
5400	648.885		5400	646.792		5400	642.488		5400	370.692
5700	673.884		5700	671.655		5700	667.191		5700	390.783
6000	693.33		6000	691.211		6000	687.007		6000	409.667
6300	715.55		6300	713.18		6300	708.619		6300	426.021
6600	726.665		6600	724.618		6600	720.666		6600	439.387
6900	729.444		6900	727.847		6900	724.67		6900	450.454

Figures B.9 and B.10 present the comparison for the time-temperature results from TAS model with a specific heat value of 1085 J/kgK and the results from Bletzacker's experiments **[1].**
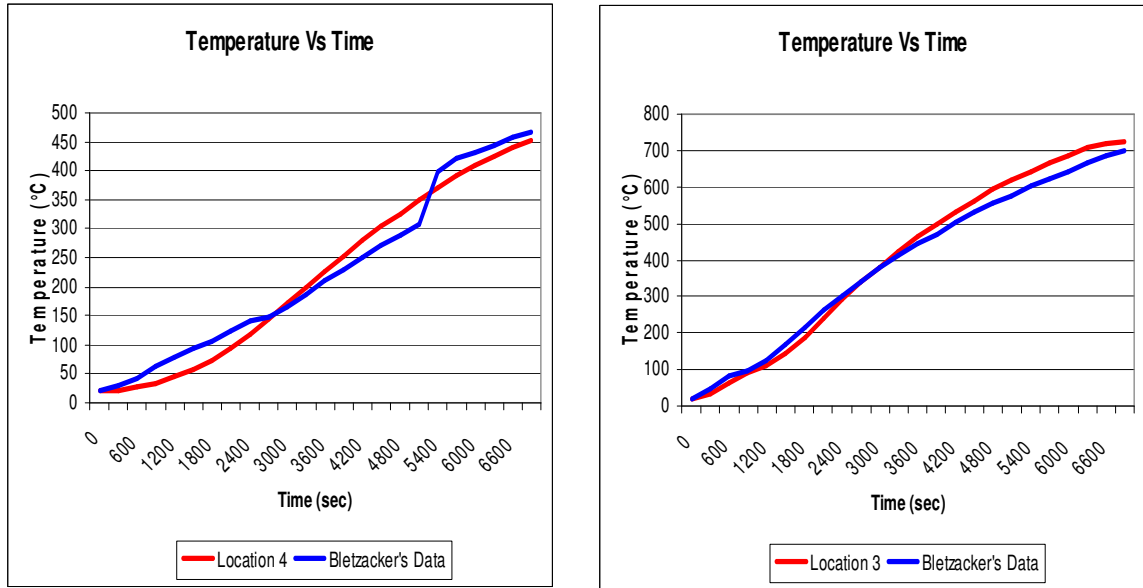
Figure B.9 Temperature Vs Time for Location 4 (left) and Location 3 (right) [C_{pc} =1085 J/kgK]
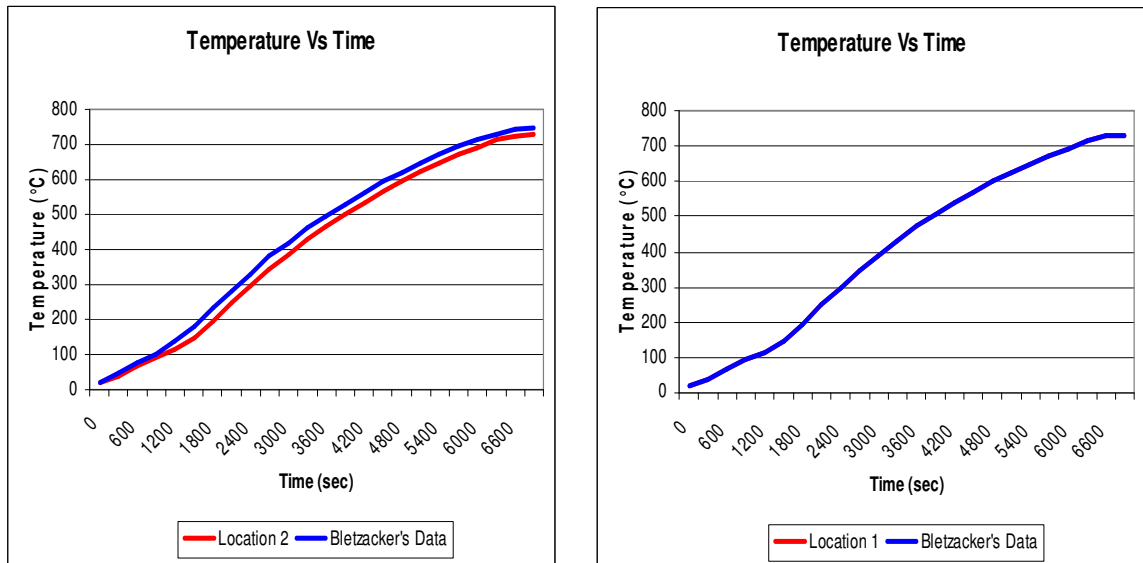
Figure B.10 Temperature Vs Time for Location 4 (left) and Location 3 (right) [C_{pc} =1085 J/kgK]

Table B-VIII Time-Temperature data for bare steel model with constant thermal characteristics of concrete k_c = 1.95W/mK, and C_{pc} =1023 J/kgK

Location 1			Location 2			Location 3			Location 4	
Time	Temperature		Time	Temperature		Time	Temperature		Time	Temperature
(sec)	°C		(sec)	°C		(sec)	°C		(sec)	°C
0	21.1111		0	20		0	20		0	20
300	37.7721		300	37.4908		300	35.0817		300	21.072
600	68.3253		600	67.7216		600	63.4197		600	25.8124
900	93.3289		900	92.7023		900	88.7432		900	34.6602
1200	112.773		1200	112.172		1200	108.659		1200	45.1103
1500	148.876		1500	147.885		1500	143.075		1500	56.8724
1800	196.098		1800	194.729		1800	189.195		1800	72.9629
2100	248.874		2100	247.198		2100	241.391		2100	94.115
2400	298.878		2400	297.066		2400	291.456		2400	119.287
2700	346.104		2700	344.187		2700	338.748		2700	146.475
3000	387.769		3000	385.844		3000	380.7		3000	174.28
3300	429.436		3300	427.394		3300	422.251		3300	201.729
3600	471.102		3600	468.939		3600	463.765		3600	229.067
3900	504.437		3900	502.379		3900	497.594		3900	256.026
4200	537.775		4200	535.637		4200	530.85		4200	281.528
4500	568.327		4500	566.191		4500	561.527		4500	306.009
4800	598.884		4800	596.674		4800	591.99		4800	329.487
5100	626.664		5100	624.469		5100	619.915		5100	352.309
5400	648.887		5400	646.813		5400	642.555		5400	374.133
5700	673.884		5700	671.677		5700	667.259		5700	394.347
6000	693.329		6000	691.233		6000	687.076		6000	413.343
6300	715.551		6300	713.203		6300	708.688		6300	429.782
6600	726.665		6600	724.641		6600	720.736		6600	443.202
6900	729.444		6900	727.871		6900	724.742		6900	454.305

Figures B.11 and B.12 present the comparison for the time-temperature results from TAS model with a specific heat value of 1023 J/kgK and the results from Bletzacker's experiments
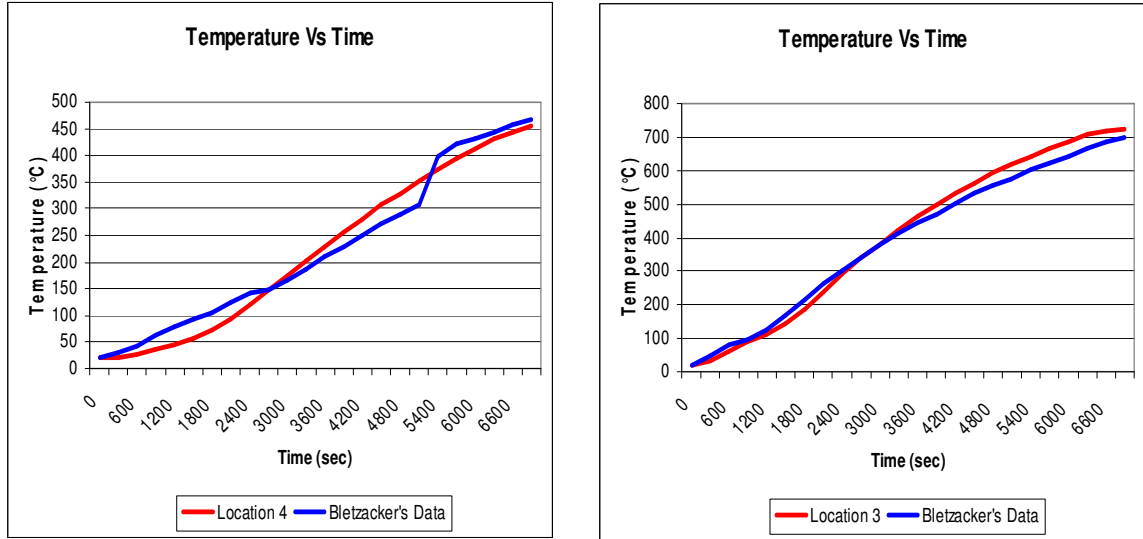
Figure B.11 Temperature Vs Time for Location 4 (left) and Location 3 (right)
[C_{pc}=1023 J/kgK]
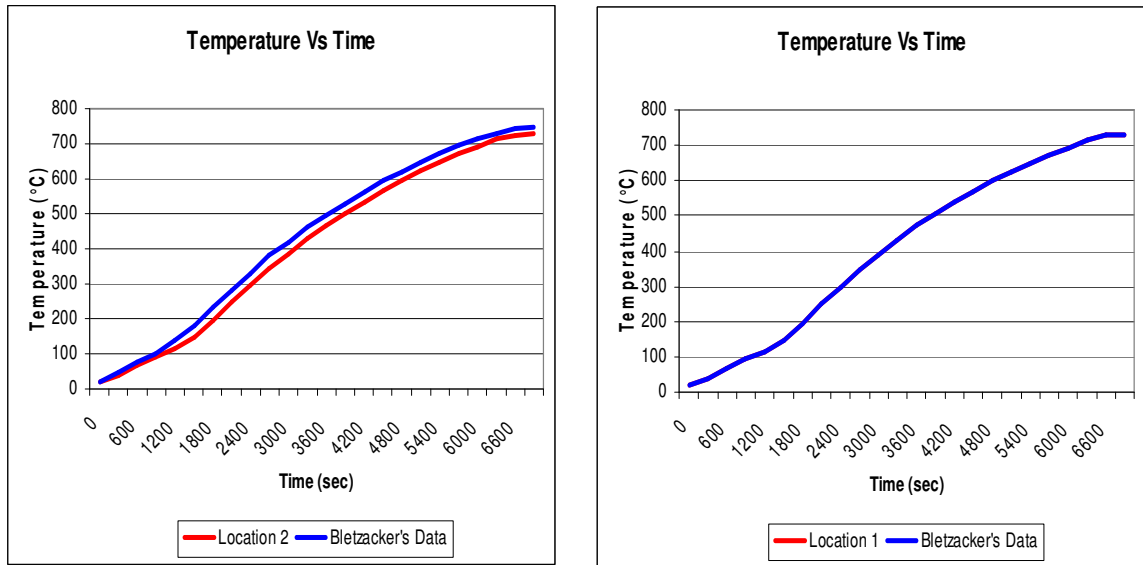
Figure B.12 Temperature Vs Time for Location 4 (left) and Location 3 (right)
[C_{pc}=1023 J/kgK]

C W 12*x*27 WITH 0.5″ THICK VERMICULITE COATING

The model was simulated for constant and variable values of thermal conductivity and specific heat of vermiculite. Table C-I presents the time-temperature data for the case of constant thermal properties for vermiculite, while Table C-II presents the data for the case of variable thermal properties for vermiculite. The data obtained from TAS simulations and was used to plot the graphs for different locations which were presented in the thesis report.

Table C-I Time-Temperature data for vermiculite model with constant values of thermal conductivity and specific heat

Location 1			Location 2			Location 3			Location 4	
Time (sec)	Temperature °C		Time (sec)	Temperature °C		Time (sec)	Temperature °C		Time (sec)	Temperature °C
0	20		0	20		0	20		0	20
300	27.2791		300	30.9247		300	23.3594		300	20.0196
600	94.1362		600	109.279		600	90.6201		600	22.2456
900	199.689		900	215.852		900	201.272		900	34.9342
1200	304.182		1200	319.268		1200	299.197		1200	57.9571
1500	398.304		1500	412.345		1500	380.866		1500	86.8885
1800	478.972		1800	491.93		1800	448.945		1800	118.772
2100	546.229		2100	558.253		2100	505.469		2100	151.811
2400	601.822		2400	613.052		2400	552.768		2400	184.895
2700	648.419		2700	658.968		2700	592.561		2700	217.189
3000	686.896		3000	696.692		3000	627.132		3000	248.048
3300	715.563		3300	723.903		3300	657.074		3300	277.169
3600	732.338		3600	740.516		3600	681.861		3600	304.425
3900	746.2		3900	755.292		3900	701.252		3900	329.71
4200	760.392		4200	769.678		4200	716.69		4200	352.926
4500	774.553		4500	783.828		4500	730.042		4500	374.061
4800	788.58		4800	797.815		4800	743.126		4800	393.191
5100	802.49		5100	811.645		5100	756.117		5100	410.485
5400	816.175		5400	825.179		5400	768.837		5400	426.155
5700	829.506		5700	838.294		5700	781.26		5700	440.377
6000	842.446		6000	851.018		6000	793.335		6000	453.317
6300	855.005		6300	863.349		6300	805.118		6300	465.151
6600	867.089		6600	875.171		6600	816.437		6600	476.024
6900	878.615		6900	886.388		6900	827.219		6900	486.069

Table C-II Time-Temperature data for vermiculite model with variable values of thermal conductivity and specific heat

Location 1			Location 2			Location 3			Location 4	
Time	**Temperature**		**Time**	**Temperature**		**Time**	**Temperature**		**Time**	**Temperature**
(sec)	**°C**		**(sec)**	**°C**		**(sec)**	**°C**		**(sec)**	**°C**
0	20		0	20		0	20		0	20
300	20.0196		300	23.3594		300	30.9247		300	27.2791
600	22.2456		600	90.6201		600	109.279		600	94.1362
900	34.9342		900	201.272		900	215.852		900	199.689
1200	57.9571		1200	299.197		1200	319.268		1200	304.182
1500	86.8885		1500	380.866		1500	412.345		1500	398.304
1800	118.772		1800	448.945		1800	491.93		1800	478.972
2100	151.811		2100	505.469		2100	558.253		2100	546.229
2400	184.895		2400	552.768		2400	613.052		2400	601.822
2700	217.189		2700	592.561		2700	658.968		2700	648.419
3000	248.048		3000	627.132		3000	696.692		3000	686.896
3300	277.169		3300	657.074		3300	723.903		3300	715.563
3600	304.425		3600	681.861		3600	740.516		3600	732.338
3900	329.71		3900	701.252		3900	755.292		3900	746.2
4200	352.926		4200	716.69		4200	769.678		4200	760.392
4500	374.061		4500	730.042		4500	783.828		4500	774.553
4800	393.191		4800	743.126		4800	797.815		4800	788.58
5100	410.485		5100	756.117		5100	811.645		5100	802.49
5400	426.155		5400	768.837		5400	825.179		5400	816.175
5700	440.377		5700	781.26		5700	838.294		5700	829.506
6000	453.317		6000	793.335		6000	851.018		6000	842.446
6300	465.151		6300	805.118		6300	863.349		6300	855.005
6600	476.024		6600	816.437		6600	875.171		6600	867.089
6900	486.069		6900	827.219		6900	886.388		6900	878.615

D   W 12*x*27 BEAM WITH 5/8″ THICK GYPSUM BOARD

The model was simulated for constant and variable values of thermal conductivity and specific heat of gypsum. Table D-I presents the time-temperature data for the case of constant thermal properties for gypsum board, while Table D-II presents the data for the case of variable thermal properties for gypsum board. The data obtained from TAS simulations was used to plot the graphs for different locations which were presented in the thesis report.

Table D-I Time-temperature data for gypsum model with constant values of thermal conductivity and specific heat

Location 1			Location 2			Location 3			Location 4	
Time	**Temperature**		**Time**	**Temperature**		**Time**	**Temperature**		**Time**	**Temperature**
(sec)	**°C**		**(sec)**	**°C**		**(sec)**	**°C**		**(sec)**	**°C**
0	20		0	20		0	20		0	20
300	28.3064		300	31.7198		300	20.1695		300	24.5406
600	68.585		600	86.1684		600	24.8693		600	56.0733
900	124.217		900	151.902		900	41.3097		900	87.3807
1200	179.994		1200	212.453		1200	68.2059		1200	114.079
1500	232.045		1500	266.629		1500	100.692		1500	138.01
1800	279.95		1800	315.367		1800	135.146		1800	160.11
2100	323.899		2100	359.457		2100	169.597		2100	180.849
2400	364.187		2400	399.497		2400	203.055		2400	200.479
2700	401.084		2700	435.917		2700	235.035		2700	219.148
3000	434.88		3000	469.112		3000	265.33		3000	236.983
3300	465.874		3300	499.455		3300	293.867		3300	254.055
3600	494.325		3600	527.232		3600	320.665		3600	270.433
3900	520.518		3900	552.776		3900	345.793		3900	286.202
4200	544.694		4200	576.316		4200	369.349		4200	301.382
4500	567.043		4500	598.043		4500	391.439		4500	315.985
4800	587.75		4800	618.189		4800	412.168		4800	330.088
5100	607.101		5100	637.034		5100	431.648		5100	343.758
5400	625.244		5400	654.636		5400	450.004		5400	356.97
5700	642.157		5700	670.97		5700	467.34		5700	369.718
6000	657.827		6000	686.046		6000	483.725		6000	382.063
6300	672.295		6300	699.854		6300	499.211		6300	394.053
6600	685.424		6600	712.118		6600	513.846		6600	405.65
6900	697.001		6900	722.739		6900	527.64		6900	416.842

Table D-II Time-temperature data for gypsum model with variable values of thermal conductivity and specific heat

Location 1			Location 2			Location 3			Location 4	
Time (sec)	Temperature °C		Time (sec)	Temperature °C		Time (sec)	Temperature °C		Time (sec)	Temperature °C
0	20		0	20		0	20		0	20
300	22.022		300	22.7005		300	20.0601		300	21.4812
600	27.9478		600	30.0624		600	20.9491		600	43.351
900	35.6002		900	38.6913		900	23.8617		900	67.0616
1200	47.1107		1200	51.7738		1200	29.6905		1200	87.4237
1500	59.4264		1500	67.3939		1500	38.3424		1500	106.672
1800	86.6316		1800	100.212		1800	49.3794		1800	126.675
2100	119.737		2100	135.86		2100	65.5588		2100	145.747
2400	153.4		2400	176.982		2400	90.0267		2400	166.063
2700	201.676		2700	231.755		2700	118.252		2700	185.684
3000	256.283		3000	289.94		3000	150.412		3000	204.963
3300	310.248		3300	345.702		3300	184.298		3300	223.029
3600	360.67		3600	397.081		3600	218.639		3600	240.283
3900	407.006		3900	444.141		3900	252.468		3900	257.039
4200	449.504		4200	487.226		4200	285.153		4200	273.332
4500	489.106		4500	526.882		4500	316.383		4500	289.209
4800	526.118		4800	563.647		4800	346.101		4800	304.757
5100	559.944		5100	597.514		5100	374.315		5100	319.998
5400	591.199		5400	627.98		5400	400.958		5400	334.866
5700	619.338		5700	654.888		5700	426.047		5700	349.321
6000	644.362		6000	679.574		6000	449.537		6000	363.414
6300	667.477		6300	701.939		6300	471.444		6300	377.157
6600	688.048		6600	720.576		6600	491.91		6600	390.475
6900	704.605		6900	734.29		6900	510.943		6900	403.336

E   W 12*x*27 BEAM WITH 0.5″ VERMICULITE COATING SUBJECTED TO ENV FIRE CURVE

The model for vermiculite was simulated for three different cases of peak fire intensities. Tables E-I, E-II, and E-III present the time-temperature histories that were formulated for the three cases of maximum fire intensities. Opening factor was modified in the range of 0.055 to 0.068 in order to test the sensitivity of the temperature results within the steel beam.

Case 1:

Opening Factor F = 0.062

Table E-I ENV Curve formulation-Maximum intensity of fire at 56 minutes

Time (sec)	Time (min)	Time (hrs)	t* (hrs)	Temperature (°C)
0	0	0.000	0.000	0
300	5	0.083	0.073	506
600	10	0.167	0.146	657
900	15	0.250	0.219	717
1200	20	0.333	0.292	752
1500	25	0.417	0.365	779
1800	30	0.500	0.439	802
2100	35	0.583	0.512	823
2400	40	0.667	0.585	842
2700	45	0.750	0.658	859
3000	50	0.833	0.731	875
3300	55	0.917	0.804	890
3360	**56**	**0.933**	**0.819**	**892**
3600	60	1.000	0.877	863
3900	65	1.083	0.950	823
4200	70	1.167	1.023	783
4500	75	1.250	1.096	743
4800	80	1.333	1.169	704
5100	85	1.417	1.242	664
5400	90	1.500	1.316	624
5700	95	1.583	1.389	584
6000	100	1.667	1.462	544
6300	105	1.750	1.535	504
6600	110	1.833	1.608	465
6900	115	1.917	1.681	425
7200	120	2.000	1.754	385

Case 2:

Opening Factor F = 0.068

Table E-II ENV Curve formulation-Maximum intensity of fire at 35.35 minutes

Time (sec)	Time (min)	Time (hrs)	t* (hrs) (hrs)	Temperature (°C)
0	0	0.000	0.000	0.000
300	5	0.083	0.088	551.638
600	10	0.167	0.176	686.878
900	15	0.250	0.264	739.931
1200	20	0.333	0.352	774.395
1500	25	0.417	0.440	802.660
1800	30	0.500	0.527	827.421
2100	35	0.583	0.615	849.498
2121	**35.35**	**0.589**	**0.622**	**850.955**
2400	40	0.667	0.703	845.072
2700	45	0.750	0.791	792.788
3000	50	0.833	0.879	740.505
3300	55	0.917	0.967	688.221
3600	60	1.000	1.055	635.938
3900	65	1.083	1.143	583.654
4200	70	1.167	1.231	531.371
4500	75	1.250	1.319	479.088
4800	80	1.333	1.407	426.804
5100	85	1.417	1.494	374.521
5400	90	1.500	1.582	322.237
5700	95	1.583	1.670	269.954
6000	100	1.667	1.758	217.670
6300	105	1.750	1.846	165.387
6600	110	1.833	1.934	113.103
6900	115	1.917	2.022	60.820
7200	120	2.000	2.110	8.536

Case 3:

Opening Factor F = 0.055

Table E-III ENV Curve formulation-Maximum intensity of fire at 102 minutes

Time (sec)	Time (min)	Time (hrs)	t* (hrs)	Temperature (°C)
0	0	0.000	0.000	0.000
300	5	0.083	0.058	444.698
600	10	0.167	0.115	611.789
900	15	0.250	0.173	684.049
1200	20	0.333	0.230	723.256
1500	25	0.417	0.288	750.239
1800	30	0.500	0.345	772.089
2100	35	0.583	0.403	791.275
2400	40	0.667	0.460	808.712
2700	45	0.750	0.518	824.783
3000	50	0.833	0.575	839.686
3300	55	0.917	0.633	853.550
3600	60	1.000	0.690	866.478
3900	65	1.083	0.748	878.554
4200	70	1.167	0.805	889.856
4500	75	1.250	0.863	900.451
4680	78	1.300	0.897	906.495
4800	80	1.333	0.920	910.401
5100	85	1.417	0.978	919.764
5400	90	1.500	1.035	928.588
5700	95	1.583	1.093	936.922
6000	100	1.667	1.150	944.806
6120	**102**	**1.700**	**1.173**	**947.843**
6300	105	1.750	1.208	595.113
6600	110	1.833	1.265	561.904
6900	115	1.917	1.323	528.694
7200	120	2.000	1.380	495.485

F   LUMPED MASS PARAMETER METHOD

The models for vermiculite and gypsum board were analyzed analytically by the method of lumped mass parameter analysis. The steps for the case of constant thermal properties for insulating materials have been described below. For the case of variable thermal properties, values were used from the tables that have been presented previously for the thermal properties of vermiculite and gypsum board.

10.1 F.1   Analytical analysis for vermiculite model

The steps for analyzing the vermiculite model analytically have been presented below,

Step 1:

Properties:

From LRFD manual for a W 12x27 section, we have the following properties

<table>
<tr><th colspan="9">BEAM PROPERTIES FOR W 12 X 27 SECTION</th></tr>
<tr><th>A (in²)</th><th>d (in)</th><th>bf (in)</th><th>tf (in)</th><th>tw (in)</th><th>$I_{xx}(in^4)$</th><th>$S_{xx}(in^3)$</th><th>$I_{yy}(in^4)$</th><th>$S_{yy}(in^3)$</th></tr>
<tr><td>7.95</td><td>11.96</td><td>6.497</td><td>0.4</td><td>0.237</td><td>204</td><td>34.2</td><td>18.30</td><td>5.63</td></tr>
</table>

Vermiculite Properties:

$k_i = 0.15 W/mK$

$\rho_i = 800 kg/m^3$

$C_{pi} = 1700 J/kgK$

Step 2: Calculation of A_i/V_s :

For, the case of steel beam which is exposed to fire from three sides the ratio is given by the following equation,

$A_i/V_s = 2(B - t_w) + B + 2D$

Here,

B = breadth of the flange

D = depth of the entire beam

A_s = Area of steel

Fire protection on three sides: profile protection
$$\frac{2(B - t_w) + B + 2D}{A_s}$$
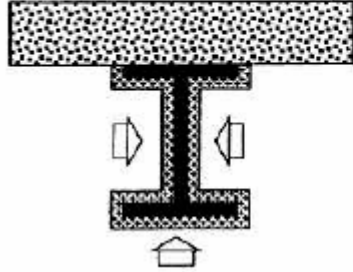
$$A_i / V_s = \left(\frac{(2x(6.497 - 0.237)) + 6.497 + (2x11.96)}{7.95} \right)$$

$A_i / V_s = 5.4 / inch$

Step 3: Calculation of ζ

$$\zeta = \left(\frac{\rho_i c_{pi} t_i}{2\rho_s c_{ps}} \right) A / V_s$$

Using the values mentioned earlier with the appropriate units, we get,

$\zeta = 0.375$

Step 4: Calculation of constant co-efficient:

$$Co - efficient = \left(\frac{\frac{k_i}{t_i}}{\rho_s C_s} \right) \left(\frac{A_i}{V_s} \right) \left(\frac{1}{1+\zeta} \right)$$

Using the values mentioned above we get,

$Co - efficient = 5.278x10^{-4}$

Similar calculations were performed for variable thermal properties for steel and vermiculite. The tables below present the results for the following cases

    1. Constant thermal properties for steel and vermiculite

    2. Variable thermal properties for steel and constant

    3. Variable thermal properties for steel and vermiculite

Table F-I Constant Thermal Properties for Steel and Vermiculite

Time	Gas Temp	Avg Gas Temp	Δt	Tg / (1/(1+ζ))	Δ Ts	Ts	Fy	Et
(sec)	(°C)	(°C)	(°C)	(°C)	(°C)	(°C)	(ksi)	(ksi)
0	20.000					20	35.82	28927.63
		106.333	86.333	23.545	-18.989			
100	192.667					20	35.82	28927.63
		279.000	86.333	23.545	-9.875			
200	365.333					20	35.82	28927.63
		451.667	86.333	23.545	-0.762			
300	538.000					20	35.82	28927.63
		565.667	27.667	7.545	21.255			
400	593.333					41.254832	35.56	28817.81
		620.997	27.663	7.545	23.054			
500	648.660					64.309061	35.22	28671.59
		676.330	27.670	7.546	24.756			
600	704.000					89.065162	34.80	28486.24
		713.165	9.165	2.500	30.440			
700	722.330					119.50561	34.22	28219.34
		731.495	9.165	2.500	29.801			
800	740.660					149.30686	33.57	27915.93
		749.830	9.170	2.501	29.195			
900	759.000					178.50156	32.87	27576.67
		764.830	5.830	1.590	29.356			
1000	770.660					207.85798	32.10	27191.14
		776.495	5.835	1.591	28.421			
1100	782.330					236.27928	31.28	26772.47
		788.165	5.835	1.591	27.537			
1200	794.000					263.81644	30.42	26320.84
		798.500	4.500	1.227	26.993			
1300	803.000					290.80977	29.52	25830.46
		807.500	4.500	1.227	26.044			
1400	812.000					316.8534	28.58	25308.63
		816.500	4.500	1.227	25.144			
1500	821.000					341.99748	27.62	24755.26
		824.665	3.665	1.000	24.476			
1600	828.330					366.47313	26.62	24165.44
		831.995	3.665	1.000	23.571			

Time	Gas Temp	Avg Gas Temp	Δt	Tg / (1/(1+ζ))	Δ Ts	Ts	Fy	Et
(sec)	(°C)	(°C)	(°C)	(°C)	(°C)	(°C)	(ksi)	(ksi)
1700	835.660					390.04382	25.61	23545.14
		839.330	3.670	1.001	22.712			
1800	843.000					412.75624	24.57	22894.19
		846.165	3.165	0.863	22.012			
1900	849.330					434.76837	23.51	22208.59
		852.495	3.165	0.863	21.184			
2000	855.660					455.9528	22.44	21492.91
		858.830	3.170	0.865	20.399			
2100	862.000					476.35211	21.36	20746.88
		864.665	2.665	0.727	19.768			
2200	867.330					496.12045	20.26	19965.43
		869.995	2.665	0.727	19.006			
2300	872.660					515.12673	19.15	19154.47
		875.330	2.670	0.728	18.283			
2400	878.000					533.41008	18.04	18313.74
		880.330	2.330	0.635	17.675			
2500	882.660					551.08506	16.92	17438.94
		884.995	2.335	0.637	16.987			
2600	887.330					568.07201	15.80	16535.07
		889.665	2.335	0.637	16.337			
2700	892.000					584.40887	14.69	15601.73
		894.165	2.165	0.590	15.758			
2800	896.330					600.16734	13.59	14635.32
		898.495	2.165	0.590	15.155			
2900	900.660					615.32262	12.55	13700.76
		902.830	2.170	0.592	14.583			
3000	905.000					629.90544	11.62	12847.89
		906.830	1.830	0.499	14.117			
3100	908.660					644.02243	10.78	12062.39
		910.495	1.835	0.500	13.564			
3200	912.330					657.5864	10.04	11342.25
		914.165	1.835	0.500	13.042			
3300	916.000					670.62816	9.36	10679.68
		917.830	1.830	0.499	12.548			
3400	919.660					683.17638	8.75	10068.09
		921.495	1.835	0.500	12.078			
3500	923.330					695.25438	8.19	9502.01
		925.165	1.835	0.500	11.634			
3600	927.000					706.88861	7.68	8976.52
		928.665	1.665	0.454	11.251			

Time	*Gas Temp*	*Avg Gas Temp*	*Δt*	*Tg / (1/(1+ζ))*	*Δ Ts*	*Ts*	*Fy*	*Et*
(sec)	*(°C)*	*(°C)*	*(°C)*	*(°C)*	*(°C)*	*(°C)*	*(ksi)*	*(ksi)*
3700	930.330					718.13988	7.22	8485.83
		931.995	1.665	0.454	10.833			
3800	933.660					728.97306	6.78	8028.82
		935.330	1.670	0.455	10.436			
3900	937.000					739.40913	6.39	7602.21
		938.500	1.500	0.409	10.099			
4000	940.000					749.50805	6.02	7201.56
		941.500	1.500	0.409	9.724			
4100	943.000					759.2323	5.68	6826.61
		944.500	1.500	0.409	9.369			
4200	946.000					768.60163	5.36	6475.00
		947.330	1.330	0.363	9.071			
4300	948.660					777.67219	5.06	6143.26
		949.995	1.335	0.364	8.731			
4400	951.330					786.4033	4.78	5831.70
		952.665	1.335	0.364	8.411			
4500	954.000					794.8145	4.53	5538.49
		955.500	1.500	0.409	8.072			
4600	957.000					802.88639	4.29	5263.30
		958.500	1.500	0.409	7.804			
4700	960.000					810.69058	4.06	5002.81
		961.500	1.500	0.409	7.551			
4800	963.000					818.24121	3.85	4755.85
		964.330	1.330	0.363	7.348			
4900	965.660					825.58905	3.65	4520.16
		966.995	1.335	0.364	7.099			
5000	968.330					832.68837	3.46	4296.66
		969.665	1.335	0.364	6.866			
5100	971.000					839.5539	3.28	4084.36
		972.165	1.165	0.318	6.681			
5200	973.330					846.23539	3.10	3881.28
		974.495	1.165	0.318	6.452			
5300	975.660					852.68721	2.94	3688.41
		976.830	1.170	0.319	6.233			
5400	978.000					858.92037	2.79	3505.01
		979.000	1.000	0.273	6.065			
5500	980.000					864.98545	2.64	3329.25
		981.000	1.000	0.273	5.851			
5600	982.000					870.83597	2.51	3162.19
		983.000	1.000	0.273	5.647			

Time	Gas Temp	Avg Gas Temp	Δt	Tg / (1/(1+ζ))	Δ Ts	Ts	Fy	Et
(sec)	(°C)	(°C)	(°C)	(°C)	(°C)	(°C)	(ksi)	(ksi)
5700	984.000					876.48326	2.38	3003.18
		985.165	1.165	0.318	5.418			
5800	986.330					881.90175	2.25	2852.66
		987.495	1.165	0.318	5.255			
5900	988.660					887.15724	2.13	2708.53
		989.830	1.170	0.319	5.100			
6000	991.000					892.25721	2.02	2570.39
		992.000	1.000	0.273	4.992			
6100	993.000					897.24891	1.91	2436.80
		994.000	1.000	0.273	4.834			
6200	995.000					902.08271	1.81	2308.94
		996.000	1.000	0.273	4.684			
6300	997.000					906.76693	1.71	2186.41
		997.830	0.830	0.226	4.580			
6400	998.660					911.34688	1.62	2067.91
		999.495	0.835	0.228	4.425			
6500	1000.330					915.77161	1.53	1954.62
		1001.165	0.835	0.228	4.279			
6600	1002.000					920.05095	1.44	1846.15
		1002.665	0.665	0.181	4.179			
6700	1003.330					924.22995	1.36	1741.25
		1003.995	0.665	0.181	4.029			
6800	1004.660					928.25859	1.28	1641.08
		1005.330	0.670	0.183	3.885			
6900	1006.000					932.14369	1.20	1545.34

Table F-II Variable Thermal Properties for Steel and Constant Thermal Properties for Vermiculite

Time (sec)	Gas Temp (°C)	k_s (W/in°C)	C_{ps} (J/lbs°C)	ζ	Tg / (1/(1+ζ)) (°C)	Δ Ts (°C)	Ts (°C)	Fy (ksi)	Et (ksi)
0	20	0.005	0.732040	0.38			20.00	35.82	28927.63
					23.56	-21.62			
100	192.6667	0.005	0.738	0.37			20.00	35.82	28927.63
					23.41	-17.64			
200	365.3333	0.005	0.745	0.37			20.00	35.82	28927.63
					23.27	-13.71			
300	538	0.005	0.750854	0.37			20.00	35.82	28927.63
					7.41	4.59			
400	593.3333	0.005	0.761	0.36			24.59	35.77	28906.17
					7.34	5.65			
500	648.66	0.005	0.772	0.36			30.25	35.70	28877.96
					7.26	6.67			
600	704	0.005	0.781972	0.35			36.91	35.62	28842.33
					2.38	12.06			
700	722.33	0.005	0.789	0.35			48.97	35.45	28771.83
					2.37	12.10			
800	740.66	0.005	0.797	0.34			61.07	35.27	28693.7
					2.35	12.15			
900	759	0.005	0.804554	0.34			73.22	35.08	28608.18
					1.48	12.97			
1000	770.66	0.005	0.810	0.34			86.19	34.85	28509.21
					1.48	12.88			
1100	782.33	0.005	0.815	0.34			99.07	34.62	28403.22
					1.47	12.79			
1200	794	0.005	0.820566	0.33			111.87	34.37	28290.36
					1.13	13.01			
1300	803	0.005	0.842	0.33			124.88	34.11	28167.73
					1.11	12.68			
1400	812	0.005	0.863	0.32			137.57	33.84	28040.53
					1.09	12.37			
1500	821	0.005	0.847296	0.32			149.94	33.56	27909.04
					0.90	12.67			
1600	828.33	0.005	0.882	0.31			162.61	33.26	27766.66
					0.87	12.18			

Time	Gas Temp	k_s	C_{ps}	ζ	$Tg / (1/(1+\zeta))$	ΔTs	Ts	Fy	Et
(sec)	*(°C)*	*(W/in°C)*	*(J/lbs°C)*		*(°C)*	*(°C)*	*(°C)*	*(ksi)*	*(ksi)*
1700	835.66	0.005	0.880	0.31			174.79	32.97	27622.21
					0.87	12.11			
1800	843	0.004963	0.877846	0.31			186.90	32.66	27471.08
					0.75	12.15			
1900	849.33	0.005	0.888	0.31			199.05	32.34	27311.69
					0.75	11.93			
2000	855.66	0.005	0.898	0.31			210.98	32.01	27147.43
					0.74	11.72			
2100	862	0.004947	0.908731	0.30			222.69	31.68	26978.38
					0.62	11.62			
2200	867.33	0.005	0.918	0.30			234.31	31.34	26802.94
					0.61	11.41			
2300	872.66	0.005	0.928	0.30			245.72	30.99	26622.91
					0.61	11.20			
2400	878	0.004931	0.937662	0.29			256.92	30.64	26438.39
					0.53	11.07			
2500	882.66	0.005	0.948	0.29			267.99	30.29	26248.14
					0.52	10.86			
2600	887.33	0.005	0.957	0.29			278.86	29.93	26053.68
					0.52	10.66			
2700	892	0.004917	0.96731	0.28			289.52	29.56	25855.02
					0.48	10.50			
2800	896.33	0.005	0.977	0.28			300.02	29.19	25651.51
					0.48	10.31			
2900	900.66	0.005	0.987	0.28			310.33	28.82	53731.95
					0.47	10.12			
3000	905	0.004904	0.997031	0.28			320.46	28.45	50936.23
					0.40	10.01			
3100	908.66	0.005	1.009	0.27			330.46	28.07	48372.89
					0.39	9.80			
3200	912.33	0.005	1.020	0.27			340.27	27.69	46035.12
					0.39	9.61			
3300	916	0.004891	1.031980	0.27			349.87	27.31	43893.94
					0.38	9.42			
3400	919.66	0.005	1.046	0.26			359.30	26.92	41925.12
					0.38	9.22			
3500	923.33	0.005	1.060	0.26			368.52	26.54	40111.87
					0.38	9.03			
3600	927	0.004878	1.073680	0.26			377.55	26.15	38436

Time	Gas Temp	k_s	C_{ps}	ζ	Tg / (1/(1+ζ))	Δ Ts	Ts	Fy	Et
(sec)	*(°C)*	*(W/in°C)*	*(J/lbs°C)*		*(°C)*	*(°C)*	*(°C)*	*(ksi)*	*(ksi)*
					0.34	8.88			
3700	930.33	0.005	1.087	0.25			386.43	25.77	36876.83
					0.34	8.70			
3800	933.66	0.005	1.100	0.25			395.14	25.38	35427.46
					0.33	8.53			
3900	937	0.004868	1.112976	0.25			403.67	24.99	34076.68
					0.30	8.40			
4000	940	0.005	1.128	0.24			412.07	24.60	32809.9
					0.29	8.22			
4100	943	0.005	1.143	0.24			420.29	24.21	31626.08
					0.29	8.05			
4200	946	0.004857	1.158436	0.24			428.34	23.83	30517.18
					0.25	7.91			
4300	948.66	0.005	1.174	0.23			436.25	23.44	29472.33
					0.25	7.75			
4400	951.33	0.005	1.190	0.23			444.00	23.05	28490.87
					0.25	7.58			
4500	954	0.004848	1.206224	0.23			451.58	22.67	27566.99
					0.28	7.40			
4600	957	0.005	1.224	0.22			458.98	22.28	26698.9
					0.27	7.24			
4700	960	0.005	1.242	0.22			466.22	21.90	25879.2
					0.27	7.09			
4800	963	0.004838	1.260512	0.22			473.32	21.52	25103.83
					0.24	6.98			
4900	965.66	0.005	1.274	0.22			480.29	21.14	24366.27
					0.24	6.85			
5000	968.33	0.005	1.287	0.21			487.15	20.76	23664.83
					0.23	6.74			
5100	971	0.004830	1.30	0.21			493.88	20.38	22996.76
					0.20	6.65			
5200	973.33	0.005	1.316	0.21			500.53	20.00	22357.09
					0.20	6.52			
5300	975.66	0.005	1.333	0.21			507.05	19.63	21748.1
					0.20	6.39			
5400	978	0.004823	1.348995	0.20			513.45	19.25	21167.63
					0.17	6.30			
5500	980	0.005	1.381	0.20			519.74	18.88	20611.28
					0.17	6.12			

Time	Gas Temp	k_s	C_{ps}	ζ	Tg / (1/(1+ζ))	Δ Ts	Ts	Fy	Et
(sec)	(°C)	(W/in°C)	(J/lbs°C)		(°C)	(°C)	(°C)	(ksi)	(ksi)
5600	982	0.005	1.412	0.19			525.87	18.51	20084.91
					0.16	5.95			
5700	984	0.004815	1.443529	0.19			531.82	18.14	19586.03
					0.19	5.77			
5800	986.33	0.005	1.492	0.18			537.58	17.78	19114.38
					0.18	5.56			
5900	988.66	0.005	1.541	0.18			543.15	17.43	18669.9
					0.18	5.37			
6000	991	0.004809	1.590216	0.17			548.52	17.09	18250.13
					0.15	5.22			
6100	993	0.005	1.750	0.16			553.74	16.75	17851.07
					0.14	4.77			
6200	995	0.005	1.909	0.14			558.51	16.44	17493.43
					0.13	4.39			
6300	997	0.004802	2.069	0.13			562.90	16.15	17169.99
					0.10	4.09			
6400	998.66	0.005	2.383	0.12			566.99	15.88	16873.89
					0.09	3.58			
6500	1000.33	0.005	2.698	0.10			570.57	15.64	16618.19
					0.08	3.19			
6600	1002	0.004799	3.012	0.09			573.76	15.42	16393.54
					0.06	2.89			
6700	1003.33	0.005	3.219	0.09			576.65	15.22	16192.55
					0.05	2.71			
6800	1004.66	0.005	3.425	0.08			579.36	15.04	16006.14
					0.05	2.55			
6900	1006	0.004798	3.631592	0.08			581.91	14.86	15832.49

Table F-III Variable Thermal Properties for Steel and Vermiculite

Time (sec)	k_s (W/in°C)	C_{ps} (J/lbs°C)	k_i (W/in°C)	C_{pi} (J/lbs°C)	Tg / (1/(1+ζ)) (°C)	Δ Ts (°C)	Ts (°C)	Fy (ksi)	Et (ksi)
0	0.005018	0.732040	0.00	1.99			20	35.82	28927.63
					23.57	-21.63			
100	0.005017	0.7383	0.00	1.83			20	35.82	28927.63
					21.97	-12.53			
200	0.005013	0.7446	0.00	1.63			20	35.82	28927.63
					20.00	1.15			
300	0.00501	0.750854	0.00	1.58			21.14985	35.81	28922.39
					6.23	35.15			
400	0.005008	0.7612	0.00	1.54			56.29914	35.34	28725.36
					6.02	38.95			
500	0.005005	0.7716	0.00	1.52			95.24865	34.69	28435.49
					5.91	42.46			
600	0.005003	0.781972	0.00	1.51			137.7055	33.83	28039.09
					1.93	48.13			
700	0.005	0.7895	0.00	1.50			185.8403	32.69	27484.58
					1.90	45.96			
800	0.004998	0.7970	0.00	1.49			231.8008	31.41	26841.55
					1.88	44.05			
900	0.004995	0.804554	0.00	1.48			275.849	30.03	26108.32
					1.18	42.48			
1000	0.004993	0.8099	0.00	1.48			318.3291	28.53	25277.54
					1.17	40.04			
1100	0.004991	0.8152	0.00	1.47			358.3687	26.96	24366.62
					1.16	37.71			
1200	0.004989	0.820566	0.00	1.46			396.0827	25.34	23377.36
					0.89	35.70			
1300	0.004985	0.8420	0.00	1.46			431.7793	23.66	22305.04
					0.87	32.86			
1400	0.004982	0.8633	0.00	1.45			464.6379	21.98	21182.42
					0.85	31.07			
1500	0.004978	0.847296	0.00	1.45			495.7117	20.28	19982.21
					0.70	30.36			
1600	0.004973	0.8824	0.00	1.44			526.0709	18.49	18658.73
					0.67	27.95			

Time	k_s	C_{ps}	k_i	C_{pi}	$Tg / (1/(1+\zeta))$	$\Delta\ Ts$	Ts	Fy	Et
(sec)	*(W/in°C)*	*(J/lbs°C)*	*(W/in°C)*	*(J/lbs°C)*	*(°C)*	*(°C)*	*(°C)*	*(ksi)*	*(ksi)*
1700	0.00497	0.8801	0.00	1.43			554.02	16.73	17287.4
					0.67	26.71			
1800	0.004963	0.877846	0.00	1.43			580.731	14.94	15817.64
					0.58	25.46			
1900	0.004958	0.8881	0.00	1.42			606.1957	13.16	14257.44
					0.57	23.84			
2000	0.004952	0.8984	0.00	1.42			630.0309	11.61	12840.74
					0.57	22.33			
2100	0.004947	0.908731	0.00	1.41			652.3584	10.32	11615.95
					0.47	20.91			
2200	0.004942	0.9184	0.00	1.41			673.2711	9.23	10548.81
					0.47	19.49			
2300	0.004936	0.9280	0.00	1.41			692.7563	8.31	9617.343
					0.46	18.18			
2400	0.004931	0.937662	0.00	1.40			710.9361	7.51	8798.072
					0.40	16.98			
2500	0.004926	0.9475	0.00	1.40			727.9155	6.83	8072.783
					0.39	15.79			
2600	0.004922	0.9574	0.00	1.40			743.7062	6.23	7430.301
					0.39	14.71			
2700	0.004917	0.96731	0.00	1.39			758.4201	5.70	6857.533
					0.36	13.74			
2800	0.004913	0.9772	0.00	1.39			772.1562	5.24	6343.999
					0.35	12.81			
2900	0.004908	0.9871	0.00	1.39			784.9616	4.83	5882.631
					0.35	11.83			
3000	0.004904	0.997031	0.00	1.38			796.789	4.47	5470.62
					0.29	11.01			
3100	0.0049	1.0087	0.00	1.38			807.7996	4.14	5098.675
					0.29	10.18			
3200	0.004895	1.0203	0.00	1.38			817.9821	3.85	4764.242
					0.29	9.45			
3300	0.004891	1.031980	0.00	1.38			827.4337	3.60	4461.689
					0.29	8.81			
3400	0.004887	1.0459	0.00	1.38			836.2388	3.36	4186.406
					0.28	8.22			
3500	0.004882	1.0598	0.00	1.38			844.4546	3.15	3935.072
					0.28	7.70			
3600	0.004878	1.073680	0.00	1.38			852.1513	2.96	3704.311
					0.25	7.24			

Time	k_s	C_{ps}	k_i	C_{pi}	Tg / (1/(1+ζ))	Δ Ts	Ts	Fy	Et
(sec)	(W/in°C)	(J/lbs°C)	(W/in°C)	(J/lbs°C)	(°C)	(°C)	(°C)	(ksi)	(ksi)
3700	0.004875	1.0868	0.00	1.38			859.396	2.78	3491.127
					0.25	6.81			
3800	0.00487	1.0999	0.00	1.38			866.203	2.62	3294.28
					0.25	6.42			
3900	0.004868	1.112976	0.00	1.38			872.6217	2.46	3111.675
					0.22	6.08			
4000	0.004864	1.1281	0.00	1.37			878.7034	2.32	2941.267
					0.22	5.73			
4100	0.004861	1.1433	0.00	1.37			884.4362	2.19	2782.924
					0.21	5.42			
4200	0.004857	1.158436	0.00	1.37			889.8593	2.07	2635.129
					0.19	5.16			
4300	0.004854	1.1744	0.00	1.37			895.0146	1.96	2496.402
					0.19	4.87			
4400	0.004851	1.1903	0.00	1.37			899.8893	1.86	2366.777
					0.18	4.63			
4500	0.004848	1.206224	0.00	1.37			904.5159	1.76	2245.124
					0.20	4.40			
4600	0.004845	1.2243	0.00	1.37			908.9152	1.67	2130.668
					0.20	4.23			
4700	0.004841	1.2424	0.00	1.37			913.1425	1.58	2021.792
					0.20	4.07			
4800	0.004838	1.260512	0.00	1.37			917.2168	1.50	1917.865
					0.17	3.94			
4900	0.004835	1.2737	0.00	1.37			921.1612	1.42	1818.179
					0.17	3.80			
5000	0.004833	1.2868	0.00	1.37			924.9658	1.34	1722.883
					0.17	3.68			
5100	0.004830	1.30	0.00	1.37			928.6459	1.27	1631.495
					0.15	3.57			
5200	0.004828	1.3163	0.00	1.37			932.2199	1.20	1543.471
					0.15	3.44			
5300	0.004825	1.3327	0.00	1.37			935.6556	1.13	1459.529
					0.14	3.31			
5400	0.004823	1.348995	0.00	1.36			938.9669	1.07	1379.242
					0.12	3.21			
5500	0.00482	1.3805	0.00	1.36			942.1735	1.01	1302.063
					0.12	3.05			
5600	0.004818	1.4120	0.00	1.36			945.2216	0.95	1229.214

Time	k_s	C_{ps}	k_i	C_{pi}	$Tg / (1/(1+\zeta))$	Δ Ts	Ts	Fy	Et
(sec)	(W/in°C)	(J/lbs°C)	(W/in°C)	(J/lbs°C)	(°C)	(°C)	(°C)	(ksi)	(ksi)
					0.12	2.91			
5700	0.004815	1.443529	0.00	1.36			948.1298	0.90	1160.17
					0.13	2.78			
5800	0.004813	1.4924	0.00	1.36			950.909	0.85	1094.609
					0.13	2.67			
5900	*0.00481*	*1.5413*	*0.00*	*1.36*			*953.577*	*0.80*	*1032.04*
					0.13	*2.57*			
6000	0.004809	1.590216	0.00	1.36			956.1489	0.75	972.094
					0.11	2.49			
6100	0.004807	1.7498	0.00	1.36			958.6422	0.70	914.2969
					0.10	2.26			
6200	0.004804	1.9094	0.00	1.36			960.9004	0.66	862.2237
					0.09	2.07			
6300	0.004802	2.069	0.00	1.36			962.9737	0.63	814.6424
					0.07	1.93			
6400	0.004801	2.3833	0.00	1.36			964.9027	0.59	770.5661
					0.06	1.68			
6500	0.0048	2.6977	0.00	1.36			966.5841	0.56	732.2996
					0.05	1.50			
6600	0.004799	3.012	0.00	1.36			968.0819	0.54	698.3313
					0.04	1.38			
6700	0.004799	3.2185	0.00	1.35			969.4639	0.51	667.0876
					0.04	1.31			
6800	0.004798	3.4251	0.00	1.34			970.7768	0.49	637.4911
					0.03	1.25			
6900	0.004798	3.631592	0.00	1.32			972.0311	0.47	609.2969

10.2 F.2 Analytical analysis for gypsum model

Step 1:

Properties:

From LRFD manual for a W 12x27 section, we have the following properties

BEAM PROPERTIES FOR W 12 X 27 SECTION								
$A\ (in^2)$	$d\ (in)$	$bf\ (in)$	$tf\ (in)$	$tw\ (in)$	$I_{xx}\ (in^4)$	$S_{xx}\ (in^3)$	$I_{yy}\ (in^4)$	$S_{yy}\ (in^3)$
7.95	11.96	6.497	0.4	0.237	204	34.2	18.30	5.63

Gypsum Properties:

$k_i = 0.25W/mK$

$\rho_i = 800kg/m^3$

$C_i = 1500J/kgK$

Step 2: Calculation of A_i/V_s :

For, the case of steel beam which is exposed to fire from three sides the ratio is given by the following equation,

$$A_i/V_s = \frac{2D+B}{A_s}$$

Here,

B = breadth of the flange

D = depth of the entire beam

A_s = Area of steel

Fire protection on three sides: board protection $\dfrac{2D + B}{A_s}$
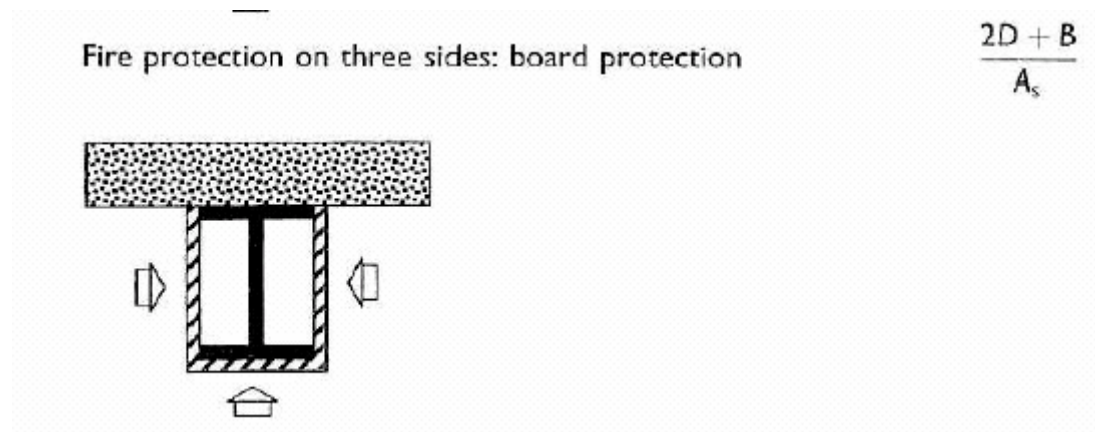
$$A_i/V_s = \left(\frac{(2x11.96)+6.5}{7.95}\right)$$

$$A_i/V_s = 3.826/inch$$

Step 3: Calculation of ζ

$$\zeta = \left(\frac{\rho_i c_{pi} t_i}{2\rho_s c_{ps}}\right) A_i/V_s$$

Using the values mentioned earlier with the appropriate units, we get,

$$\zeta = 0.414$$

Step 4: Calculation of constant co-efficient:

$$Co-efficient = \left(\frac{\frac{k_i}{t_i}}{\rho_s C_s}\right)\left(\frac{A_i}{V_s}\right)\left(\frac{1}{1+\zeta}\right)$$

Using the values mentioned above we get,

$$Co-efficient = 4.85x10^{-4}$$

Similar calculations were performed by varying the necessary parameters depending on the following cases:

1. Variable thermal properties of steel and constant thermal properties for gypsum.
2. Variable thermal properties of steel and gypsum

Table F-IV Constant Thermal Properties for Steel and Gypsum

Time	Gas Temp	Avg Gas Temp	Δt	Tg / (1/(1+ζ))	Δ Ts	Ts	Fy	Et
(sec)	*(°C)*	*(°C)*	*(°C)*	*(°C)*	*(°C)*	*(°C)*	*(ksi)*	*(ksi)*
0	20.000					20	35.82	28927.63
		106.333	86.333	23.545	-19.358			
100	192.667					20	35.82	28927.63
		279.000	86.333	23.545	-10.984			
200	365.333					20	35.82	28927.63
		451.667	86.333	23.545	-2.610			
300	538.000					20	35.82	28927.63
		565.667	27.667	7.545	18.919			
400	593.333					38.919379	35.59	28831.12
		620.997	27.663	7.545	20.686			
500	648.660					59.605582	35.29	28703.54
		676.330	27.670	7.546	22.365			
600	704.000					81.970352	34.93	28542.28
		713.165	9.165	2.500	28.113			
700	722.330					110.08375	34.41	28306.54
		731.495	9.165	2.500	27.639			
800	740.660					137.72265	33.83	28038.91
		749.830	9.170	2.501	27.186			
900	759.000					164.90895	33.21	27739.94
		764.830	5.830	1.590	27.506			
1000	770.660					192.41512	32.51	27399.68
		776.495	5.835	1.591	26.737			
1100	782.330					219.15163	31.78	27030.31
		788.165	5.835	1.591	26.006			
1200	794.000					245.15741	31.01	26631.98
		798.500	4.500	1.227	25.610			
1300	803.000					270.76725	30.20	26199.24
		807.500	4.500	1.227	24.804			
1400	812.000					295.57152	29.35	25738.75
		816.500	4.500	1.227	24.038			
1500	821.000					319.60928	28.48	25250.44
		824.665	3.665	1.000	23.496			
1600	828.330					343.10494	27.58	24729.70
		831.995	3.665	1.000	22.712			

Time	Gas Temp	Avg Gas Temp	Δt	Tg / (1/(1+ζ))	Δ Ts	Ts	Fy	Et
(sec)	(°C)	(°C)	(°C)	(°C)	(°C)	(°C)	(ksi)	(ksi)
1700	835.660					365.81656	26.65	24181.96
		839.330	3.670	1.001	21.964			
1800	843.000					387.78105	25.71	23607.05
		846.165	3.165	0.863	21.368			
1900	849.330					409.14949	24.74	23001.26
		852.495	3.165	0.863	20.639			
2000	855.660					429.78857	23.76	22368.67
		858.830	3.170	0.865	19.944			
2100	862.000					449.73253	22.76	21709.04
		864.665	2.665	0.727	19.397			
2200	867.330					469.12994	21.75	21017.72
		869.995	2.665	0.727	18.715			
2300	872.660					487.84507	20.72	20299.92
		875.330	2.670	0.728	18.065			
2400	878.000					505.90991	19.69	19555.39
		880.330	2.330	0.635	17.524			
2500	882.660					523.43383	18.65	18780.19
		884.995	2.335	0.637	16.899			
2600	887.330					540.33273	17.61	17978.70
		889.665	2.335	0.637	16.306			
2700	892.000					556.63853	16.56	17150.53
		894.165	2.165	0.590	15.780			
2800	896.330					572.41811	15.51	16293.15
		898.495	2.165	0.590	15.224			
2900	900.660					587.64238	14.46	15409.03
		902.830	2.170	0.592	14.695			
3000	905.000					602.33716	13.43	14498.35
		906.830	1.830	0.499	14.269			
3100	908.660					616.60597	12.46	13623.93
		910.495	1.835	0.500	13.753			
3200	912.330					630.35914	11.59	12822.04
		914.165	1.835	0.500	13.264			
3300	916.000					643.62327	10.81	12084.08
		917.830	1.830	0.499	12.800			
3400	919.660					656.4232	10.10	11402.73
		921.495	1.835	0.500	12.356			
3500	923.330					668.77873	9.46	10771.93
		925.165	1.835	0.500	11.934			
3600	927.000					680.71301	8.87	10186.22

Time	Gas Temp	Avg Gas Temp	Δt	Tg / (1/(1+ζ))	Δ Ts	Ts	Fy	Et
(sec)	(°C)	(°C)	(°C)	(°C)	(°C)	(°C)	(ksi)	(ksi)
3700	930.330					692.28459	8.33	9639.22
		931.995	1.665	0.454	11.172			
3800	933.660					703.45645	7.83	9129.59
		935.330	1.670	0.455	10.790			
3900	937.000					714.24687	7.38	8653.72
		938.500	1.500	0.409	10.467			
4000	940.000					724.71405	6.95	8206.73
		941.500	1.500	0.409	10.105			
4100	943.000					734.81908	6.56	7788.23
		944.500	1.500	0.409	9.760			
4200	946.000					744.57951	6.20	7395.62
		947.330	1.330	0.363	9.471			
4300	948.660					754.05019	5.86	7025.13
		949.995	1.335	0.364	9.139			
4400	951.330					763.18942	5.54	6676.98
		952.665	1.335	0.364	8.825			
4500	954.000					772.01489	5.25	6349.18
		955.500	1.500	0.409	8.490			
4600	957.000					780.50483	4.97	6041.36
		958.500	1.500	0.409	8.224			
4700	960.000					788.7285	4.71	5749.97
		961.500	1.500	0.409	7.970			
4800	963.000					796.69883	4.47	5473.71
		964.330	1.330	0.363	7.767			
4900	965.660					804.46622	4.24	5210.13
		966.995	1.335	0.364	7.519			
5000	968.330					811.98477	4.02	4960.13
		969.665	1.335	0.364	7.283			
5100	971.000					819.26817	3.82	4722.64
		972.165	1.165	0.318	7.098			
5200	973.330					826.36594	3.62	4495.50
		974.495	1.165	0.318	6.867			
5300	975.660					833.23247	3.44	4279.70
		976.830	1.170	0.319	6.645			
5400	978.000					839.87786	3.27	4074.43
		979.000	1.000	0.273	6.475			
5500	980.000					846.35256	3.10	3877.75
		981.000	1.000	0.273	6.258			
5600	982.000					852.61023	2.94	3690.69
		983.000	1.000	0.273	6.051			

Time	Gas Temp	Avg Gas Temp	Δt	Tg / (1/(1+ζ))	Δ Ts	Ts	Fy	Et
(sec)	*(°C)*	*(°C)*	*(°C)*	*(°C)*	*(°C)*	*(°C)*	*(ksi)*	*(ksi)*
5700	984.000					858.66141	2.80	3512.57
		985.165	1.165	0.318	5.818			
5800	986.330					864.4791	2.66	3343.83
		987.495	1.165	0.318	5.649			
5900	988.660					870.12765	2.52	3182.29
		989.830	1.170	0.319	5.486			
6000	991.000					875.61412	2.40	3027.51
		992.000	1.000	0.273	5.372			
6100	993.000					880.98611	2.27	2877.96
		994.000	1.000	0.273	5.208			
6200	995.000					886.19456	2.16	2734.79
		996.000	1.000	0.273	5.053			
6300	997.000					891.24739	2.04	2597.61
		997.830	0.830	0.226	4.943			
6400	998.660					896.19029	1.94	2465.00
		999.495	0.835	0.228	4.783			
6500	1000.330					900.97284	1.83	2338.17
		1001.165	0.835	0.228	4.632			
6600	1002.000					905.60443	1.74	2216.69
		1002.665	0.665	0.181	4.526			
6700	1003.330					910.1305	1.64	2099.26
		1003.995	0.665	0.181	4.371			
6800	1004.660					914.50157	1.55	1987.02
		1005.330	0.670	0.183	4.222			
6900	1006.000					918.72402	1.47	1879.67

Table F-V Variable Thermal Properties for Steel and Constant

Thermal Properties for Gypsum

Time	Gas Temp	k_s	C_{ps}	ζ	Tg / (1/(1+ζ))	Δ Ts	Ts	Fy	Et
(sec)	(°C)	(W/in°C)	(J/lbs°C)		(°C)	(°C)	(°C)	(ksi)	(ksi)
0	20.00	0.005018	0.732040	0.415			20.00	35.82	28927.63
					25.32	-21.13			
100	192.67	0.005017	0.738	0.411			20.00	35.82	28927.63
					25.16	-12.68			
200	365.33	0.005013	0.745	0.408			20.00	35.82	28927.63
					25.01	-4.33			
300	538.00	0.005010	0.750854	0.405			20.00	35.82	28927.63
					7.97	18.02			
400	593.33	0.005008	0.761	0.399			38.02	35.60	28836.17
					7.89	19.60			
500	648.66	0.005005	0.772	0.394			57.62	35.32	28716.68
					7.82	21.08			
600	704.00	0.005003	0.781972	0.388			78.71	34.98	28567.28
					2.56	26.79			
700	722.33	0.005000	0.789	0.385			105.49	34.50	28347.54
					2.55	26.21			
800	740.66	0.004998	0.797	0.381			131.71	33.96	28100.24
					2.53	25.67			
900	759.00	0.004995	0.804554	0.378			157.38	33.39	27826.37
					1.60	25.93			
1000	770.66	0.004993	0.810	0.375			183.31	32.75	27516.65
					1.59	25.16			
1100	782.33	0.004991	0.815	0.373			208.47	32.08	27182.58
					1.58	24.44			
1200	794.00	0.004989	0.820566	0.370			232.91	31.38	26824.58
					1.22	24.05			
1300	803.00	0.004985	0.842	0.361			256.96	30.64	26437.74
					1.19	22.94			
1400	812.00	0.004982	0.863	0.352			279.90	29.89	26034.58
					1.17	21.92			
1500	821.00	0.004978	0.847296	0.358			301.82	29.13	25615.89
					0.97	21.85			
1600	828.33	0.004973	0.882	0.344			323.67	28.33	25163.62
					0.94	20.59			

Time	*Gas Temp*	*k$_s$*	*C$_{ps}$*	*ζ*	*Tg / (1/(1+ζ))*	*Δ Ts*	*Ts*	*Fy*	*Et*
(sec)	*(°C)*	*(W/in°C)*	*(J/lbs°C)*		*(°C)*	*(°C)*	*(°C)*	*(ksi)*	*(ksi)*
1700	835.66	0.004968	0.880	0.345			344.25	27.53	24703.05
					0.94	20.06			
1800	843.00	0.004963	0.877846	0.346			364.32	26.71	24219.56
					0.81	19.67			
1900	849.33	0.004958	0.888	0.342			383.98	25.87	23709.76
					0.81	18.94			
2000	855.66	0.004952	0.898	0.338			402.92	25.03	23182.80
					0.80	18.25			
2100	862.00	0.004947	0.908731	0.334			421.17	24.17	22638.84
					0.67	17.70			
2200	867.33	0.004942	0.918	0.331			438.87	23.31	22074.41
					0.66	17.06			
2300	872.66	0.004936	0.928	0.327			455.93	22.44	21493.81
					0.66	16.44			
2400	878.00	0.004931	0.937662	0.324			472.37	21.57	20897.14
					0.57	15.94			
2500	882.66	0.004926	0.948	0.321			488.31	20.70	20281.58
					0.57	15.36			
2600	887.33	0.004922	0.957	0.317			503.66	19.82	19650.97
					0.56	14.81			
2700	892.00	0.004917	0.96731	0.314			518.47	18.95	19005.26
					0.52	14.33			
2800	896.33	0.004913	0.977	0.311			532.80	18.08	18342.81
					0.51	13.83			
2900	900.66	0.004908	0.987	0.308			546.63	17.21	17665.74
					0.51	13.35			
3000	905.00	0.004904	0.997031	0.305			559.97	16.34	16974.04
					0.43	12.97			
3100	908.66	0.004900	1.009	0.301			572.94	15.48	16263.81
					0.42	12.49			
3200	912.33	0.004895	1.020	0.298			585.43	14.61	15540.99
					0.42	12.05			
3300	916.00	0.004891	1.031980	0.294			597.48	13.76	14805.51
					0.42	11.63			
3400	919.66	0.004887	1.046	0.290			609.11	12.96	14077.61
					0.41	11.21			
3500	923.33	0.004882	1.060	0.287			620.32	12.22	13403.33
					0.41	10.82			
3600	927.00	0.004878	1.073680	0.283			631.14	11.54	12777.45
					0.37	10.48			

Time	*Gas Temp*	k_s	C_{ps}	ζ	*Tg / (1/(1+ζ))*	*Δ Ts*	*Ts*	*Fy*	*Et*
(sec)	*(°C)*	*(W/in°C)*	*(J/lbs°C)*		*(°C)*	*(°C)*	*(°C)*	*(ksi)*	*(ksi)*
3700	930.33	0.004875	1.087	0.279			641.63	10.92	12193.11
					0.36	10.12			
3800	933.66	0.004871	1.100	0.276			651.75	10.35	11648.12
					0.36	9.79			
3900	937.00	0.004868	1.112976	0.273			661.54	9.83	11138.60
					0.32	9.50			
4000	940.00	0.004864	1.128	0.269			671.03	9.34	10659.55
					0.32	9.17			
4100	943.00	0.004861	1.143	0.266			680.20	8.89	10210.84
					0.31	8.86			
4200	946.00	0.004857	1.158436	0.262			689.06	8.48	9789.61
					0.28	8.60			
4300	948.66	0.004854	1.174	0.259			697.66	8.09	9391.98
					0.27	8.30			
4400	951.33	0.004851	1.190	0.255			705.96	7.72	9017.95
					0.27	8.02			
4500	954.00	0.004848	1.206224	0.252			713.98	7.39	8665.37
					0.30	7.73			
4600	957.00	0.004845	1.224	0.248			721.71	7.07	8333.56
					0.30	7.48			
4700	960.00	0.004841	1.242	0.244			729.20	6.78	8019.60
					0.29	7.25			
4800	963.00	0.004838	1.260512	0.241			736.45	6.50	7721.98
					0.26	7.06			
4900	965.66	0.004835	1.274	0.238			743.51	6.24	7438.28
					0.26	6.86			
5000	968.33	0.004833	1.287	0.236			750.36	5.99	7168.12
					0.25	6.67			
5100	971.00	0.004830	1.30	0.234			757.03	5.75	6910.45
					0.22	6.52			
5200	973.33	0.004828	1.316	0.231			763.55	5.53	6663.38
					0.22	6.32			
5300	975.66	0.004825	1.333	0.228			769.87	5.32	6428.02
					0.22	6.13			
5400	978.00	0.004823	1.348995	0.225			776.01	5.11	6203.53
					0.18	5.99			
5500	980.00	0.004820	1.381	0.220			781.99	4.92	5988.17
					0.18	5.75			
5600	982.00	0.004818	1.412	0.215			787.75	4.74	5784.42
					0.18	5.54			

Time	Gas Temp	k_s	C_{ps}	ζ	Tg / (1/(1+ζ))	Δ Ts	Ts	Fy	Et
(sec)	(°C)	(W/in°C)	(J/lbs°C)		(°C)	(°C)	(°C)	(ksi)	(ksi)
5700	984.00	0.004815	1.443529	0.210			793.29	4.57	5591.30
					0.20	5.31			
5800	986.33	0.004813	1.492	0.204			798.60	4.41	5408.75
					0.20	5.09			
5900	988.66	0.004811	1.541	0.197			803.68	4.26	5236.45
					0.19	4.87			
6000	991.00	0.004809	1.590216	0.191			808.56	4.12	5073.46
					0.16	4.70			
6100	993.00	0.004807	1.750	0.174			813.26	3.99	4918.15
					0.15	4.27			
6200	995.00	0.004804	1.909	0.159			817.53	3.87	4778.75
					0.14	3.91			
6300	997.00	0.004802	2.069	0.147			821.45	3.76	4652.44
					0.11	3.63			
6400	998.66	0.004801	2.383	0.127			825.08	3.66	4536.50
					0.09	3.17			
6500	1000.33	0.004800	2.698	0.113			828.24	3.57	4436.20
					0.08	2.81			
6600	1002.00	0.004799	3.012	0.101			831.05	3.50	4347.87
					0.06	2.54			
6700	1003.33	0.004799	3.219	0.094			833.59	3.43	4268.61
					0.06	2.37			
6800	1004.66	0.004798	3.425	0.089			835.96	3.37	4194.99
					0.05	2.23			
6900	1006.00	0.004798	3.631592	0.084			838.19	3.31	4126.30

Table F-VI Variable Thermal Properties for Steel and Gypsum

Time	k_s	C_{ps}	k_i	C_{pi}	$Tg / (1/(1+\zeta))$	ΔTs	Ts	Fy	Et
(sec)	*(W/in°C)*	*(J/lbs°C)*	*(W/in°C)*	*(J/lbs°C)*	*(°C)*	*(°C)*	*(°C)*	*(ksi)*	*(ksi)*
0	0.005018	0.732040	2.33E-05	2.4923			20.00	35.82	28927.63
					25.32	-21.13			
100	0.005017	0.7383	1.12E-05	2.4923			20.00	35.82	28927.63
					25.17	-19.18			
200	0.005013	0.7446	1.12E-05	1.0800			20.00	35.82	28927.63
					12.97	-1.10			
300	0.00501	0.750854	1.58E-05	1.0384			20.00	35.82	28927.63
					3.99	17.25			
400	0.005008	0.7612	2.05E-05	0.9138			37.25	35.61	28840.44
					3.53	26.04			
500	0.005005	0.7716	2.28E-05	4.9845			63.29	35.24	28678.59
					12.19	9.69			
600	0.005003	0.781972	2.51E-05	0.9138			72.98	35.08	28609.92
					1.14	37.73			
700	0.005	0.7895	2.51E-05	0.9061			110.71	34.40	28300.89
					1.12	36.29			
800	0.004998	0.7970	2.51E-05	0.8985			147.00	33.63	27940.94
					1.11	34.96			
900	0.004995	0.804554	2.51E-05	0.8908			181.96	32.78	27533.60
					0.69	33.93			
1000	0.004993	0.8099	2.51E-05	0.8859			215.89	31.87	27077.46
					0.69	32.44			
1100	0.004991	0.8152	2.51E-05	0.8810			248.34	30.91	26580.53
					0.68	31.06			
1200	0.004989	0.820566	2.51E-05	0.8761			279.39	29.91	26043.87
					0.52	29.85			
1300	0.004985	0.8420	2.51E-05	0.8723			309.24	28.86	25466.41
					0.50	28.00			
1400	0.004982	0.8633	2.63E-05	0.8723			337.23	27.81	24864.02
					0.49	27.61			
1500	0.004978	0.847296	2.73E-05	0.8723			364.84	26.69	24206.45
					0.41	28.05			
1600	0.004973	0.8824	2.83E-05	0.8723			392.89	25.48	23466.63
					0.39	26.77			

Time	k_s	C_{ps}	k_i	C_{pi}	$Tg / (1/(1+\zeta))$	$\Delta\ Ts$	Ts	Fy	Et
(sec)	(W/in°C)	(J/lbs°C)	(W/in°C)	(J/lbs°C)	(°C)	(°C)	(°C)	(ksi)	(ksi)
1700	0.004968	0.8801	2.93E-05	0.8723			419.66	24.24	22685.25
					0.40	26.55			
1800	0.004963	0.877846	3.02E-05	0.8723			446.21	22.94	21829.29
					0.34	26.15			
1900	0.004958	0.8881	3.11E-05	0.8723			472.36	21.57	20897.45
					0.34	25.30			
2000	0.004952	0.8984	3.19E-05	0.8723			497.66	20.17	19902.03
					0.34	24.44			
2100	0.004947	0.908731	3.27E-05	0.8723			522.10	18.73	18841.03
					0.28	23.51			
2200	0.004942	0.9184	3.34E-05	0.8723			545.62	17.27	17716.44
					0.28	22.54			
2300	0.004936	0.9280	3.41E-05	0.8723			568.16	15.80	16530.40
					0.27	21.60			
2400	0.004931	0.937662	3.47E-05	0.8723			589.75	14.31	15281.72
					0.24	20.64			
2500	0.004926	0.9475	3.54E-05	0.8723			610.40	12.87	13998.88
					0.24	19.67			
2600	0.004922	0.9574	3.6E-05	0.8723			630.07	11.61	12838.60
					0.23	18.75			
2700	0.004917	0.96731	3.66E-05	0.8723			648.81	10.51	11804.19
					0.21	17.85			
2800	0.004913	0.9772	3.72E-05	0.8723			666.67	9.56	10878.02
					0.21	16.97			
2900	0.004908	0.9871	3.72E-05	0.8723			683.64	8.73	10046.00
					0.21	15.90			
3000	0.004904	0.997031	3.75E-05	0.8723			699.54	8.00	9306.29
					0.18	15.05			
3100	0.0049	1.0087	3.79E-05	0.8723			714.59	7.36	8638.82
					0.17	14.19			
3200	0.004895	1.0203	3.82E-05	0.8723			728.78	6.79	8036.63
					0.17	13.40			
3300	0.004891	1.031980	3.85E-05	0.8723			742.19	6.28	7490.78
					0.17	12.67			
3400	0.004887	1.0459	3.89E-05	0.8723			754.86	5.83	6993.85
					0.17	11.97			
3500	0.004882	1.0598	3.92E-05	0.8723			766.84	5.42	6540.54
					0.17	11.33			
3600	0.004878	1.073680	3.95E-05	0.8723			778.17	5.05	6125.32
					0.15	10.74			

Time	k_s	C_{ps}	k_i	C_{pi}	$Tg / (1/(1+\zeta))$	ΔTs	Ts	Fy	Et
(sec)	*(W/in°C)*	*(J/lbs°C)*	*(W/in°C)*	*(J/lbs°C)*	*(°C)*	*(°C)*	*(°C)*	*(ksi)*	*(ksi)*
3700	0.004875	1.0868	3.98E-05	0.8723			788.91	4.71	5743.74
					0.15	10.17			
3800	0.004871	1.0999	4.01E-05	0.8723			799.07	4.40	5392.50
					0.15	9.65			
3900	0.004868	1.112976	4.04E-05	0.8723			808.72	4.12	5068.07
					0.13	9.16			
4000	0.004864	1.1281	4.07E-05	0.8723			817.88	3.86	4767.56
					0.13	8.67			
4100	0.004861	1.1433	4.1E-05	0.8723			826.55	3.62	4489.62
					0.13	8.22			
4200	0.004857	1.158436	4.12E-05	0.8723			834.77	3.40	4231.74
					0.11	7.81			
4300	0.004854	1.1744	4.15E-05	0.8723			842.58	3.20	3991.83
					0.11	7.40			
4400	0.004851	1.1903	4.17E-05	0.8723			849.98	3.01	3768.87
					0.11	7.02			
4500	0.004848	1.206224	4.2E-05	0.8723			857.01	2.84	3561.03
					0.12	6.68			
4600	0.004845	1.2243	4.23E-05	0.8723			863.69	2.68	3366.62
					0.12	6.38			
4700	0.004841	1.2424	4.25E-05	0.8723			870.07	2.52	3183.90
					0.12	6.11			
4800	0.004838	1.260512	4.28E-05	0.8723			876.18	2.38	3011.68
					0.10	5.85			
4900	0.004835	1.2737	4.3E-05	0.8723			882.03	2.25	2849.00
					0.10	5.62			
5000	0.004833	1.2868	4.33E-05	0.8723			887.65	2.12	2695.05
					0.10	5.40			
5100	0.004830	1.30	4.35E-05	0.8723			893.05	2.00	2549.03
					0.09	5.20			
5200	0.004828	1.3163	4.37E-05	0.8723			898.25	1.89	2410.30
					0.09	4.97			
5300	0.004825	1.3327	4.39E-05	0.8723			903.22	1.79	2279.13
					0.09	4.77			
5400	0.004823	1.348995	4.41E-05	0.8723			907.98	1.69	2154.83
					0.07	4.57			
5500	0.00482	1.3805	4.43E-05	0.8723			912.56	1.59	2036.81
					0.07	4.33			
5600	0.004818	1.4120	4.45E-05	0.8723			916.89	1.50	1926.22

Time	*k_s*	*C_{ps}*	*k_i*	*C_{pi}*	*Tg / (1/(1+ζ))*	*Δ Ts*	*Ts*	*Fy*	*Et*
(sec)	*(W/in°C)*	*(J/lbs°C)*	*(W/in°C)*	*(J/lbs°C)*	*(°C)*	*(°C)*	*(°C)*	*(ksi)*	*(ksi)*
					0.07	4.11			
5700	0.004815	1.443529	4.47E-05	0.8723			921.00	1.42	1822.25
					0.08	3.92			
5800	0.004813	1.4924	4.49E-05	0.8723			924.91	1.34	1724.16
					0.08	3.72			
5900	0.004811	1.5413	4.51E-05	0.8723			928.63	1.27	1631.83
					0.08	3.54			
6000	0.004809	1.590216	4.53E-05	0.8723			932.18	1.20	1544.56
					0.06	3.39			
6100	0.004807	1.7498	4.55E-05	0.8723			935.56	1.13	1461.80
					0.06	3.04			
6200	0.004804	1.9094	4.57E-05	0.8723			938.60	1.08	1388.17
					0.05	2.76			
6300	0.004802	2.069	4.58E-05	0.8723			941.35	1.02	1321.76
					0.04	2.53			
6400	0.004801	2.3833	4.6E-05	0.8723			943.88	0.98	1261.18
					0.04	2.18			
6500	0.0048	2.6977	4.61E-05	0.8723			946.06	0.94	1209.18
					0.03	1.93			
6600	0.004799	3.012	4.63E-05	0.8723			947.99	0.90	1163.49
					0.02	1.73			
6700	0.004799	3.2185	4.64E-05	0.8723			949.72	0.87	1122.66
					0.02	1.61			
6800	0.004798	3.4251	4.65E-05	0.8723			951.33	0.84	1084.68
					0.02	1.52			
6900	0.004798	3.631592	4.65E-05	0.8723			952.85	0.81	1049.14